European Commission

European Reference Materials

CERTIFICATION REPORT

The certification of equivalent diameters of a mixture of silica nanoparticles in aqueous solution: ERM®- FD102

EUR 26656 EN - 2014

European Commission
Joint Research Centre
Institute for Reference Materials and Measurements

Contact information
Reference materials sales
Retieseweg 111
B-2440 Geel, Belgium
E-mail: jrc-irmm-rm-sales@ec.europa.eu
Tel.: +32 (0)14 571 705
Fax: +32 (0)14 590 406

http://irmm.jrc.ec.europa.eu/
http://www.jrc.ec.europa.eu/

JRC 90438

EUR 26656 EN
ISBN 978-92-79-38396-0 (pdf)

ISSN 1831-9424 (online)

doi:10.2787/95996

Luxembourg: Publications Office of the European Union

CERTIFICATION REPORT

The certification of equivalent diameters of a mixture of silica nanoparticles in aqueous solution: ERM®- FD102

V. Kestens and G. Roebben

European Commission, Joint Research Centre
Institute for Reference Materials and Measurements (IRMM)
Geel, Belgium

Disclaimer

Certain commercial equipment, instruments, and materials are identified in this paper to specify adequately the experimental procedure. In no case does such identification imply recommendation or endorsement by the European Commission, nor does it imply that the material or equipment is necessarily the best available for the purpose.

Summary

This report describes the production of ERM®-FD102, silica nanoparticles in an aqueous solution certified for different equivalent diameters. The material was produced following ISO Guide 34:2009 [1].

The certified reference material (CRM), which has been produced by the Institute for Reference Materials and Measurements (IRMM) of the European Commission's Joint Research Centre (JRC), is a mixture of two monomodal populations of silica nanoparticles with distinct nominal particle sizes of 20 nm and 80 nm. These nominally 20 nm and 80 nm particle populations are further referred to as size class A and size class B, respectively. The CRM was prepared from two commercially available silica sols, moderately diluted in an aqueous solution and bottled in 10 mL pre-scored amber glass ampoules.

Between unit-homogeneity was quantified and stability during dispatch and storage were assessed in accordance with ISO Guide 35:2006 [2]. The minimum sample intake for the different methods was determined from the results and information provided by the laboratories that participated in the interlaboratory comparison (ILC) exercises of the characterisation study.

The material was characterised, for size classes A and B, by an intercomparison amongst laboratories of demonstrated competence and adhering to ISO/IEC 17025 [3]. Technically invalid results were removed but no outlier was eliminated on statistical grounds only.

Uncertainties of the certified values were calculated in accordance with the Guide to the Expression of Uncertainty in Measurement (GUM) [4] and include uncertainty contributions related to possible inhomogeneity and instability and to characterisation.

The material is intended for quality control and assessment of method performance. As any reference material, it can also be used for control charts or validation studies. The certified values are regarded as reliable estimates of the true values and ERM-FD102 can therefore be used for calibration purposes. The CRM is available in amber glass ampoules containing about 9 mL of suspension.

The CRM was accepted as European Reference Material (ERM®) after peer evaluation by the partners of the European Reference Materials consortium.

The following certified values were assigned:

	Equivalent diameter			
	Size class A		Size class B	
	Certified value [4] [nm]	Uncertainty [5] [nm]	Certified value [4] [nm]	Uncertainty [5] [nm]
Scattered light intensity-weighted arithmetic mean hydrodynamic diameter [1]	17.8 [a]	1.5	88.5 [a]	2.2
Light extinction intensity-weighted modal Stokes' diameter [2]	23.9 [b]	2.3	88.0 [b]	6.6
Number-weighted modal area-equivalent diameter [3]	18.2 [a]	1.6	84.0 [a]	2.1

Number-weighted median area-equivalent diameter [3]	18.3 [a]	1.7	83.3 [a]	2.3

1) Arithmetic mean from a transformed density function as obtained by dynamic light scattering (DLS) and by applying non-negative least square (NNLS), CONTIN or Dynals algorithms for data analysis.

2) As obtained by centrifugal liquid sedimentation (CLS), with turbidimetric detection, according to ISO 13318-1:2001; effective particle density 2.0 g/cm^3.

3) As obtained by transmission and scanning electron microscopy.

4) Unweighted mean value of the means of accepted sets of data; each set being obtained in a different laboratory and/or with a different method of determination. The certified value and its uncertainty are traceable to:

a) the International System of Units (SI)

b) the size values provided for the PVC calibrants supplied by CPS Instruments, Inc.

5) The uncertainty of the certified value is the expanded uncertainty with a coverage factor k = 2 corresponding to a level of confidence of about 95 % estimated in accordance with ISO/IEC Guide 98-3, Guide to the Expression of Uncertainty in Measurement (GUM:1995), ISO, 2008.

Table of contents

Glossary

aFlFFF	Asymmetrical flow field-flow fractionation
ACF	Autocorrelation function
AFM	Atomic force microscopy
ANOVA	Analysis of variance
APD	Avalanche photodiode detector
AUC	Analytical ultracentrifugation
CCL	Consultative Committee for Length
CIPM	Comité International des Poids et Mesures (International Committee of Weights and Measures)
CLS	Centrifugal liquid sedimentation
CRM	Certified reference material
D	Diameter of an equivalent sphere
DLS	Dynamic light scattering
ELS	Electrophoretic light scattering
EM	Electron microscopy
ERM®	Trademark of European Reference Materials
EU	European Union
GUM	Guide to the Expression of Uncertainty in Measurements
IEC	International Electrotechnical Commission
ILC	Interlaboratory comparison
IRMM	Institute for Reference Materials and Measurements of the JRC
ISO	International Organization for Standardization
JRC	Joint Research Centre of the European Commission
k	Coverage factor
MALLS	Multi-angle laser light scattering
$MS_{between}$	Mean of squares between-unit from an ANOVA
MS_{within}	Mean of squares within-unit from an ANOVA
n.a.	Not applicable (or not available)
n.c.	Not calculated
n.d.	Not detectable
NIST	National Institute of Standards and Technology (US)
NNLS	Non-negative least square
p	Number of technically valid datasets
PMT	Photomultiplier tube

PSD	Particle size distribution
PTA	Particle tracking analysis
PVC	Polyvinyl chloride
q	Scattering vector
QC	Quality control
R	Radius of an equivalent sphere
R_g	Radius of gyration
RI	Refractive index
RM	Reference material
rpm	Revolutions per minute
RSD	Relative standard deviation
s	Standard deviation
SAXS	Small-angle X-ray scattering
s_{bb}	Between-unit standard deviation; an additional index "rel" is added when appropriate
$s_{between}$	Standard deviation between groups as obtained from ANOVA
SE	Secondary electron
SEM	Scanning electron microscopy
SI	International System of Units
s_{within}	Standard deviation within groups as obtained from ANOVA
s_{wb}	Within-unit standard deviation; an additional index "rel" is added when appropriate
$\bar{t}$	Mean of all t_i
t_i	Time elapsed at time point i
t_{sl}	Shelf life
t_{tt}	Transport time
TEM	Transmission electron microscopy
U	Expanded uncertainty; an additional index "rel" is added when appropriate
u	Standard uncertainty; an additional index "rel" is added when appropriate
u^*_{bb}	Standard uncertainty related to a maximum between-unit inhomogeneity that could be hidden by method repeatability; an additional index "rel" is added when appropriate
u_{bb}	Standard uncertainty related to a possible between-unit inhomogeneity; an additional index "rel" is added when appropriate
u_c	Combined uncertainty
u_{cal}	Standard uncertainty of a common calibrant
u_{char}	Standard uncertainty of the material characterisation; an additional index "rel" is added when appropriate

u_{CRM}	Combined standard uncertainty of the certified value; an additional index "rel" is added as appropriate
U_{CRM}	Expanded uncertainty of the certified value; an additional index "rel" is added when appropriate
u_{Δ}	Combined standard uncertainty of measurement result and certified value
u_{lts}	Standard uncertainty of the long-term stability; an additional index "rel" is added when appropriate
u_{sts}	Standard uncertainty of the short-term stability; an additional index "rel" is added when appropriate
u_{ρ}	Standard uncertainty of the effective particle density; an additional index "rel" is added when appropriate
$\overline{x}$	Arithmetic mean
Δ_{meas}	Absolute difference between mean measured value and the certified value
ν_{eff}	Effective degrees of freedom
$\nu_{MSwithin}$	Degrees of freedom of MS_{within}

1 Introduction

1.1 Background

Nanoparticles are particles with all three external dimensions between 1 nm and 100 nm [5], that may exhibit unique properties due to their size. To implement the European Commission's Recommendation (2011/696/EU) on the definition of a nanomaterial [6], and to better understand the different properties of nanoparticles, reliable size and size distribution measurements are needed. In this respect, fit-for-purpose reference materials including quality control and calibration materials are necessary. A variety of techniques exists to analyse the size and size distribution of nanoparticles. In reality, it is very rare that particles have a perfectly spherical shape. Since different size parameters would need to be carefully investigated in order to determine the effective particle size [7], most of the techniques therefore try to describe the size of the particles with an "equivalent" diameter.

Different techniques report different equivalent particle diameters due to the various established measurement principles. Discrepancy of the results obtained with different sizing techniques is expected: particle size is a method-defined measurand. The certified, indicative and additional material information particle size values of ERM-FD102 are specified in this report as equivalent diameters corresponding to the methods used, and to the type of distribution reported. A summary of the techniques used in this study is given below.

1. Atomic force microscopy (AFM) [8] is a kind of stylus technique that uses the force acting between a sharp tip that is attached to a flexible cantilever and a specimen surface. When brought in close proximity to a specimen surface, net attractive or repulsive forces resulting from interactions between the tip and the surface will cause vertical bending and torsion of the cantilever. The bending is commonly detected by means of a laser beam that is focussed onto the back reflective surface of the cantilever. The reflected laser beam strikes a position-sensitive photodetector which captures the vertical displacement and rotation of the cantilever. Images are typically generated based on the principle of either keeping the cantilever deflection (and hence the force) constant and tracking the height variations of the surface, or by keeping the height constant. In the contact mode the tip is in permanent contact with the sample surface. In this mode, which is also referred to as static or DC mode, the tip is in the repulsive regime. In the dynamic (AC) mode, the cantilever is oscillating in z-direction and the tip is either in non-contact (net attractive interactions) or in the intermittent contact where the tip is submitted successively to repulsive and attractive forces. The tip-sample force interactions cause variations in the cantilever resonance frequency. These can be detected either directly (frequency modulation) or indirectly (amplitude modulation) through changes in the cantilever oscillation amplitude at a drive frequency slightly below or above its resonance peak frequency.

   An AFM instrument can be operated in the so-called open-loop and closed-loop modes. The open-loop mode provides very good performance in terms of imaging resolution. However, due to the absence of positional feedback, images are very often distorted. These distortions are typically introduced by nonlinearities that are caused by phenomena such as creep, hysteresis and ageing effects which originate from the piezoelectric scanners. In the closed-loop mode, the actual position of the AFM probe is tracked by sensors. The software-controlled feedback compensates for the nonlinear behaviour of the piezoelectric scanner, which is especially relevant for tests over large scanning areas. Measurement of the lateral dimensions of small particles, deposited onto a substrate, are not straightforward as this requires deconvolution of the shape of the AFM cantilever tip, which has a radius that is similar

to the diameter of a nanoparticle. However, if the particles are assumed to be near spherical and the substrate around the particles is accessible for the AFM tip, then the maximum particle height, which corresponds to the diameter of the particles, can be accurately measured.

2. Analytical centrifugation or centrifugal liquid sedimentation (CLS) methods [9] use an increased centrifugal force to fractionate and settle particles in a suspension. CLS instruments contain the suspension in a disc or a cuvette.

   (i) A *disc centrifuge* instrument is based on an optically clear spinning disc that is partly filled with a liquid (e.g., a sucrose or dextrose solution). Under the influence of the centrifugal force the liquid is held against the outside edge of the chamber forming a liquid ring. If this ring is created by a series of injections of liquid with decreasing density, the liquid at the outside edge of the ring is denser than the liquid near the inside edge. The latter density is chosen to be slightly denser than the density of the sample's dispersing medium. When the density gradient is created and stabilised a small volume of a dilute suspension of particles is injected into the centre of the spinning disc. A laser light or X-ray beam passes through the liquid near the outside edge of the disc and particles passing the beam reduce the light intensity in proportion to their concentration.

   Commercially available disc centrifuge instruments can be operated in the line-start or homogeneous mode and are either equipped with (laser) light [10] or X-ray absorption [11] optical detection systems. Their rotational speed varies from 500 revolutions per minute (rpm) to 24000 rpm. Both types of systems either measure the attenuation of light (turbidity) or X-rays. The measured time is then converted to an equivalent particle size using Stokes' Law of sedimentation and assuming an effective particle density. For instruments with turbidity optics, the obtained particle size distribution is light extinction intensity-based. The transmission data can be converted to a relative mass-based distribution using Mie theory. The mass-based distribution can be further converted to a number-based distribution by calculating the volume of the particles. For instruments with X-ray absorption optics the attenuation of the X-ray beam is directly proportional to the mass of the detected particles. As a result, the particle size distribution is relative mass-based.

   (ii) In the *cuvette centrifuge*, particles do not travel through a pre-constructed density gradient but sediment out of their native dispersant in which they are initially homogeneously distributed. There are two types of cuvette centrifuges which can generally be distinguished depending on their maximum rotational speed. The first group of instruments have a rotational speed up to 4000 rpm and are equipped with turbidity optics [12]. The second group of cuvette centrifuges, which are known as analytical ultracentrifugation (AUC) instruments, can be operated at rotational speeds up to 60000 rpm. Today's commercially available AUC instruments are typically equipped with Rayleigh interference optics. Such detection system determines the distribution of sedimentation coefficients by measuring the difference in refractive index between a test sample and a reference sample [13]. The difference in refractive index directly corresponds to the mass of the detected particles. Hence, the particle size distribution obtained from the initial sedimentation coefficient distribution, and following the Stokes-Einstein equation, is relative mass-based.

3. Dynamic light scattering (DLS), also referred to as photon correlation spectroscopy or quasi-elastic light scattering, measures the fluctuation of light intensity that is scattered by a quiescent particle suspension upon irradiation by a beam of coherent and monochromatic (laser) light [14]. The intensity of the scattered light, which fluctuates in time due to the Brownian motion of the particles, is registered by a highly sensitive photodetector such as a photomultiplier tube (PMT) or an avalanche photodiode (APD). These detectors are commonly positioned at an angle of about 90°

or at about 180° with respect to the incident light beam. DLS instruments are intrinsically absolute in nature and instrument response calibration or correction factors are thus not required. DLS instruments can be classified according to the principle of data acquisition and processing.

(i) The main group of DLS instruments are operating in the time-domain. These instruments either measure the scattered light intensity fluctuations directly (homodyne or correlation analysis method) at the detector, or superimpose the light of a reference beam on that of the light scattered by the particles (heterodyne or cross-correlation function analysis method). For both the homodyne and heterodyne methods, the raw signal is collected and processed via a digital correlator and subsequently extracted as an approximated intensity autocorrelation function (ACF). For highly monomodal dispersions of solid spherical particles, the ACF linearly decays with a rate that is proportional to the apparent translational diffusion coefficient of the particles. This decay rate can be precisely determined by fitting the ACF with a first-order or single linear exponential function. The apparent translational diffusion coefficient then yields, via the Stokes-Einstein relationship, the hydrodynamic harmonic particle size. The term "harmonic" describes the inverse proportionality between the particle diameter and the translational diffusion coefficient. In reality, monomodal samples have a degree of polydispersity. As a result, the ACF consists of a distribution of decay constants and describes a multi-exponential behaviour that can only be fitted by a cumulant generating polynomial power function. This power function is generally known as the method of cumulants [15,16,17]. The first cumulant of the power function, which corresponds to the initial slope of the ACF, provides the mean translational diffusion coefficient. The Stokes-Einstein equation then relates the mean translational diffusion coefficient with the scattering intensity-weighted harmonic mean (also commonly referred to as harmonic z-average) particle size. In addition, a dimensionless qualitative estimation that expresses the degree of polydispersity can be obtained from the ratio of the first and second cumulant. The cumulants method is the simplest and most widely used method for measuring the average size of nanoparticles in dispersion. In addition to the cumulants method, intensity-, volume- and number-based particle size distributions (PSD) can be computed by deconvoluting the ACF via Laplace transformation. The main disadvantage of Laplace transformation is that the process is ill-defined: a given ACF can be described by an infinite number of solutions. The existing algorithms try to overcome this difficulty by using criteria to limit the number of possible solutions and to choose the most reasonable one. One such algorithm, called CONTIN, has been developed by Provencher [18,19]. CONTIN is a generalised inverse Laplace transform algorithm that seeks the simplest (most parsimonious) solution for experimental data based on statistical prior knowledge. The algorithm additionally contains a non-negative least square (NNLS) routine that is often effectively used as stand-alone PSD algorithm [20]. Another algorithm being Dynals behaves similar to CONTIN. Since a single universally-accepted Laplace transformation algorithm does not exist, most manufacturers of DLS instruments have developed their own specific algorithms that are typically grafted on either the CONTIN or NNLS (or a combination of both) algorithm. Most of these algorithms differ from each other in the grade of smoothing of the ACF. Because of the different smoothing approaches, in combination with the noise sensitivity, PSD results tend to be less repeatable and reproducible than cumulants results.

(ii) The second group of DLS instruments are equipped with spectrum analysers that obtain the frequency spectra by Fourier transforming the scattered intensity fluctuations into a power spectrum. The power spectrum is then converted into a PSD using an NNLS, or equivalent, algorithm [21].

4. Transmission electron microscopy (TEM) and scanning electron microscopy (SEM) are versatile techniques that allow analysing the morphology, crystallographic structure and chemical composition of nanomaterials. An electron microscope uses an electron source to generate a primary electron beam, which can be focused onto a specimen through a set of lenses and apertures. In a TEM instrument, part of the electron beam passes through the very thin specimen and the information contained in the electron waves that exit the specimen is used to create an image. The contrast in this image originates from the absorption and scattering of electrons in the specimen, due to the thickness and composition of the material (i.e. mass-thickness contrast), and from the crystal orientation (i.e. diffraction contrast). An SEM instrument scans the surface of a specimen with a focused beam of electrons. An image is created, for example, by detecting the secondary electrons generated from the interactions of the electron beam with the specimen surface at every point during the scan.

   SEM and TEM instruments have in common that they both produce 2D projections of 3D objects like nanoparticles. Nanoparticles, typically dispersed in a liquid solvent, are first deposited onto a suitable substrate (e.g., grid, mica, silicon wafer). Due to the difference in contrast between the nanoparticles and the substrate, well-dispersed nanoparticles can be detected also in an automated image analysis process, by applying grey-level threshold limits and then be quantified i.e. in terms of particle size and particle size distribution.

   The particle size obtained by electron microscopy (EM) can be quantitatively defined in a number of ways (e.g., minimum and maximum Feret's diameter, Martin's diameter, projected area-equivalent circular diameter) [22,23,24,25]. Automated, semi-automated and manual image analysis can be performed by using designated software.

5. Particle tracking analysis (PTA), also referred to as nanoparticle tracking analysis, dynamic ultramicroscopy, or orthogonal tracking microscopy, combines laser light scattering microscopy with a digital camera. The latter enables visualisation of the light scattered by particles that are moving under Brownian motion. The PTA software detects, based on their scattering behaviour, individual particles suspended in a liquid and monitors in real-time their trajectories in the suspension. The movement of the particles, expressed as a mean square displacement, is then related to a particle diameter via a formula derived from the Stokes-Einstein equation.

6. In a small-angle X-ray scattering (SAXS) experiment, a narrow beam of X-ray is passed through (transmission mode) a sample, i.e. suspension of nanoparticles [26]. The electrons of the atomic shell in the particles interfere with the incident X-rays and hence emit photons in all directions thereby creating elastic scattering waves (Rayleigh scattering). These scattering waves interfere with one another forming a scattering pattern (also referred to as speckles). The scattering angle, which is inversely related to the particle size, together with the individual unit vectors in the incident and scattered X-ray directions are the basis for the scattering vector (q). If the suspended particles have an electron density contrast different than that of the surrounding dispersant, a scattering intensity curve can be obtained. The shape of the scattering curve contains the information of particle size and particle shape. At small scattering vectors the intensity only depends on the contrast (= difference in electron density of the particle versus dispersing medium), concentration, particle volume and radius of gyration (R_g). The latter is a model independent size parameter that corresponds to the root mean square (quadratic mean) distance to the centre of mass weighted by the contrast of electron density and which can be determined by applying the Guinier law [27]. The initial part of the scattering curve can be approximated by a Gaussian function; its natural logarithm versus q^2 yields a straight line with R_g that can be calculated from the slope of the fitted linear curve. After fitting,

the mean values of R_g^2 are intensity weighted (i.e. proportional to the radius of a sphere to the power six), hence, the mean values of R_g are volume- (or mass)-weighted (i.e. proportional to R^3). Following this approach only an overall mean particle size can be obtained. In order to obtain the PSD from SAXS data, a theoretical scattering curve assuming a certain model for statistical distribution must be fitted to the experimental curve, i.e. by using the indirect Fourier transformation method [28]. This method allows computation of volume- and intensity-based PSDs under the assumption of homogeneous particle shape.

1.2 Choice of the material

ERM-FD102 was produced from two commercially available sols which both consisted of silica nanoparticles suspended in electrolyte solution. In order to allow the users of ERM-FD102 to use the CRM as-received (e.g., for DLS and CLS), the original silica sols were diluted in ultrapure water. The forced dilution with ultrapure water increases the versatility with respect to the preparation of test specimens for microscopy analysis and it allows using values of commonly required physical properties (e.g., viscosity, density, refractive index) that are generally known for water and which are often needed by ensemble characterisation methods.

Given its industrial relevance, and the ability to remain colloidally stable for several years, silica nanoparticles were selected as analyte.

1.3 Design of the project

The stability and homogeneity of the material was evaluated through studies involving measurement of DLS and CLS measurands. The certified and indicative values were established by an interlaboratory comparison of different laboratories with different measurement methods and techniques.

2 Participants

2.1 Project management and evaluation

European Commission, Joint Research Centre, Institute for Reference Materials and Measurements (IRMM), Geel, BE
(accredited to ISO Guide 34 for production of certified reference materials, BELAC No. 268-RM)

2.2 Processing

European Commission, Joint Research Centre, Institute for Reference Materials and Measurements (IRMM), Geel, BE
(accredited to ISO Guide 34 for production of certified reference materials, BELAC No. 268-RM)

2.3 Homogeneity study

European Commission, Joint Research Centre, Institute for Reference Materials and Measurements (IRMM), Geel, BE
(accredited to ISO Guide 34 for production of certified reference materials, BELAC No. 268-RM; measurements under the scope of ISO/IEC 17025 accreditation BELAC No. 268-TEST)

2.4 Stability study

European Commission, Joint Research Centre, Institute for Reference Materials and Measurements (IRMM), Geel, BE
(accredited to ISO Guide 34 for production of certified reference materials, BELAC No. 268-RM; measurements under the scope of ISO/IEC 17025 accreditation BELAC No. 268-TEST)

2.5 Characterisation

The participants in the interlaboratory comparison study were (alphabetically):

Agfa Gevaert NV, Agfa-Labs, Mortsel, BE

Anton Paar GmbH, Graz, AT

AQura GmbH, Marl, DE
(accredited to ISO/IEC 17025, measurements under the scope of DAkkS No. D-PL-14093-01-00)

Beijing Center for Physical and Chemical Analysis (BCPCA), Beijing, CN
(accredited to ISO/IEC 17025, measurements under the scope of CNAS No. L0066)

Delft Solids Solutions B.V., Wateringen, NL

Dr. Lerche KG, Berlin, DE

European Commission, Joint Research Centre, Institute for Reference Materials and Measurements (IRMM), Geel, BE
(accredited to ISO/IEC 17025, measurements under the scope of BELAC No. 268-TEST)

Horiba Instruments Inc., Irvine, US

LGC Ltd., Teddington, UK

LUM GmbH, Berlin, DE

Malvern Instruments Inc., Westborough, US

Malvern Instruments Ltd., Malvern, UK

Max Planck Institute of Colloids and Interfaces, Potsdam, DE

microParticles GmbH, Berlin, DE

NanoSight Ltd., Amesbury, UK

National Center for Nanoscience and Technology (NCNST), CAS Key Lab for Biomedical Effects of Nanomaterials and Nanosafety, Beijing, CN

National Institute of Metrology (NIM), Division of Nano Metrology and Materials Measurement, Beijing, CN

National Institute of Standards and Technology (NIST), Semiconductor and Dimensional Metrology Division, Gaithersburg, US

National Measurement Institute Australia (NMIA), Nanometrology, West Lindfield, AU

National Physical Laboratory (NPL), Analytical Science Division, Teddington, UK

Sirris, Seraing, BE

Solvias AG, Kaiseraugst, CH

Sympatec GmbH, Clausthal-Zellerfeld, DE

Technical University Bergakademie, Institute for Mechanical Process Engineering and Mineral Processing, Laboratory for Particle Characterisation, Freiberg, DE

Technical University of Dresden, Faculty of Mechanical Engineering, Institute of Process Engineering and Environmental Technology, Research Group Mechanical Process Engineering, Dresden, DE

Umicore N.V., Group Research and Development, Fine Particle Technology, Olen, BE

University of Konstanz, Physical Chemistry, Konstanz, DE

University of Namur, Namur Nanosafety Centre, Namur, BE

Veterinary and Agrochemical Research Centre (CODA-CERVA), Service Electron Microscopy, Brussels, BE

Wageningen University and Research Centre (RIKILT), Wageningen, NL

3 Material processing and process control

3.1 Origin of the starting material

Two different colloidal silica starting materials, Köstrosol 1530 and Klebosol 30R50 were supplied by Chemiewerk Bad Köstritz GmbH (Bad Köstritz, DE) and AZ Electronic Materials France SAS (Trosly-Breuil, FR), respectively. Material specifications for the starting materials, as provided by both product manufacturers and as obtained in a preliminary characterisation study, are listed in Table 1.

Table 1: Köstrosol 1530 and Klebosol 30R50 starting material information

Property	**Specifications**	
	Köstrosol 1530	**Klebosol 30R50**
Batch identification	K430	19019/L1
Appearance	Slightly turbid	Milky turbid
Nominal particle diameter	20 nm	80 nm
Specific surface area	160-210 m^2/g	40-60 m^2/g
Nominal SiO_2 mass fraction	300 g/kg	300 g/kg
Free alkalinity as Na_2O	≤ 0.3 g/kg	≤ 0.2 g/kg
pH (at 25 °C)	9-10	8.5-9.5
Viscosity (at 25 °C)	6 mPa·s	n.a.
Suspension density (at 20 °C)	1.2 g/cm^3	1.2 g/cm^3
Particle aspect ratio [1)]	1.1*	1.0*

[1)] ratio of the major diameter (length) to the minor diameter (width) of a fitted ellipse

n.a., information not available

* Preliminary characterisation

Preliminary TEM analyses were commissioned by IRMM to an independent qualified laboratory. TEM grids were dipped in the as-received mixture of the aforementioned materials and imaged on a Philips CM120 transmission electron microscope at an acceleration voltage of 100 kV. A typical TEM micrograph (Fig. 1) shows both nominally 20 nm (Köstrosol 1530) and nominally 80 nm (Klebosol 30R50) near-spherical silica nanoparticles.

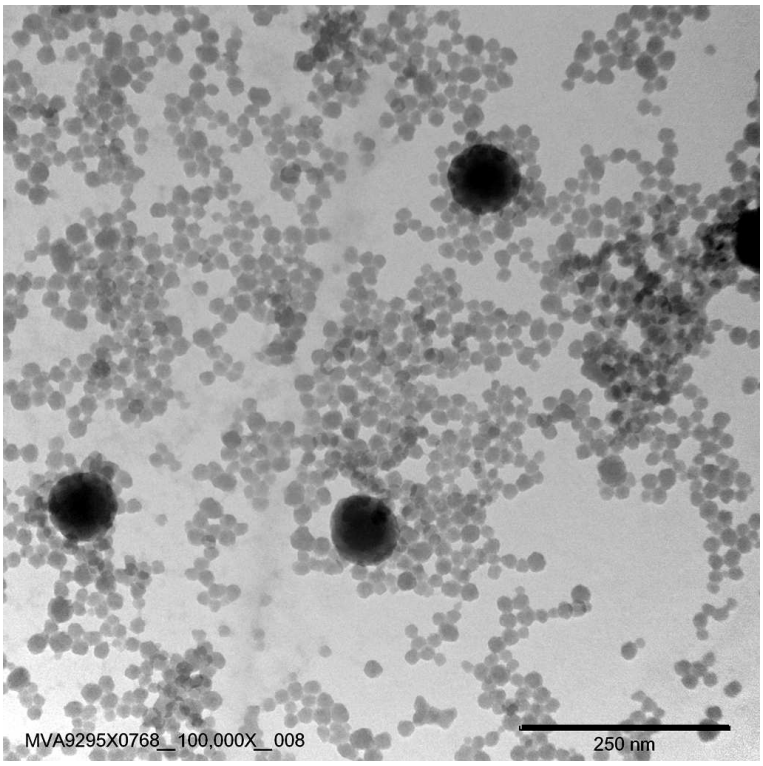

Fig 1 TEM micrograph (MVA Scientific Consultants, Duluth, US) of a mixture of Köstrosol 1530 and Klebosol 30R50 silica nanoparticles

3.2 Processing

The delivered Köstrosol 1530 and Klebosol 30R50 starting materials were diluted to a target SiO_2 mass fraction of 10 g/kg and 2.5 g/kg, respectively, by the addition of ultrapure water (resistivity 18.2 MΩ.cm at 25 °C) produced by an Elix 35 water purification system (Merck Millipore, Molsheim, FR). The diluted Köstrosol 1530 sub-batch was prepared by addition of 667 g of the initial starting material into 19333 g of ultrapure water. The diluted Klebosol 30R50 sub-batch was prepared by addition of 33 g of the initial starting material into 3967 g of ultrapure water. Both diluted sub-batches were vigorously hand shaken for 30 s followed by resting overnight to allow coarse and high density particles to settle down.

On the following day, before preparing the final batch, both diluted sub-batches were intermediately transferred to two new bottles. To ensure that potentially settled particles were left behind, the lower end of the transfer tube was kept about 2 cm away from the bottom of the bottle. During siphoning, special care was taken to minimise turbulence. 17000 g of the Köstrosol 1530 sub-batch and 3418 g of the Klebosol 30R50 sub-batch were transferred into new bottles. The final bimodal colloidal silica batch (8.8 g/kg) was prepared by adding together 16668 g of diluted Köstrosol 1530 (10 g/kg) and 3334 g of diluted Klebosol 30R50 (2.5 g/kg).

It was decided to use pre-scored 10 mL amber glass ampoules (Nederlandse Ampullenfabriek B.V., Nijmegen, NL) to provide a rugged and gas tight containment for the colloidal silica samples. Ampoules were filled semi-automatically using a Rota ampouling machine R 910 PA (Rota, Wehr, DE). The transfer lines between the bottle containing the bimodal colloidal silica batch and pump were made of Teflon/Tygon, the tubes between the pump and the filling needle were made of silicone. The solution was under constant stirring until about 1200 ampoules were filled. Because of the limited void volume, no stirring could

be applied for the ampoules filled after that. First, the sealed empty ampoules were manually loaded on the feeding belt. The ampoules were then passed automatically into a continuous rotating worm gear at the end of which the ampoules were pushed into a moving star wheel. The wheel passed the ampoules through the following processing steps: preheating of the neck and top of the ampoules, opening the ampoules at the top, flushing the ampoules with Ar gas, filling the ampoules with about 9.2 mL from the final bimodal colloidal silica batch, purging the headspace of the ampoules with Ar gas, preheating the neck of the ampoules, and finally flame sealing the ampoules and removal from the star wheel. In this way, a total of 2061 units were produced.

4 Homogeneity

A key requirement for any reference material (RM) produced as a batch of different units is the equivalence between the various units. In this respect, it is relevant whether the variation between units is significant compared to the uncertainty of the certified value. In contrast to that, it is not relevant if this variation between units is significant compared to the analytical variation. Consequently, ISO Guide 34 requires RM producers to quantify the between-unit variation. This aspect is covered in between-unit homogeneity studies.

The within-unit inhomogeneity does not influence the uncertainty of the certified value when the minimum sample intake is respected, but determines the minimum size of an aliquot that is representative for the whole unit. Quantification of within-unit heterogeneity is therefore necessary to determine the minimum sample intake.

4.1 Between-unit homogeneity

The between-unit homogeneity was evaluated to ensure that the certified values of the CRM are valid for all units of the material, within the stated uncertainty.

The number of selected units corresponds to approximately the cubic root of the total number of the produced units. Therefore 20 units were selected using a random stratified sampling scheme covering the whole batch for the between-unit homogeneity test. For this, the batch was divided into 20 groups (with a similar number of units) and one unit was selected randomly from each group. 15 out of the 20 selected units were actually tested; the 5 remaining units were available as adequate safety margin. From each of the 15 units, two independent sub-samples (aliquots) were taken and analysed in triplicate by means of dynamic light scattering (DLS) following a validated method based on a non-negatively constrained least squares algorithm (NNLS). The ability of the NNLS method to discriminate between two or more particle populations in a given sample lies within the value of the smoothing or regularisation parameter. For the given study, the value of the smoothing parameter was set at 0.01. In addition to the DLS measurements, a limited number of five units was analysed in duplicate by means of line-start centrifugal liquid sedimentation (disc centrifuge). CLS has the advantage over DLS that it has a much higher sensitivity and resolution to detect multiple particle size populations in a given sample. Due to the relatively short stability (about 7 hours) of the CLS sucrose density gradient and the long measurement time (about 40 min) for a single replicate, only 10 aliquots could be analysed under repeatability conditions.

The DLS and CLS measurements were performed under repeatability conditions, and in a randomised manner to be able to separate a potential analytical drift from a potential trend in the filling sequence. Typical intensity-based bimodal particle size distributions (PSD) obtained from the DLS NNLS and the CLS methods are depicted in Fig. 2 and Fig. 3, respectively. An overview of the DLS and CLS results associated to the two individual particle size populations is shown in Annex A.

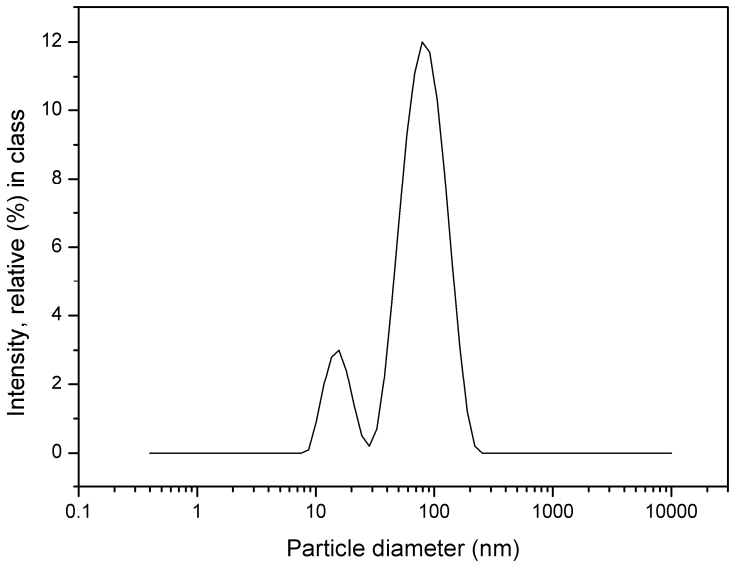

Fig. 2 Transformed density function of an intensity-based PSD for ERM-FD102 determined by means of DLS NNLS

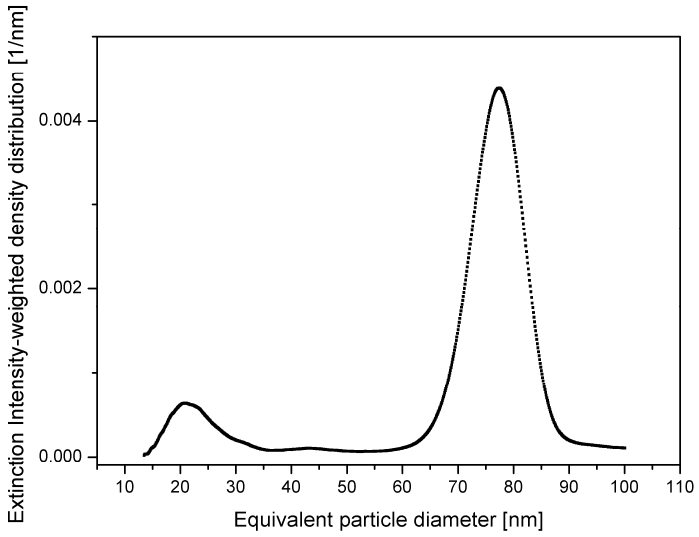

Fig. 3 Intensity-based PSD for ERM-FD102 determined by means of line-start CLS (disc centrifuge)

Regression analyses were performed on the DLS data to evaluate potential trends in the analytical sequence as well as trends in the filling sequence. No trends in the filling sequence or the analytical sequence were visible.

Quantification of between-unit inhomogeneity was accomplished by analysis of variance (ANOVA), which can separate the between-unit variation (s_{bb}) from the within-unit variation (s_{wb}). The latter is equivalent to the method repeatability if the individual samples are representative for the whole unit.

Evaluation by ANOVA requires unit means which follow at least a unimodal distribution and results for each unit that follow unimodal distributions with approximately the same standard deviations. For each size class, the distribution of the unit means was visually tested using histograms and normal probability plots. Since too few data were available for each unit, all individual data were pooled. From the obtained histograms and normal probability plots, it was concluded that all data followed a normal and unimodal distribution. Minor deviations from unimodality of the individual values do not significantly affect the estimate of between-unit standard deviations. Data were checked and scrutinised for single and double outliers by applying the Grubbs' test at a confidence level of 99 %. For both the DLS and CLS results, statistical outliers were neither detected for data grouped according to unit means, nor for data grouped according to individual results.

One has to bear in mind that s_{bb} and s_{wb} are estimates of the true standard deviations and are therefore subject to random fluctuations. Therefore, the mean square between groups ($MS_{between}$) can be smaller than the mean squares within groups (MS_{within}), resulting in negative arguments under the square root used for the estimation of the between-unit variation, whereas the true variation cannot be lower than zero. In this case, u^*_{bb}, the maximum inhomogeneity that could be hidden by method repeatability, was calculated as described by Linsinger *et al.* [29]. u^*_{bb} is comparable to the limit of detection of an analytical method, yielding the maximum inhomogeneity that might be undetected by the given study setup. The larger value of s_{bb} or u^*_{bb} was used as uncertainty contribution for homogeneity, u_{bb}.

Method repeatability ($s_{wb,rel}$), between–unit standard deviation ($s_{bb,rel}$) and $u^*_{bb,rel}$ were calculated in accordance to ISO Guide 35:

$$s_{wb,rel} = \frac{\sqrt{MS_{within}}}{\bar{y}} \qquad \textbf{Equation 1}$$

$$s_{bb,rel} = \frac{\sqrt{\frac{MS_{between} - MS_{within}}{n}}}{\bar{y}} \qquad \textbf{Equation 2}$$

$$u^*_{bb,rel} = \frac{\sqrt{\frac{MS_{within}}{n}}\sqrt[4]{\frac{2}{v_{MSwithin}}}}{\bar{y}} \qquad \textbf{Equation 3}$$

MS_{within}	mean square within a unit from an ANOVA
$MS_{between}$	mean squares between-unit from an ANOVA
$\bar{y}$	mean of all results of the homogeneity study
n	mean number of replicates per unit
$v_{MSwithin}$	degrees of freedom of MS_{within}

The results of the evaluation of the between-unit variation are summarised in Table 2 and Table 3.

Table 2: Results of the homogeneity study for size class A

Particle sizing method	$s_{wb,rel}$ [%]	$s_{bb,rel}$ [%]	$u^*_{bb,rel}$ [%]	$u_{bb,rel}$ [%]
DLS [1)]	3.0	3.2	1.3	3.2
CLS [2)]	2.2	1.0	1.2	1.2

[1)] Scattered light intensity-weighted arithmetic mean hydrodynamic particle diameter by NNLS

[2)] Light extinction intensity-weighted modal Stokes' particle diameter (turbidimetric detection)

Table 3: Results of the homogeneity study for size class B

Particle sizing method	$s_{wb,rel}$ [%]	$s_{bb,rel}$ [%]	$u^*_{bb,rel}$ [%]	$u_{bb,rel}$ [%]
DLS [1)]	1.1	0.6	0.5	0.6
CLS [2)]	0.4	0.4	0.2	0.4

[1)] Scattered light intensity-weighted arithmetic mean hydrodynamic particle diameter by NNLS

[2)] Light extinction intensity-weighted modal Stokes' particle diameter (turbidimetric detection)

The homogeneity study showed no outlying unit means or trends in the filling sequence. Therefore the between-unit standard deviation can be used as estimate of u_{bb}. As u^*_{bb} sets the limits of the study to detect inhomogeneity, the larger value of s_{bb} and u^*_{bb} is adopted as uncertainty contribution to account for potential inhomogeneity.

4.2 Within-unit homogeneity and minimum sample intake

The within-unit homogeneity is closely correlated to the minimum sample intake. The minimum sample intake is the minimum amount of sample that is representative for the whole unit and thus can be used in an analysis. Sample sizes equal or above the minimum sample intake guarantee the certified value within its stated uncertainty.

Characterisation study:

The minimum sample intake was determined from the results of the characterisation study, using the method information supplied by the participants. The smallest sample intake that still yielded results with acceptable accuracy to be included in the respective studies was taken as minimum sample intake. Using the data from Annex D (Tables D.1 to D.6), the following minimum sample intakes are derived:

- AFM: 20 µL of an aliquot as received. One shall measure at least 1000 discrete particles of size class A and at least 300 discrete particles of size class B;
- CLS (turbidimetric detection): 100 µL of an aliquot as received;
- CLS (Rayleigh interference): 330 µL of an aliquot as received;
- DLS: 50 µL of an aliquot as received;

- EM: 2.5 μL of an aliquot as received. One shall measure at least 1000 discrete particles of size class A and at least 300 discrete particles of size class B;
- PTA: 10 μL of an aliquot as received. One shall analyse at least 800 tracks per measurement;
- SAXS: 25 μL of an aliquot as received.

5 Stability

Time and temperature were regarded as the most relevant influences on stability of the material. The influence of visible radiation was minimised by the choice of the containment which eliminates most of the incoming light.

Stability testing is necessary to establish conditions for storage (long-term stability) as well as conditions for dispatch to the customers (short-term stability). During transport, especially in summer time, temperatures up to 60 °C may be reached and stability under these conditions must be demonstrated if transport at ambient temperature will be applied.

The stability studies have been carried out using an isochronous design [30]. In that approach, samples are stored for a certain time at different temperature conditions. Systematically, more samples are moved to conditions where further degradation can be assumed to be negligible (reference conditions), effectively "freezing" the degradation status of the material. At the end of the isochronous storage, the samples are analysed simultaneously under repeatability conditions. Analysis of the material (after various exposure times and temperatures) under repeatability conditions greatly improves the sensitivity of the stability tests.

5.1 Short-term stability study

For the short-term stability study, samples were stored at 4 °C and 60 °C for 0, 1, 2 and 4 weeks (at each temperature). The reference temperature was set to 18 °C. For the storage temperatures 4 °C and 60 °C, four units per storage time point were selected. For the storage temperature of 18 °C, a total of 8 units were taken. All units were selected from the produced batch using a random stratified sampling scheme. From each unit, two aliquots were measured by DLS (NNLS method) and line-start CLS (disc centrifuge). Each DLS aliquot was measured three times in a consecutive manner. Due to the high number of units and the relatively long CLS measurement time, measurements could not be performed under strict repeatability conditions. Instead, measurements were equally spread over four different days and performed in a randomised manner to be able to separate a potential analytical drift from a trend over storage time.

The sets of results obtained from the four measurement days were first analysed by one-way ANOVA to identify potential day-to-day differences. At a 5 % significance level none of the sets showed to be different. The particle size results obtained by CLS revealed a clear systematic trend throughout each measurement day: the modal values decreased slightly towards the end of the day. Possible reasons were the increase of temperature in the laboratory and/or the degradation of the sucrose density gradient. The within-day variations for size class A and size class B of the CLS PSDs were within the 3.4 % and 0.6 % measurement uncertainties, respectively. No analytical drift was observed within the DLS sets of results.

After having corrected the CLS results for the analytical drift, data were pooled together according to the storage temperatures 4 °C and 60 °C. The new sets of results were then evaluated individually for each temperature. The results were screened for outliers using the single and double Grubbs' tests on 99 % confidence levels. No outlying individual results were found (Table 4). The individual DLS and CLS measurement results are shown in Fig. B1 and Fig. B2 of Annex B.

Furthermore, the data were plotted against storage time, and regression lines of particle diameter *versus* time were calculated. The slopes of the regression lines were then tested for statistical significance (loss/increase due to shipping conditions). For both CLS and DLS sets

of results and a 60 °C storage temperature, slopes of the regression lines corresponding to the size class B of the PSD were found to be significantly different from zero. During the production of similar, but monodisperse, colloidal silica CRM, ERM-FD100, slopes of the regression lines were also found to be significant at a confidence level of 99 % [31].

Table 4: Results of the short-term stability tests

Particle sizing method	**Number of individual outlying results**				**Significance of the trend on a 99% confidence level**			
	4 °C		**60 °C**		**4 °C**		**60 °C**	
	Size class A	**Size class B**	**Size class A**	**Size class B**	**Size class A**	**Size class B**	**Size class A**	**Size class B**
DLS [1)]	None	None	None	None	No	No	No	Yes
CLS [2)]	None	None	None	None	No	No	No	Yes

[1)] Scattered light intensity-weighted arithmetic mean hydrodynamic particle diameter by NNLS

[2)] Light extinction intensity-weighted modal Stokes' particle diameter (turbidimetric detection)

When stored at a temperature of 60 °C, the slopes of the regression lines (size class B) were significantly different from zero (at 99 % confidence level). These trends, which correspond to an increase of the measured particle size with about 1 nm, mainly stem from the fourth week at 60 °C. To better investigate the possible instability of the material when subjected to elevated temperatures, four units (# 118, # 681, # 1417 and # 1947) were randomly selected across the produced batch and kept at 60 °C for three months. The particle size results (Fig. B3 of Annex B), which were measured by DLS (NNLS method) and line-start CLS (disc centrifuge), agree with the certified values. In practice, the possibility that samples during dispatch are exposed at 60 °C for four weeks is rather unlikely; instead, a dispatch period of one week is more realistic. At these conditions, the corresponding slopes were found not to be significantly different from zero.

During the production of a similar, but monomodal, colloidal silica CRM, ERM-FD304 [32], it was observed that freezing of the suspension significantly affected the particle size distribution measured after thawing. Therefore, ERM-FD102 must be protected against freezing temperatures.

Supported by the additional experimental data and taking into account a dispatch period of one week, it can be concluded that the material can be safely shipped under ambient conditions. Hence, cooled transportation is not required.

5.2 Long-term stability study

For the long-term stability study, samples were stored at 18 °C for 0, 4, 8 and 12 months. The reference temperature was set to 4 °C. A total of 24 units per storage time were selected using a random stratified sampling scheme. From each unit, two aliquots were measured by DLS (NNLS method) and line-start CLS (disc centrifuge). Each DLS aliquot was measured three times in a consecutive manner. Due to the high number of units and the relatively long CLS measurement time, measurements could not be performed under strict repeatability conditions. Instead, measurements were equally spread over three different days and performed in a randomised manner to be able to separate a potential analytical drift from a trend over storage time.

The sets of results obtained from the three measurement days were first analysed by one-way ANOVA to identify potential day-to-day differences. At a 5 % significance level none of the sets showed to be different. The particle size results obtained by CLS revealed a clear systematic trend throughout each measurement day: the modal values decreased slightly towards the end of the day. Possible reasons were the increase of temperature in the laboratory and/or the degradation of the sucrose density gradient. The within-day variations for size class A and size class B of the CLS PSDs were within the 3.4 % and 0.6 % measurement uncertainties, respectively. No analytical drift was observed within the DLS sets of results.

After having corrected the CLS results for the analytical drift, data were pooled together according to the storage temperature of 18 °C. The new sets of results were then screened for outliers using the single and double Grubbs' test. No outlying individual results were found. The results of the long-term stability measurements are shown in Annex C. The results of the statistical evaluation of the long-term stability study are summarised in Table 5.

Furthermore, the data were plotted against storage time and linear regression lines of particle diameter *versus* time were calculated. The slope of the regression lines was tested for statistical significance (loss/increase due to storage conditions). For both CLS and DLS sets of results, the slopes of the regression lines were not significantly different from zero (on a 99 % confidence level) for 18 °C.

Table 5: Results of the long-term stability tests

Particle sizing method	**Number of individual outlying results**		**Significance of the trend on a 99 % confidence level**	
	Size class A	**Size class B**	**Size class A**	**Size class B**
DLS [1)]	None	None	No	No
CLS [2)]	None	None	No	No

[1)] Scattered light intensity-weighted arithmetic mean hydrodynamic particle diameter by NNLS

[2)] Light extinction intensity-weighted modal Stokes' particle diameter (turbidimetric detection)

No technically unexplained outliers were observed and none of the trends was statistically significant on a 99 % confidence level for any of the temperatures. The material can therefore be stored at 18 °C.

5.3 Estimation of uncertainties

Due to the intrinsic variation of measurement results, no study can rule out degradation of materials completely, even in the absence of statistically significant trends. It is therefore necessary to quantify the potential degradation that could be hidden by the method repeatability, i.e. to estimate the uncertainty of stability. This means, even under ideal conditions, the outcome of a stability study can only be "degradation is 0 ± x % per given unit of time".

Uncertainties of stability during dispatch and storage were estimated as described in [33] for each measurand. For this approach, the uncertainty of the linear regression line with a slope of zero is calculated. The uncertainty contributions $u_{sts,rel}$ and $u_{lts,rel}$ are calculated as the product of the chosen transport time/shelf life and the uncertainty of the regression lines as:

$$u_{sts,rel} = \frac{RSD}{\sqrt{\sum (t_i - \bar{t})^2}} \cdot t_{tt}$$ **Equation 4**

$$u_{lts,rel} = \frac{RSD}{\sqrt{\sum (t_i - \bar{t})^2}} \cdot t_{sl}$$ **Equation 5**

RSD	relative standard deviation of all results of the stability study
t_i	time elapsed at time point *i*
$\bar{t}$	mean of all t_i
t_{tt}	chosen transport time (1 week at 60 ºC)
t_{sl}	chosen shelf life (24 months at 18 ºC)

The following uncertainties were estimated:

- u_{sts}, the uncertainty of degradation during dispatch. This was estimated from the 60 °C studies. The uncertainty describes the possible change during a dispatch at 60 °C lasting for one week, which can be considered to be a realistic transport time.
- u_{lts}, the stability during storage. This uncertainty contribution was estimated from the 18 °C study. The uncertainty contribution describes the possible degradation during 24 months storage at 18 °C.

The results of these evaluations are summarised in Table 6.

Table 6: Uncertainties of stability during dispatch and storage. $u_{sts,rel}$ was calculated for a temperature of 60 °C and one week; $u_{lts,rel}$ was calculated for a storage temperature of 18 °C and two years

Particle sizing method	$u_{sts,rel}$ **[%]**		$u_{lts,rel}$ **[%]**	
	Size class A	**Size class B**	**Size class A**	**Size class B**
DLS [1)]	0.4	0.2	2.6	0.8
CLS [2)]	0.1	< 0.1	1.1	0.1

[1)] Scattered light intensity-weighted arithmetic mean hydrodynamic particle diameter by NNLS

[2)] Light extinction intensity-weighted modal Stokes' particle diameter (turbidimetric detection)

After the certification campaign, the released CRM will be subjected to IRMM's regular stability monitoring programme to control and evidence its further stability.

5.4 Effect of ultrasound

In the frame of *in vitro* toxicity testing, nanomaterial test suspensions may require exposure to ultrasound (sonication). The ultrasonic energy causes cavitation bubbles which on their turn have the potential to break agglomerates or clusters of particles.

Two randomly chosen units (# 471 and # 1774) of ERM-FD102 were exposed to modest sonication energies using a 3510E-MTH Bransonic® sonication bath (Branson Ultrasonic Corp., Danbury, CT, US). The power and frequency of the bath sonicator were 100 W and 42 kHz, respectively. The sonication time varied from 1 min to 10 min. The effect of sonication energy on the material's PSD was investigated by means of line-start CLS (disc centrifuge) and DLS NNLS. Each unit was tested in duplicate under repeatability conditions. The mean results and their associated expanded measurement uncertainties (k = 2) for repeatability are summarised in Fig. 4. For the applied sonication conditions, measurable differences were not observed between the as-received suspension and suspensions that were subjected to ultrasound.

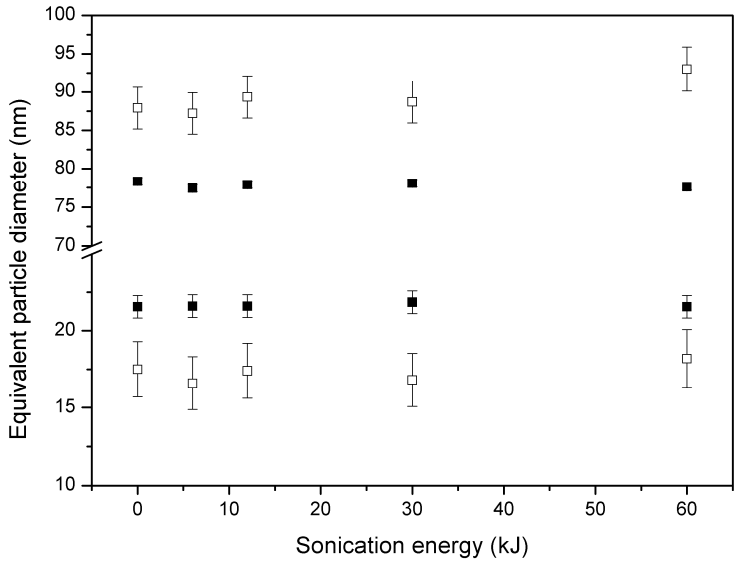

Fig. 4 Sonication energy *vs*. equivalent particle diameter of ERM-FD102 as measured by DLS NNLS and CLS; DLS scattered light intensity-weighted arithmetic mean particle diameter (open squares), CLS light extinction intensity-weighted modal Stokes' particle diameter (solid squares), error bars correspond to the relative expanded (k = 2) measurement uncertainties for method repeatability; CLS measurement uncertainties for results of size class A are only about 0.5 nm and error bars are therefore not visible in the graph.

6 Characterisation

The material characterisation is the process of determining the property values of a reference material.

The material characterisation was based on a series of intercomparisons of expert laboratories, i.e. the physical properties, being different method-defined equivalent particle diameters, of the material were determined in different laboratories that applied fundamentally different measurement procedures. Within each method-defined measurand group, all ILC participants applied the same method. Crucial in this characterisation approach is, however, that the measurements must be performed under intermediate precision and reproducibility conditions and that the results from different laboratories are independent.

6.1 Selection of participants

31 laboratories were selected based on criteria that comprised both technical competence and quality management aspects. Each participant was required to operate a quality system and to deliver documented evidence of its laboratory proficiency in the field of size analysis of nanoparticles. Having a formal accreditation was not mandatory, but meeting the requirements of ISO/IEC 17025 [3] was obligatory. Where measurements are covered by the scope of accreditation, the corresponding accreditation number is stated in the list of participants (Section 2).

6.2 Study setup

Each laboratory received three units of the candidate CRM together with a detailed measurement protocol. This protocol included a description of the measurement scheme as well as guidelines for sample handling and relevant measurement method parameters. The involved SAXS, EM, CLS and AFM laboratories were requested to provide six independent results (two replicates per unit). The participating DLS and PTA laboratories were requested to provide nine independent results (three replicates/aliquots per unit) and each aliquot had to be consecutively measured three and five times, respectively. The units for material characterisation were selected using a random stratified sampling scheme and covered the whole batch. The sample preparations and measurements had to be spread over at least three different days to ensure intermediate precision conditions.

Blinded CRMs and non-certified RMs were sent as quality control (QC) samples along with the candidate CRMs to allow independent assessment of method trueness. Because EM methods are not typically calibrated on a daily basis, an additional polystyrene latex QC sample was provided in order to verify the appropriateness of calibration. The following quality control samples were used:

- ERM-FD100 (colloidal silica, IRMM) for SAXS and EM methods;
- ERM-FD304 (colloidal silica, IRMM) for DLS and CLS (disc and cuvette) methods with turbidity optics;
- Nanosphere Size Standard 3080A (polystyrene latex, Thermo Scientific) for PTA, AFM and CLS (cuvette) methods with Rayleigh interference optics;

- Nanosphere Size Standard 3100A (polystyrene latex, Thermo Scientific) for EM methods.

The results of the QC samples were used to support the evaluation of the characterisation results, i.e. to ensure reliability of the results obtained on the candidate CRM.

Laboratories were also requested to give realistic estimations of the expanded uncertainties of the mean value of the replicate results. No approach for the estimation was prescribed, i.e. top-down and bottom-up were regarded as equally valid procedures.

6.3 Methods used

6.3.1 Atomic force microscopy

ERM-FD102 was characterised by means of conventional AFM instruments operated in closed-loop control. The as-received material was first diluted in ultrapure water after which a small volume of the diluted suspension was transferred to a flat substrate (e.g., silicon wafer, mica). After incubation, rinsing and drying, the deposited nanoparticles remained attached onto the substrate mainly through electrostatic and van der Waals forces. Because of the relatively weak nature of these physical forces images were recorded in the amplitude modulation ("tapping") mode. By raster-scanning the sample surface with an AFM probe consisting of a silicon cantilever and tip, 3D topographic images were generated. These images were then processed (e.g., flatness tilt, levelling and removal of image artefacts) and analysed using commercially available software packages. For each test specimen (replicate), at least 1000 discrete particles of size class A and at least 300 discrete particles of size class B were automatically detected and their maximum height (with reference to the substrate) was individually measured and depicted in a number-based PSD. For each test specimen the detected and measured particles originated from at least two different randomly (but widely separated) selected scan areas. The height responses of the AFM instruments were SI traceably calibrated using different step-height transfer standards that were characterised and calibrated in a metrologically accepted manner.

An overview of the instrument specifications and measurement conditions is given in Table D.1 of Annex D. The laboratory code (e.g., L15) is a random number and does not correspond to the order of laboratories listed in Section 2. The information in this annex is presented as reported by the ILC participants.

6.3.2 Centrifugal liquid sedimentation

ERM-FD102 was characterised by means of CLS. The group of CLS instruments can be generally classified according to the type of detection system (i.e. turbidity and Rayleigh interference optics) and according to their geometry (i.e. disc and cuvette type). Furthermore, instruments can be operated either in the line-start mode or in the so-called homogeneous mode. Turbidity and Rayleigh interference optics target distinctly different measurands: the former directly determines the light extinction intensity-based Stokes' PSD whereas the latter directly arrives at the mass-based Stokes' PSD. All laboratories analysed ERM-FD102 as-received and applied the general guidelines as stipulated in documentary standards ISO 13318-1 [9] and ISO 13318-2 [10]. These documentary standards include both the line-start and homogeneous CLS methods.

The effective particle density of the test material (ERM-FD102), and of the calibrant (if applicable), directly affects the value of the particle size. Hence, to eliminate potential systematic errors the effective density of the suspended silica nanoparticles has to be accurately known. During previous studies, the effective density of the silica nanoparticles of both starting materials (Köstrosol 1530 and Klebosol 30R50) was *in situ* determined by means of a "zero velocity" and a "two velocity" sedimentation approach. The former method is also referred to as isopycnic sedimentation. The resulting effective particle densities were found to be 2.0 g/cm^3 ± 0.1 g/cm^3 [34].

An overview of the instrument specifications and measurement conditions is given in Table D.2 of Annex D. The laboratory code (e.g., L1) is a random number and does not correspond to the order of laboratories listed in Section 2. The information in this annex is presented as reported by the ILC participants.

6.3.3 Dynamic light scattering

The characterisation of ERM-FD102 by DLS was performed in terms of the intensity-weighted particle diameter of a transformed density function [35], as obtained by a suitable PSD data evaluation algorithm. Datasets were grouped according to the kind of mean (e.g., arithmetic, harmonic, geometric) [36]. The majority of the laboratories reported arithmetic mean values. Measurements on the monomodal colloidal silica QC sample (ERM-FD304) had to be performed using the cumulants method. All measurements were performed on the as-received material. The measurement protocol recommended the use of optical-quality glass (e.g., quartz) cuvettes, disposable plastic cuvettes were however acceptable too. Furthermore, the protocol required measurements to be performed at 25 °C ± 0.3 °C, an equilibration time of 300 s, a viscosity (at 25 °C） of the dispersing medium of 0.8872 mPa.s and a refractive index (at 25 °C) of the dispersing medium of 1.330. From each ampoule, three aliquots had to be taken and each aliquot had to be measured at least three times under repeatability conditions. Although the use of PSD data evaluation algorithms is not covered by documentary standards ISO 13321 [16] and ISO 22412 [17], laboratories were nevertheless asked to perform sample handling, preparation and measurements as much as possible according to these standards.

An overview of the instrument specifications and measurement conditions is given in Table D.3 of Annex D. The laboratory code consists of a number assigned to each laboratory (e.g., L2) and abbreviation of the data analysis algorithm used (e.g., NNLS, CONTIN, Dynals). The assigned number does not correspond to the order of laboratories listed in Section 2. The information in this annex is presented as reported by the ILC participants.

6.3.4 Electron microscopy

Scanning and transmission electron microscopes were used to characterise ERM-FD102 in terms of area-equivalent diameters. For the obtained number-based PSDs, the modal and median values of both peaks were determined. Due to the much lower number of particles belonging to size class B, the majority of the participants diluted the as-received material in ultrapure water and performed measurements at different magnifications. To minimise the risk of contamination during the preparation of EM test specimens, participants were recommended to prepare the test specimens in a clean room or in a low contamination environment and to analyse the acquired micrographs according to documentary standard ISO 13322-1 [22]. For each prepared test specimen, at least 1000 discrete (i.e. non-

touching) particles of size class A and at least 300 discrete particles of size class B had to be measured.

An overview of the instrument specifications and measurement conditions is given in Table D.4 of Annex D. The laboratory code consists of a random number assigned to each laboratory (e.g., L8) and abbreviation of the type of EM instrument used (e.g., SEM, TEM). The assigned number does not correspond to the order of laboratories listed in Section 2. The information in this annex is presented as reported by the ILC participants.

6.3.5 Particle tracking analysis

For the characterisation of ERM-FD102 by means of PTA, laboratories were asked to dilute the as-received material using ultrapure water (resistivity of 18.2 MΩ.cm at 25 °C and additionally filtered through a membrane with nominal pore size of 0.1 μm) depending on the optical specifications of their instruments. At the given particle concentration of the undiluted suspension, the intensity levels of the scattered light are too high and this causes that individual particles cannot easily be resolved. As a rule of thumb, test samples should contain between 10^7 and 10^9 particles/mL. In order to allow determination of the particle concentration, sample loading (and dilution) had to be performed by using accurately calibrated micropipettes and/or syringes. Additional measurement conditions that were fixed in the test protocol were: measurement temperature (25 °C ± 0.5 °C), equilibration time between measurements (30 s), viscosity (0.8872 mPa.s at 25 °C) and refractive index (1.330 at 25 °C) of the dispersion liquid. The mode, mean and median values of the number-based PSDs had to be reported, as well as the determined particle concentration.

An overview of the instrument specifications and measurement conditions is given in Table D.5 of Annex D. The laboratory code (e.g., L6) is a random number and does not correspond to the order of laboratories listed in Section 2. The information in this annex is presented as reported by the ILC participants.

6.3.6 Small-angle X-ray scattering

ERM-FD102 was additionally characterised by means of SAXS. Measurements were performed on the as-received material. The experimental scattering curves were corrected for background noise and deconvoluted (beam-length profile). Following Guinier approximation, the initial parts (at low *q*-ranges) of the scattering curves were approached with linear regression fits from which the volume-weighted Guinier radii (R_g) were deduced. These results were then converted into the mean equivalent spherical diameter (D) following Equation 6.

$$D = 2\sqrt{\frac{5}{3}}R_g \qquad \textbf{Equation 6}$$

In addition, volume- and intensity-based PSDs were determined by applying the indirect Fourier transformation method.

An overview of the instrument specifications and measurement conditions is given in Table D.6 of Annex D. The laboratory code (e.g., L13) is a random number and does not correspond to the order of laboratories listed in Section 2. The information in this annex is presented as reported by the ILC participants.

6.4 Evaluation of results

The characterisation campaign resulted in a total of 70 independent datasets of which 2 for AFM, 10 for CLS (turbidity), 2 for CLS (Rayleigh interference optics), 26 for DLS, 20 for EM, 9 for PTA and 1 for SAXS. All individual results of the participants, grouped per technique/method/measurand are displayed in tabular and graphical form in Annex E.

6.4.1 Technical evaluation

The obtained data were first checked for compliance with the requested measurement protocol and for their validity based on technical criteria. The following criteria were considered during the evaluation:

- appropriate validation of the measurement procedure;
- compliance with the provided measurement protocol: sample preparations and measurements performed on three days;
- method performance, i.e. agreement of the measurement results with the assigned value of the QC sample following the procedure described in ERM Application Note 1 [37].

Based on the above criteria, the following datasets were rejected as not technically valid (Table 7)

Table 7: Datasets that showed non-compliances with the analysis protocol and technical specifications, and action taken

Particle sizing method	Lab-method code	Description of problem	Action taken
EM	L1a	Results for QC sample ERM-FD304 15 % below certified value Results originate from a different measurand	Data not used for evaluation
EM	L1b	Results for QC sample ERM-FD304 about 20 % above certified value Results originate from a different measurand	Data not used for evaluation
DLS	L2	Results for QC sample ERM-FD304 about 20 % below certified value	Data not used for evaluation

CLS (disc, turbidimetry)	L4	Results for QC sample ERM-FD304 about 50 % above certified value	Data not used for evaluation
CLS (cuvette, turbidimetry)	L18	Results for QC sample ERM-FD304 about 20 % below assigned value	Data not used for evaluation
EM	L27	Less than 300 particles of size class B were measured	Data not used for evaluation

Atomic force microscopy

Two laboratories participated with AFM to the characterisation study and submitted one dataset each. The provided measurement protocol did not outline the specimen preparation (deposition) procedures. Hence each participant followed their own in-house established nanoparticle deposition procedure. Only non-touching particles that were detected as single particles (i.e. non agglomerates) were retained and their maximum height was measured (Fig. 5). The obtained results were plotted in number-based maximum height PSDs, from which the modal values were reported.

The results of the technical evaluation of the AFM datasets are summarised in Table 8 and Annex E1.

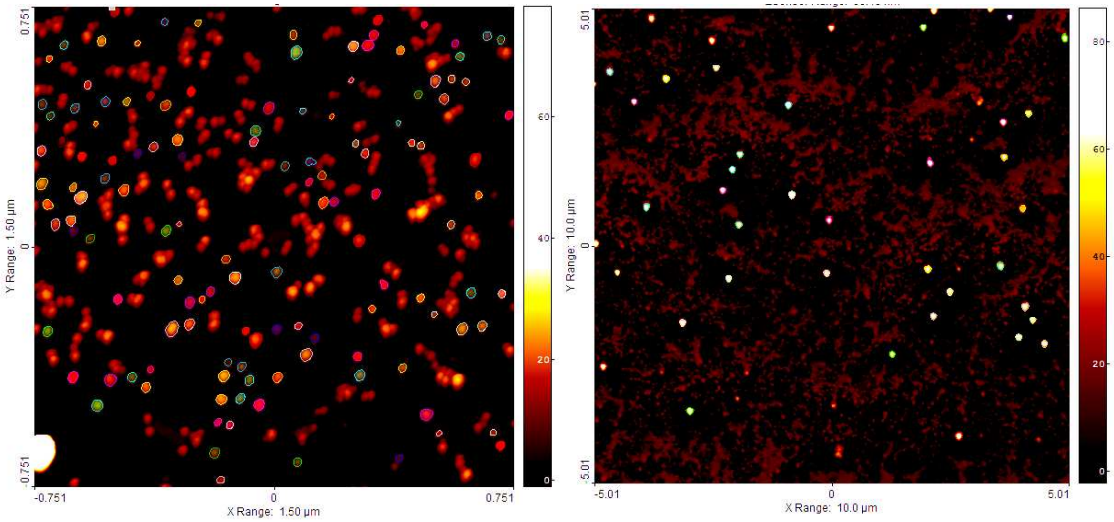

Fig. 5 Topography AFM images of silica nanoparticles deposited onto silicon substrate, non-touching particles belonging to size class A (left) and size class B (right) were automatically detected (coloured) and measured for their maximum height

Table 8: Summary of the technical evaluation of the received AFM datasets

Lab-code	Protocol followed?	Result QC sample	u_{rel} [%] [1)] of modal value		Uncertainty contributions
			Size class A	Size class B	
L15	Yes	OK	12.0	12.0	Repeatability, intermediate precision, calibration and deformation bias
L25	Yes	OK	1.6	1.5	Repeatability, intermediate precision and trueness

[1)] Relative standard measurement uncertainty (confidence level of 68 %) as reported by the participant

Centrifugal liquid sedimentation

Twelve laboratories were involved in the CLS ILC study. Four out of the 12 laboratories participated with homogeneous CLS (ultracentrifugation or cuvette) methods whereas the other eight laboratories all applied line-start CLS (disc centrifugation) methods with turbidity detection optics. The former CLS group is further split into two laboratories that used AUC with Rayleigh interference optics and two laboratories that performed measurements using benchtop ultracentrifuges equipped with turbidity optics. Because of the different measurands, datasets originating from CLS instruments with turbidity-based detection systems and CLS instruments equipped with Rayleigh interference optics (L5 and L11), were evaluated separately.

The results of the technical evaluation of the CLS datasets are summarised in Table 9 and Annex E2.

Table 9: Summary of the technical evaluation of the received CLS datasets

Lab-code	Protocol followed?	Result QC sample	u_{rel} [%] [1)] of modal value		Uncertainty contributions
			Size class A	Size class B	
L1	Yes	OK	14.4	3.9	Precision and trueness
L3	Yes	OK	8.0	8.0	Precision, trueness, calibration and effective density
L4	Yes	Not OK	1.0	1.0	Reproducibility
L5	Yes	OK	0.4	1.8	Intermediate precision, trueness and calibration
L7	Yes	OK	5.5	5.5	Calibration, instrument operation and handling
L10	Yes	OK	6.1	7.2	Intermediate precision and trueness

L11	Yes	OK	1.8	1.8	Trueness
L14	Yes	OK	8.5	7.6	Trueness
L15	Yes	OK	6.0	6.0	Repeatability, intermediate precision and trueness
L18	Yes	Not OK	5.0	5.0	ILC and repeatability
L19	Yes	OK	5.0	5.0	ILC and repeatability
L25	Yes	OK	3.9	3.6	Repeatability, intermediate precision and trueness

[1)] Relative standard measurement uncertainty (confidence level of 68 %) as reported by the participant

Dynamic light scattering

Nineteen laboratories were involved in the DLS ILC study of which one failed to submit a dataset. Two of the remaining 18 laboratories performed the analyses using two DLS instruments which differed with respect to the optical system. In addition, several laboratories provided multiple datasets for different measurands (e.g., mode, harmonic mean, arithmetic mean and geometric mean). A total of 26 datasets were received and analysed. All laboratories used commercially available equipment, i.e. customised DLS setups were not included in the study. The participants' DLS instruments were either applying the conventional correlation function analysis (homodyne) principle or the 3D cross-correlation (heterodyne) principle. For both particle populations, unpaired two-tailed Students' *t*-tests showed no significant differences ($P < 0.05$) between the mean values of the two instrument groups. Following the same statistical evaluation approach, no significant differences were observed between instruments that collect the scattered light at an angle of 90° and 173° and between samples measured in quartz and disposable plastic cuvettes.

The results of the technical evaluation of the DLS datasets are summarised in Table 10 and Annex E3.

Table 10: Summary of the technical evaluation of the received DLS datasets

Lab-code	**Protocol followed?**	**Result QC sample**	**u_{rel} [%] [1)] of arithmetic mean value**		**Uncertainty contributions**
			Size class A	**Size class B**	
L2	Yes	Not OK	8.0	n.d.	Control chart
L3	Yes	OK	4.5	2.1	Repeatability, intermediate precision and trueness
L7	Yes	OK	4.5	4.5	Device-related, temperature and sample handling
L8	Yes	OK	6.5	2.7	Repeatability, reproducibility and trueness
L10	Yes	OK	0.9	0.9	NIST nanosphere size

					standard of nominal 50 nm
L15	Yes	OK	16.0	10.0	Repeatability, intermediate precision and trueness
L16	Yes	OK	4.4	2.9	All parameters of Stokes-Einstein equation
L17a	Yes	OK	11.9	3.8	Mixture of two polystyrene latex standards
L17b	Yes	OK	12.4	3.8	Mixture of two polystyrene latex standards
L20	Yes	OK	11.8	3.8	Mixture of two polystyrene latex standards
L21a	Yes	OK	6.7	5.4	Repeatability and intermediate precision
L22	Yes	OK	1.0	4.0	All parameters of Stokes-Einstein equation
L23	Yes	OK	3.1	1.1	Intermediate precision
L24	Yes	OK	3.8	3.8	Repeatability, intermediate precision and trueness
L25	Yes	OK	8.0	4.2	Repeatability, intermediate precision and trueness
L26	Yes	OK	4.0	4.0	Intermediate precision
L29	Yes	OK	2.5	1.9	Intermediate precision
L30	Yes	OK	2.0	2.0	Expert judgement

n.d. = not detectable, amount of scattered light below method's limit of detection

[1)] Relative standard measurement uncertainty (confidence level of 68 %) as reported by the participant

Electron microscopy

Nine laboratories participated in the ILC study with SEM and TEM methods. A total of 11 datasets were received. Two participants performed measurements using both SEM and TEM. An unpaired two-tailed Students' *t*-test showed no significant difference ($P < 0.05$) between the mean values of the two instrument groups. The results of the technical evaluation of the EM datasets are summarised in Table 11 and Annex E4. Representative examples of SEM and TEM micrographs are shown in Fig. 6 and Fig. 7, respectively.

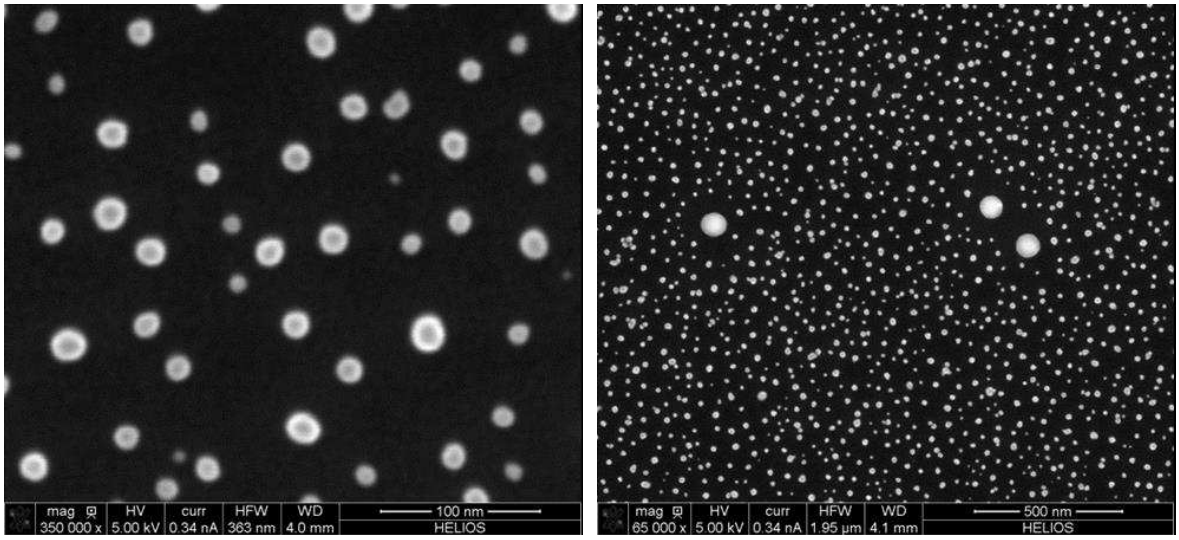

Fig. 6 Representative SEM micrographs of ERM-FD102 with nanoparticles belonging to size class A (left) and a mixture of nanoparticles belonging to size class A and B (right) deposited onto silicon substrate

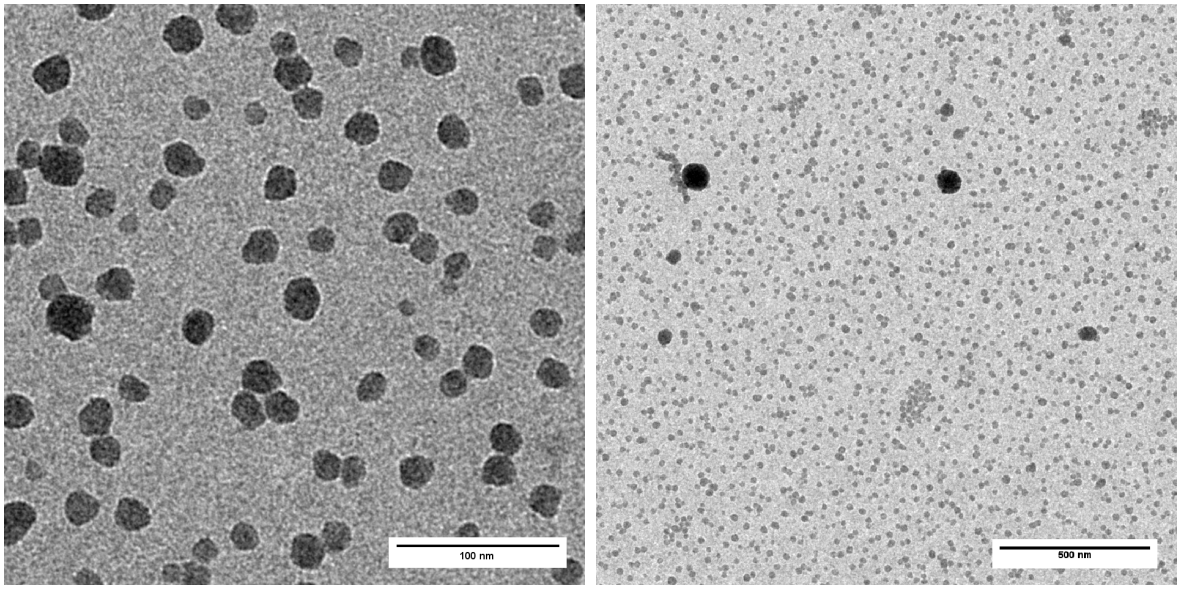

Fig. 7 Representative TEM micrographs of ERM-FD102 with nanoparticles belonging to size class A (left) and a mixture of nanoparticles belonging to size class A and B (right) deposited onto an electron-transparent substrate

Table 11: Summary of the technical evaluation of the received EM datasets

Lab-code	Protocol followed?	Result QC sample	u_{rel} [%] [1] of modal value		u_{rel} [%] [1] of median value		Uncertainty contributions
			Size class A	Size class B	Size class A	Size class B	
L1a	Yes	Not OK	5.0	5.0	5.0	5.0	ILC and expert judgement
L1b	Yes	Not OK	5.0	5.0	5.0	5.0	ILC and expert judgement
L8	Yes	OK	8.4	1.9	8.4	1.9	Repeatability, reproducibility, threshold correction and background, particle boundary determination, calibration and image drift
L9	Yes	OK	2.7	2.4	3.1	2.4	Repeatability, intermediate precision, calibration and trueness
L10	Yes	OK	3.0	3.0	3.0	3.0	Standard error and trueness
L11a	Yes	OK	3.0	3.0	3.0	3.0	Trueness
L11b	Yes	OK	3.0	3.0	3.0	3.0	Trueness
L16	Yes	OK	9.4	2.4	9.4	2.4	Repeatability, calibration, threshold, stage drift and spot size
L24	Yes	OK	4.0	4.0	4.0	4.0	Repeatability, intermediate precision and trueness
L25	Yes	OK	8.0	8.0	6.0	6.0	Repeatability, intermediate precision and trueness
L27	Yes	OK	3.5	3.5	3.5	3.5	Repeatability, number of particles, calibration and magnification

[1] Relative standard measurement uncertainty (confidence level of 68 %) as reported by the participant

Particle tracking analysis

Three laboratories characterised ERM-FD102 using PTA and submitted one dataset each. In contrast to the AFM, DLS, CLS and EM methods, the PTA methods were not able to detect both particle populations, only the nanoparticles belonging to size class B appeared in the number-based PSDs (Fig. 8). From these results, it can be concluded that the amount of light scattered by nanoparticles of size class A is insufficient to be detected. As can be seen from the representative example in Fig. 8, the PSD exhibits a shoulder towards lower particle sizes. This indicates the presence of an additional particle population with diameters in the range of about 40 nm to 50 nm. The presence of such minor third mode was also observed and indicated by several other laboratories applying EM, SAXS and CLS methods.

The results of the technical evaluation of the PTA datasets are summarised in Table 12 and Annex E5.

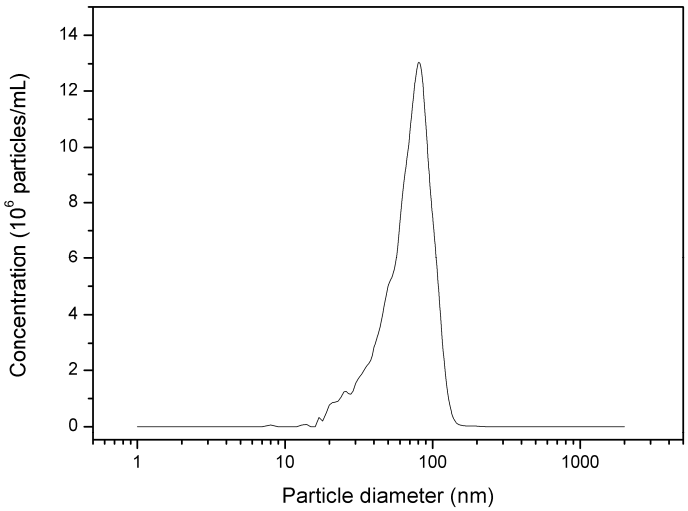

Fig. 8 Representative PTA number-based PSD

Table 12: Summary of the technical evaluation of the received PTA datasets

Lab-code	Protocol followed?	Result QC sample	u_{rel} [%] [1)]			Uncertainty contributions
			Mode	Mean	Median	
L6	Yes	OK	1.7	2.5	1.4	Intermediate precision and repeatability
L12	Yes	OK	3.5	5.7	2.9	Intermediate precision, repeatability and trueness
L16	Yes	OK	2.7	2.7	2.7	Repeatability and trueness

[1)] Relative standard measurement uncertainty (confidence level of 68 %) as reported by the participant

In addition to particle size measurements, the PTA method can also determine the absolute particle concentration by counting particles in a well-defined volume. The *RSD* calculated from the laboratory mean particle concentration results was about 50 %. Therefore, the results were considered to be insufficiently reliable and hence excluded from the study.

Small-angle X-ray scattering

Two laboratories signed up for the SAXS ILC study, but only one laboratory submitted one dataset. Test samples were analysed as-received and the experimental scattering curves were evaluated following the Guinier method and the indirect Fourier transformation method.

Laboratory 13 performed all measurements according to the provided measurement scheme and protocol and successfully analysed the monomodal colloidal silica QC sample (ERM-FD100). The obtained QC result (mean of two replicate results) of 22.0 nm ± 0.9 nm (two times standard deviation) agreed with the certified value (21.8 nm ± 0.7 nm) of the QC sample.

The laboratory reported results obtained from the Guinier as well as from the indirect Fourier transformation methods. For the Guinier method, at low *q*-range the scattering curve showed two linear regimes that are originating from two particle populations. Both regimes (0.05/nm to 0.09/nm and 0.09/nm to 0.11/nm) were fitted independently. Fitting of the regime at higher *q*-range resulted in a model independent volume-weighted mean R_g of 8.7 nm ± 2.9 nm (two times standard deviation) and a corresponding equivalent diameter (*D*) of 22.6 nm ± 7.2 nm (two times standard deviation). The volume-weighted mean R_g and *D* associated to the second regime were 19.8 nm ± 0.2 nm (two times standard deviation) and 51.2 nm ± 2.2 nm (two times standard deviation), respectively. The theoretical upper limit of detection for this method was reported to be approximately 70 nm in diameter.

The volume-based PSD obtained via indirect Fourier transformation showed four resolved peaks, one main peak with a particle diameter mode of about 20 nm and three smaller peaks with particle diameter modes of approximately 7 nm, 40 nm and 80 nm. The laboratory indicated that the peak with mode of 7 nm is rather a matter of speculation as this might reflect the presence of particles or pores within larger particles. The peak representing the 40 nm particles fairly agrees with the one of 51.2 nm found via the Guinier method. The last mode agrees with the particles of size class B that were mixed into ERM-FD102. The converted intensity-based PSD (Fig. 9) shows two distinct particle populations with equivalent radii of about 10 nm and 40 nm. The shoulder visible in the PSD represents the third minor mode which was also observed by several EM, CLS and PTA laboratories.

The indirect Fourier transformation evaluates the whole scattering curve to determine the PSD. The contribution of the nominally 80 nm particles (size class B) is not only limited to the Guinier regime, but it also influences its progression at higher *q*-ranges. According to the laboratory that performed the analyses, the indirect Fourier transformation method could detect the nanoparticles that are belonging to size class B, despite the theoretical upper detection limit.

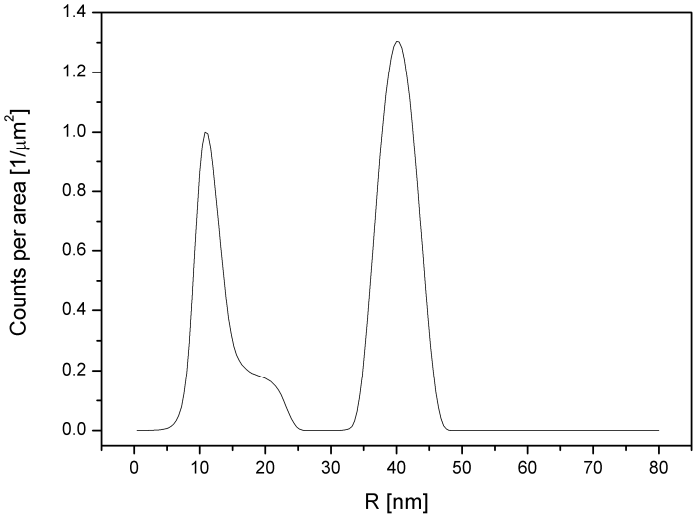

Fig. 9 Intensity-based PSD obtained by SAXS (indirect Fourier transformation)

6.4.2 Statistical evaluation

The DLS, CLS (turbidimetric detection) and EM datasets that were accepted on the basis of technical criteria, and used for certification, were statistically evaluated. This evaluation included testing for the normality of dataset means using kurtosis/skewness tests as well as normal probability plots, and testing for outlying means and standard deviations (both at 99 % confidence level) using the Grubbs' and Cochran tests, respectively. Standard deviations within (s_{within}) and between ($s_{between}$) laboratories were calculated using one-way ANOVA. The results of these evaluations are shown in Table 13 and Table 14. The technically accepted AFM, CLS (Rayleigh interference), PTA and SAXS datasets were not evaluated for their normality and outlying means and standard deviations because of the limited number of datasets available.

Table 13: Statistical evaluation of the technically accepted datasets for ERM-FD102 (size class A). *p*: number of technically valid datasets

Particle sizing method	*p*	Outliers		Normally distributed	Statistical parameters			
		Means	Variances		Mean [nm]	*s* [nm]	$s_{between}$ [nm]	s_{within} [nm]
CLS [1)]	8	None	None	Yes	23.9	1.9	1.8	0.7
DLS [2)]	17	L7	None	No	17.8	0.9	0.8	0.7
EM [3)]	9	None	None	Yes	18.2	0.8	0.7	0.9
EM [4)]	9	None	L16	Yes	18.3	0.8	0.8	0.7

[1)] Disc or cuvette setup with turbidimetric detection

[2)] Scattered light intensity-weighted arithmetic mean hydrodynamic particle diameter

[3)] Number-weighted modal area-equivalent particle diameter

[4)] Number-weighted median area-equivalent particle diameter

Statistical evaluation of the datasets associated to size class A of the PSDs of ERM-FD102 flags laboratory L7 as an outlier for the intensity-weighted arithmetic mean particle diameter (DLS) and additionally determines the data as unimodal non-normally distributed. However, it must be borne in mind that outlier tests do not take uncertainty information into consideration. A closer investigation reveals that the difference between the mean value of laboratory L7 and the other results is covered by the measurement uncertainties. Therefore, it can be reliably concluded that there is no clear evidence that the results of laboratory L7 significantly deviate from the other results. Taking into account the ill-posed nature of DLS Laplace transformation algorithms, the range of results (16.8 nm to 20.6 nm) is small, and small enough to assign a certified value.

In addition to laboratory L7, the variance of laboratory L16 was determined as an outlier for the number-weighted median area-equivalent particle diameter. In essence, outliers of variance show that repeatability varies between laboratories. The heterogeneity of variance prevents pooling of all individual results, so the evaluation is based on the mean of laboratory means instead. In conclusion, outlying variances are not a reason for exclusion of data.

Table 14: Statistical evaluation of the technically accepted datasets for ERM-FD102 (size class B). *p*: number of technically valid datasets

Particle sizing method	*p*	Outliers		Normally distributed	Statistical parameters			
		Means	Variances		Mean [nm]	*s* [nm]	$s_{between}$ [nm]	s_{within} [nm]
CLS [1)]	8	None	L7, L10, L14, L19	Yes	88.0	4.0	3.8	1.3
DLS [2)]	17	L8	None	Yes	88.5	2.1	2.1	1.2
EM [3)]	8	None	None	Yes	84.0	1.6	1.4	1.5
EM [4)]	8	None	None	Yes	83.3	2.1	2.1	1.2

[1)] Disc or cuvette setup with turbidimetric detection

[2)] Scattered light intensity-weighted arithmetic mean hydrodynamic particle diameter

[3)] Number-weighted modal area-equivalent particle diameter

[4)] Number-weighted median area-equivalent particle diameter

Statistical evaluation of the datasets associated to size class B of the PSDs of ERM-FD102 determines the data of laboratory L8 as unimodal non-normally distributed. In addition to laboratory L8, the variances of laboratories L7, L10, L14 and L19 were identified as statistical outliers for the intensity-weighted modal Stokes' particle diameter (turbidimetry). The exact sources of these variations are difficult to identify. These variations may partly reflect the possible intrinsic variations within the different methods applied when operating the disc centrifugation instruments and variations between disc centrifugation instruments and cuvette centrifugation. As the measurement methods were found technically sound and the submitted datasets were evaluated to be technically valid, results of the concerned laboratories were retained.

The uncertainty related to the characterisation (u_{char}) is estimated as the standard error of the means, i.e. $s/\sqrt{p}$ with s and p taken from Table 13 and Table 14. An overview of the estimated uncertainties for characterisation is shown in Table 15 and Table 16.

Table 15: Uncertainty of characterisation for ERM-FD102 (size class A)

Particle sizing method	*p*	Mean [nm]	*s* [nm]	u_{char} [nm]
CLS [1)]	8	23.9	1.9	0.7
DLS [2)]	17	17.8	0.9	0.2
EM [3)]	9	18.2	0.8	0.3
EM [4)]	9	18.3	0.8	0.3

[1)] Disc or cuvette setup with turbidimetric detection

[2)] Scattered light intensity-weighted arithmetic mean hydrodynamic particle diameter

[3)] Number-weighted modal area-equivalent particle diameter

[4)] Number-weighted median area-equivalent particle diameter

Table 16: Uncertainty of characterisation for ERM-FD102 (size class B)

Particle sizing method	*p*	Mean [nm]	*s* [nm]	u_{char} [nm]
CLS [1)]	8	88.0	4.0	1.4
DLS [2)]	17	88.5	2.1	0.5
EM [3)]	8	84.0	1.6	0.6
EM [4)]	8	83.3	2.1	0.8

[1)] Disc or cuvette setup with turbidimetric detection

[2)] Scattered light intensity-weighted arithmetic mean hydrodynamic particle diameter

[3)] Number-weighted modal area-equivalent particle diameter

[4)] Number-weighted median area-equivalent particle diameter

7 Value Assignment

Certified, indicative and information values were assigned for ERM-FD102.

Certified values are values that fulfil the highest standards of accuracy. Procedures at IRMM require generally pooling of not less than six datasets to assign certified values. Full uncertainty budgets in accordance with the 'Guide to the Expression of Uncertainty in Measurement' [4] were established.

Indicative values are values where either the uncertainty is deemed too large or where too few independent datasets were available to allow certification. Uncertainties are evaluated according to the same rules as for certified values.

Additional material information refers to values that were obtained in the course of the study. For example, results reported from only one or two laboratories or in cases where individual measurement uncertainty is high, would fall under this category.

7.1 Certified values and their uncertainties

The unweighted mean of the means of the accepted CLS (turbidity), DLS and EM datasets, as shown in Table 17 and Table 18, were assigned as certified values for the different measurands.

The assigned uncertainties consist of uncertainties related to characterisation, u_{char} (Section 6), potential between-unit inhomogeneity, u_{bb} (Section 4), potential degradation during transport (u_{sts}) and long-term storage, u_{lts} (Section 5).

For the CLS methods, an uncertainty of 2.5 % [34], which accounts for the uncertainty related to the effective particle density (u_{ρ}) was included. In addition, the CLS methods (disc centrifuge) require calibration. With the exception of one laboratory, all laboratories applied calibration by using PVC calibrants that were supplied by CPS Instruments, Inc. It has been experimentally confirmed that the particle size values assigned to the different PVC calibrants agree very well (measuring calibrant A after calibration with calibrant B produces, within the given measurement uncertainty, the value assigned to calibrant A, and vice versa). Therefore these calibrants can be considered as a "common" calibrant. Hence, the uncertainty (u_{cal}) contribution (2.2 %) of these calibrants cannot be neglected in the overall uncertainty budget.

The different contributions were combined to estimate the expanded, relative uncertainty of the certified value (U_{CRM}) with a coverage factor k as:

$$U_{CRM,rel} = k \cdot \sqrt{u^2_{char,rel} + u^2_{bb,rel} + u^2_{sts,rel} + u^2_{lts,rel} (+u^2_{cal,rel} + u^2_{\rho,rel})}$$ **Equation 7**

- u_{char} was estimated as described in Section 6
- u_{bb} was estimated as described in Section 4
- u_{sts} was estimated as described in section 5
- u_{lts} was estimated as described in Section 5
- u_{cal} was estimated (only for CLS (disc centrifuge) methods)

- u_{ρ} was estimated (only for CLS methods)

Because of the sufficient numbers of the degrees of freedom of the different uncertainty contributions, a coverage factor $k = 2$ was applied, to obtain the expanded uncertainties.

According to ISO Guide 35:2006 [2], reference materials must be characterised with respect to the degree of inhomogeneity and stability for each characteristic or measurand of interest. Inhomogeneity and in particular instability of ERM-FD102 will typically be manifested by the formation of agglomerates and/or aggregates of the primary particles. In the given study, homogeneity and stability experiments were conducted under repeatability conditions by means of DLS and CLS (turbidity) methods.

One can in theory also evaluate material homogeneity and stability from characterisation data (e.g., EM). However, whereas DLS and CLS measurements were performed on the as-received material, EM measurements required preparation of specimens that included deposition of the nanoparticles on a substrate and drying. During this specimen preparation step, agglomerates/aggregates may have been formed. The EM method is not capable of distinguishing between agglomerates/aggregates that are potentially present in the as-received suspension and those that may be formed during specimen preparation. As a result, the reliability of the values of u_{bb} that were calculated from the EM characterisation data cannot be considered to be sufficiently reliable. Therefore, the conclusions (i.e. u_{bb}, u_{sts} and u_{lts}) drawn from the DLS homogeneity and DLS stability studies were considered and used as realistic contributions in the calculations for u_{char} of the EM measurands.

The certified values and their uncertainties are summarised in Table 17 and Table 18.

Table 17: Certified values and their uncertainties for ERM-FD102 (size class A)

Particle sizing method	Certified value [nm]	$u_{char,rel}$ [%]	$u_{bb,rel}$ [%]	$u_{sts,rel}$ [%]	$u_{lts,rel}$ [%]	$u_{\rho,rel}$ [%]	$u_{cal,rel}$ [%]	$U_{CRM,rel}$ [%]	U_{CRM} [nm] [5)]
CLS [1)]	23.9	2.8	1.2	0.1	1.1	2.5	2.2	9.4	2.3
DLS [2)]	17.8	1.2	3.2	0.4	2.6	n.a.	n.a.	8.7	1.5
EM [3)]	18.2	1.4	3.2	0.4	2.6	n.a.	n.a.	8.8	1.6
EM [4)]	18.3	1.5	3.2	0.4	2.6	n.a.	n.a.	8.9	1.7

[1)] Disc or cuvette setup with turbidimetric detection

[2)] Scattered light intensity-weighted arithmetic mean hydrodynamic particle diameter

[3)] Number-weighted modal area-equivalent particle diameter

[4)] Number-weighted median area-equivalent particle diameter

[5)] Expanded ($k = 2$) and rounded uncertainty

Table 18: Certified values and their uncertainties for ERM-FD102 (size class B)

Particle sizing method	Certified value [nm]	$u_{char,rel}$ [%]	$u_{bb,rel}$ [%]	$u_{sts,rel}$ [%]	$u_{lts,rel}$ [%]	$u_{\rho,rel}$ [%]	$u_{cal,rel}$ [%]	$U_{CRM,rel}$ [%]	U_{CRM} [nm] [5)]
CLS [1)]	88.0	1.6	0.4	< 0.1	0.1	2.5	2.2	7.5	6.6
DLS [2)]	88.5	0.6	0.6	0.2	0.8	n.a.	n.a.	2.4	2.2
EM [3)]	84.0	0.7	0.6	0.2	0.8	n.a.	n.a.	2.5	2.1
EM [4)]	83.3	0.9	0.6	0.2	0.8	n.a.	n.a.	2.8	2.3

[1)] Disc or cuvette setup with turbidimetric detection

[2)] Scattered light intensity-weighted arithmetic mean hydrodynamic particle diameter

[3)] Number-weighted modal area-equivalent particle diameter

[4)] Number-weighted median area-equivalent particle diameter

[5)] Expanded (k = 2) and rounded uncertainty

7.2 Indicative values and their uncertainties

Indicative values were assigned to the scattered light intensity-weighted harmonic mean and to the scattered light intensity-weighted modal hydrodynamic particle diameters (DLS), the number-weighted modal maximum particle height (AFM) and the number-weighted hydrodynamic modal, mean and median particle diameters (PTA). Technically valid datasets were received from at least two different laboratories and/or methods. For PTA, several of the laboratories have successfully participated to previous ILC studies [38], and their reported results agreed within the stated measurement uncertainties. Taking into account the successful results of the QC samples, the quality of the results is sufficiently trustworthy to assign indicative values. The uncertainty budgets (Table 19 and Table 20) were set up in a similar way as for the certified values. The individual standard uncertainties were taken from the DLS homogeneity and stability studies because the PTA and DLS methods both tackle the same (hydrodynamic equivalent diameter) property. In contrast to the certified values, where a fixed coverage factor was used to calculate the expanded uncertainty, the combined uncertainties of the indicative values were multiplied with t-factors that were extracted from the t-distribution table following calculation of the effective degrees of freedom according to the Welch-Satterthwaite equation [4].

$$\nu_{\text{eff}} = \frac{u_{\text{c}}^4(y)}{\sum_{i=1}^{N} \frac{u_{\text{i}}^4(y)}{\nu_{\text{i}}}}$$ **Equation 8**

ν_{eff} effective number of degrees of freedom

u_{c} combined uncertainty obtained by combining of u_{char}, u_{bb}, u_{sts} and u_{lts}

u_{i} individual standard measurement uncertainties

ν_{i} degrees of freedom corresponding to u_{i}

The above described approach is required because the standard uncertainties are estimated from evaluations with inadequate degrees of freedom and therefore the true coverage probability for the resulting interval may be lower than expected.

Table 19: Indicative values and their uncertainties for ERM-FD102 (size class A)

Particle sizing method	Indicative value [nm]	$u_{char,rel}$ [%]	$u_{bb,rel}$ [%]	$u_{sts,rel}$ [%]	$u_{lts,rel}$ [%]	$u_{\rho,rel}$ [%]	$U_{CRM,rel}$ [%]	U_{CRM} [nm] [5)]
DLS [1)]	17.3	7.3	3.2	0.4	2.6	n.a.	19.0	3.3
DLS [2)]	17.1	5.3	3.2	0.4	2.6	n.a.	14.0	2.4
AFM [3)]	17	0.3	3.2	0.4	2.6	n.a.	10.7	2
CLS [4)]	18.0	3.6	3.2	0.4	2.6	2.5	14.8	2.7

[1)] Scattered light intensity-weighted harmonic mean hydrodynamic particle diameter

[2)] Scattered light intensity-weighted modal hydrodynamic particle diameter

[3)] Number-weighted modal maximum particle height

[4)] Mass-weighted modal Stokes' particle diameter (Rayleigh interference optics)

[5)] Expanded (k = 2) and rounded uncertainty

Table 20: Indicative values and their uncertainties for ERM-FD102 (size class B)

Particle sizing method	Indicative value [nm]	$u_{char,rel}$ [%]	$u_{bb,rel}$ [%]	$u_{sts,rel}$ [%]	$u_{lts,rel}$ [%]	$u_{\rho,rel}$ [%]	$U_{CRM,rel}$ [%]	U_{CRM} [nm] [8)]
DLS [1)]	84.8	0.3	0.6	0.2	0.8	n.a.	2.4	2.2
DLS [2)]	83.6	4.4	0.6	0.2	0.8	n.a.	10.0	8.4
PTA [3)]	77.8	2.2	0.6	0.2	0.8	n.a.	5.2	4.1
PTA [4)]	82.4	2.0	0.6	0.2	0.8	n.a.	4.8	4.0
PTA [5)]	79.2	0.8	0.6	0.2	0.8	n.a.	2.7	2.2
AFM [6)]	80	2.4	0.6	0.2	0.8	n.a.	6.7	6
CLS [7)]	88.5	2.2	0.6	0.2	0.8	2.5	7.9	7.0

[1)] Scattered light intensity-weighted harmonic mean hydrodynamic particle diameter

[2)] Scattered light intensity-weighted modal hydrodynamic particle diameter

[3)] Number-weighted modal hydrodynamic particle diameter

[4)] Number-weighted mean hydrodynamic particle diameter

[5)] Number-weighted median hydrodynamic particle diameter

[6)] Number-weighted modal maximum particle height

[7)] Mass-weighted modal Stokes' particle diameter (Rayleigh interference optics)

[8)] Expanded (k = 2) and rounded uncertainty

The effective density of the suspended silica nanoparticles is essential for the accurate determination of the particle size distribution by sedimentation techniques such as CLS. The

effective density, which may significantly differ from the density of the dry particle bulk material, was determined by means of two different ultracentrifugation methods: zero-velocity (also referred to as isopycnic centrifugation) and a two-velocity sedimentation approach [34]. The effective density and associated uncertainty of the silica nanoparticles present in ERM-FD102 is given in Table 21.

Table 21: Effective particle density of silica nanoparticles present in EM-FD102

Property	Indicative value [g/cm^3]	U_{CRM} [g/cm^3] [1)]
Effective particle density	2.0	0.1

[1)] Expanded (k = 2) and rounded uncertainty

7.3 Additional material information

For each of the SAXS measurands, as well as for one DLS measurand, only one technically valid dataset was received (Table 22 and Table 23).

Laboratory 11 additionally analysed ERM-FD102 using asymmetrical flow field-flow fractionation (aFlFFF) instrument which was coupled to refractive index (RI) and multi-angle laser light scattering (MALLS) detectors. Instrumental details are listed in Table D.7 of Annex D. A representative fractogram obtained on ERM-FD102 is given in Fig. 10. The corresponding results (averages of six replicates) are given in Table 22 and Table 23.

One laboratory (L3) also reported pH, zeta potential and electrolytic conductivity results (Table 24), instrumental details are listed in Table D.8 of Annex D. One other laboratory provided additional TEM-based morphology results which are related to the number-based distributions of the particles' aspect ratio and convexity (Table 25 and Table 26).

Because of the limited number of datasets, the evaluated results are only listed as additional material information values. These values must be regarded as informative only on the general composition of the material and can not be, in any case, used as certified or indicative value.

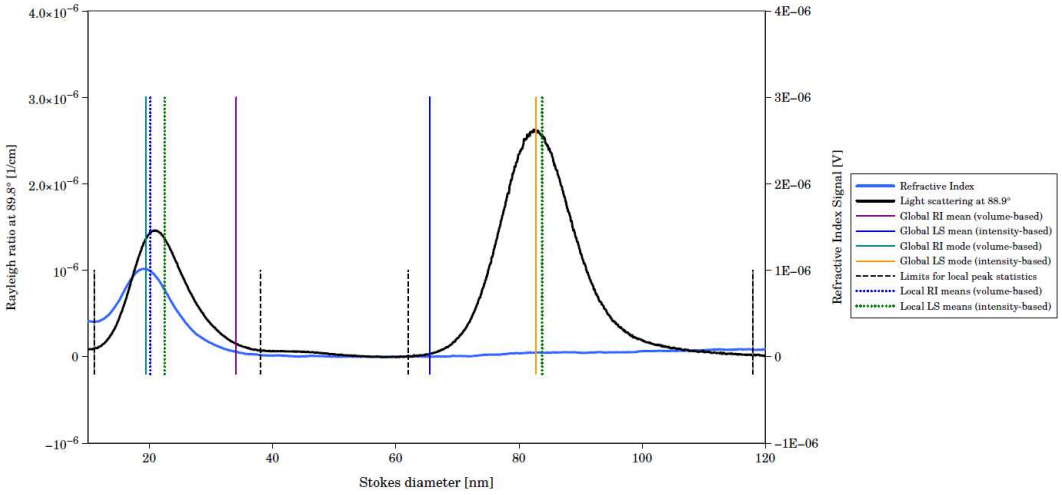

Fig. 10 Overlay of aFlFFF-MALLS and aFlFFF-RI fractograms

Table 22: Additional material information values for ERM-FD102 (size class A)

Particle sizing method	Information value [nm]
DLS [1)]	16.8
DLS [2)]	18.0
SAXS [3)]	22.6
SAXS [4)]	19.8
SAXS [5)]	21.4
aFlFFF-RI [6)]	20.4
aFlFFF-MALLS [7)]	22.9

[1)] Scattered light intensity-weighted geometric mean hydrodynamic particle diameter

[2)] Scattered light intensity-weighted median hydrodynamic particle diameter

[3)] Volume-weighted mean particle diameter (Guinier's approximation)

[4)] Volume-weighted mean particle diameter (indirect Fourier transformation method)

[5)] Scattered X-ray intensity-weighted mean particle diameter (indirect Fourier transformation method)

[6)] Volume-weighted arithmetic mean particle diameter

[7)] Scattered light intensity-weighted arithmetic mean particle diameter

Table 23: Additional material information values for ERM-FD102 (size class B)

Particle sizing method	Information value [nm]
DLS [1)]	85.2
DLS [2)]	85.9
SAXS [3)]	80.1
SAXS [4)]	81.0
aFlFFF-MALLS [5)]	87.5

[1)] Scattered light intensity-weighted geometric mean hydrodynamic particle diameter

[2)] Scattered light intensity-weighted median hydrodynamic particle diameter

[3)] Volume-weighted mean particle diameter (indirect Fourier transformation method)

[4)] Scattered X-ray intensity-weighted mean particle diameter (indirect Fourier transformation method)

[5)] Scattered light intensity-weighted arithmetic mean particle diameter

Table 24: Additional material information values

Measurement method	Information value
Zeta potential [1)]	-52 mV
pH [2)]	9
Electrolytic conductivity [3)]	2.0 x 10^2 µS/cm

[1)] As obtained by electrophoretic light scattering (ELS)

[2)] As determined by a potentiometric method at 23 °C ± 1 °C

[3)] Determined at 25 °C ± 1 °C using a folded capillary cell (Malvern Zetasizer Nano ZS instrument) and a conductivity meter equipped with a 2-electrode sensor with a nominal cell constant of 0.475 cm^{-1}

Table 25: Additional material information values of particle morphology for ERM-FD102 (size class A)

Parameter	Information value
Median aspect ratio [1)]	1.17
Modal aspect ratio [1)]	1.13
Median convexity [2)]	0.95
Modal convexity[2)]	0.96

[1)] The maximum ratio of the width and height of a bounding rectangle

[2)] The fraction of the measured object's area and the area of its convex hull

Table 26: Additional material information values of particle morphology for ERM-FD102 (size class B)

Parameter	Information value
Median aspect ratio [1)]	1.07
Modal aspect ratio [1)]	1.06
Median convexity [2)]	0.97
Modal convexity[2)]	0.97

[1)] The maximum ratio of the width and height of a bounding rectangle

[2)] The fraction of the measured object's area and the area of its convex hull

8 Metrological traceability and commutability

8.1 Metrological traceability

Identity

The size of particles is a method-defined property and different techniques and methods measure mostly an equivalent diameter (or radius). The actual realisation of the term "equivalent" strongly depends on the nature of the measurement principle of each method. From a metrological perspective, this means that the measurement results originate from measurands that are intrinsically defined by the applied method.

ERM-FD102 has been characterised by multiple methods and the different assigned property values are intrinsically linked to their corresponding operationally- or method-defined measurands. The certified values can be regarded as reliable estimates of the true equivalent particle sizes, and are underpinned by the agreement of the laboratories' results with the assigned values for the CRMs (ERM-FD100 and ERM-FD304) that were used as QC samples.

Quantity value

Metrological traceability of the assigned particle size values to a higher order accepted reference, ultimately to a practical realisation of the definition of a unit of the International System of Units (SI) such as the metre, requires traceability of all relevant input factors through an unbroken network of calibrations. Properly characterised and fit-for-purpose calibrants are essential links in order to establish the traceability network. Considering the method-defined nature of the different measurands, the traceability network and final references have been specific for each method. A summary of the traceability network for the different methods used in this study is given below. Detailed information regarding the calibrants used by the different laboratories in the study is listed in the tables of Annex D.

Atomic force microscopy: The AFM measurand in this certification study is the modal value of the number-based distribution of the measured maximum particle heights. The indicative values are traceable to the SI unit metre. An unbroken traceability network was established by calibrating the height responses of the laboratories' AFM instruments with physical transfer step-height standards. The heights of the calibration features present on these standards were interferometrically determined. The wavelength of the interferometry laser light was calibrated by comparing it with that of the laser source used in the practical realisation of the SI unit metre.

Centrifugal liquid sedimentation (turbidimetric detection): The measurand of the CLS method, being the extinction intensity-weighted modal Stokes' particle diameter, is method-defined according to the procedures described in documentary standards ISO 13318-1 [9] and 13318-2 [10]. Whereas the cuvette methods do not require calibration for particle size, the disc centrifuges were all calibrated using particle size standards. With the exception of one laboratory, all laboratories used calibration standards of PVC beads that were supplied by CPS Instruments, Inc. During different series of in-house experiments PVC standards of different particle sizes have been checked against each other as well as against colloidal silica and polystyrene materials. The obtained results indicate consistency, in terms of particle size, amongst the different PVC standards. Therefore, measurement results obtained

by CLS (turbidimetric detection) are traceable to size values provided for the PVC standards supplied by CPS Instruments, Inc.

Dynamic light scattering: The scattered light intensity-weighted mean hydrodynamic particle diameter, as determined by the NNLS, CONTIN and Dynals algorithms, is a method-defined length measurand. Since the DLS method is intrinsically absolute in nature, there is no need for instrument response calibration or for introducing corrective terms. Traceability of the measured diameter values depends on the traceability of the values corresponding with the parameters occurring in the Stokes-Einstein equation:

- Temperature: the sample temperatures have been measured by sensors which had either been accurately calibrated by its manufacturer or which had been verified following alpha testing using Pt100 sensors.
- Detector angle: the angle at which the detector was fixed had been geometrically determined as it depends on the mechanical design of the DLS systems. The accuracy of the angle is determined by the applied mechanical tolerances.
- Measured decay rate: the traceability of the measured decay rates depends on the accurately known constant resonant frequency of quartz crystal oscillators that are integrated in programmable logic devices such as a field-programmable gate array (FPGA).
- Refractive index and viscosity of the sample/particle: refractive index and viscosity values were obtained from tables in the literature (e.g., CRC Handbook) reporting traceably measured values.
- Laser wavelength: Direct (without calibration) traceability of the measurement result to the SI was established via the wavelength of an uncalibrated or unstabilised helium neon (He-Ne) laser with a nominal wavelength of 633 nm. In the ILC study, 18 out of the 20 DLS instruments were equipped with such a laser.

  Unstabilised He-Ne lasers of 633 nm are used in most laser interferometers and many instruments used for length measurements. These instruments, including DLS instruments, are very often used at uncertainty levels that are large compared to the possible variation of the He-Ne laser vacuum wavelength. Based on these considerations, the International Committee of Weights and Measures (CIPM) recognised the need for providing documentary evidence regarding the value of the vacuum wavelength and its uncertainty that can be expected in the absence of calibration. During its 96^{th} meeting, the CIPM adopted a wavelength of 632.9908 nm with a relative standard uncertainty of 1.5×10^{-6} [39]. Following thorough evaluation of the Consultative Committee for Length (CCL) of the CIPM, the CCL recommended including unstabilised red He-Ne lasers, operating on the 633 ($3s_2 \rightarrow 2p_4$) neon transitions, in the new list of standard frequencies, "*Recommended values of standard frequencies for applications including the practical realization of the metre and secondary representations of the second*". This list replaces the *Mise en Pratique* for the definition of the metre.

Electron microscopy: The measurands investigated by SEM and TEM were the number-weighted modal and median area-equivalent particle diameters. The magnifications of the instruments were calibrated using different types of standards which were all suitable for calibration of lateral dimensional measurement systems. Several laboratories used pitch size standards that were calibrated on a metrological AFM, thereby linking the assigned pitch sizes to the SI unit metre through the calibrated laser light wavelength of the interferometer. Hence, the certified value and uncertainty are traceable to the SI through the SI traceable calibrants used by the different laboratories.

8.2 Commutability

According to ISO Guide 34 [1], the assessment of commutability for a CRM requires a comparison and establishment of a numerical correlation between the property value assigned to the CRM and to routine test samples using both a "higher-order" reference measurement procedure and one or more "lower-order" routine measurement procedures. If the ratio between the results of the compared measurement procedures is the same as the ratio of the results for routine test samples, then the CRM is said to be commutable.

ERM-FD102 has been characterised by multiple techniques and methods which all target different method-defined measurands and the size measurement results for near-spherical particles are uncorrelated. Therefore, commutability cannot be assessed.

9 Instructions for use

9.1 Safety information

This material should be handled with care. Nanoparticles can have an impact on environment and human health. Any spilling of the suspension should be handled according to the usual laboratory safety precautions.

For further details refer to the safety data sheet.

9.2 Storage conditions

The materials shall be stored at 18 °C ± 5 °C. Ampoules must not be allowed to freeze, as this will irreversibly compromise the integrity of the material.

Please note that the European Commission cannot be held responsible for changes that happen during storage of the material at the customer's premises, especially of opened ampoules.

9.3 Instructions for use and intended use

The intended use is to check the performance of instruments and/or methods that characterise the particle size distribution of nanoparticles (particle size ranging from approximately 1 nm to approximately 100 nm) that are either suspended in a liquid medium or deposited onto a suitable substrate. The certified values are regarded as reliable estimates of the true values and ERM-FD102 can therefore be used for calibration purposes (e.g., EM methods). Due to its long measurement time, ERM-FD102 may, however, not be ideal for calibration of CLS methods that apply the disc centrifugation measurement principle.

Before opening, the ampoule should be gently inverted several times to ensure the homogeneity of the suspension and to re-suspend any settled particles. Remove any suspension that remains in the upper part (conical tip) of the ampoule by gently flicking the conical part with the forefinger while tilting the ampoule. The ampoule is pre-scored and can be opened by applying moderate pressure with one's thumb to snap off the conical part. The contents of an ampoule should be used the same day as opened.

DLS method: Aliquots of ERM-FD102 shall be measured as-received, i.e. without dilution. A measurement temperature of 25 °C is recommended, the corresponding viscosity and refractive index of the dispersing medium (water) are 0.8872 mPa•s and 1.330, respectively.

CLS (turbidity) method: Aliquots of ERM-FD102 shall be measured as-received, i.e. without dilution. The effective particle density (silica) used in the evaluation was 2.0 g/cm^3.

Electron microscopy method: A drop of the material should be transferred to a suitable grid/substrate; after drying at least 300 discrete particles of the large particle population (size class B) and 1000 discrete particles of the small particle population (size class A) should be counted and measured. If necessary, ERM-FD102 can be diluted with ultrapure water.

9.4 Minimum sample intake

The minimum amount of sample to be used is for:

- AFM: 20 µL of an aliquot as received. One shall measure at least 1000 discrete particles of size class A and at least 300 discrete particles of size class B;
- CLS (turbidimetric detection): 100 µL of an aliquot as received;
- CLS (Rayleigh interference): 330 µL of an aliquot as received;
- DLS: 50 µL of an aliquot as received;
- EM: 2.5 µL of an aliquot as received. One shall measure at least 1000 discrete particles of size class A and at least 300 discrete particles of size class B;
- PTA: 10 µL of an aliquot as received. One shall analyse at least 800 tracks per measurement;
- SAXS: 25 µL of an aliquot as received.

9.5 Use of the certified value

The main purpose of this material is to assess the performance of instruments and/or methods that are used for measuring the size of nanoparticles. As any reference material, ERM-FD102 can also be used for control charts or validation studies.

Use as a calibrant

The certified values that have been assigned to the number-weighted modal and median area-equivalent diameters are regarded as reliable estimates of the true values and ERM-FD102 can therefore be used for calibration purposes for EM methods.

Comparing an analytical result with the certified value

A result is unbiased if the combined standard uncertainty of measurement and certified value covers the difference between the certified value and the measurement result (see also ERM Application Note 1, www.erm-crm.org [37].

For assessing the method performance, the measured values of the CRMs are compared with the certified values. The procedure is described here in brief:

- Calculate the absolute difference between mean measured value and the certified value (Δ_{meas}).
- Combine measurement uncertainty (u_{meas}) with the uncertainty of the certified value (u_{CRM}): $u_{\Delta} = \sqrt{u_{meas}^2 + u_{CRM}^2}$
- Calculate the expanded uncertainty (U_{Δ}) from the combined uncertainty ($u_{\Delta,}$) using an appropriate coverage factor, corresponding to a level of confidence of approximately 95 %
- If $\Delta_{meas} \leq U_{\Delta}$ no significant difference between the measurement result and the certified value, at a confidence level of about 95 % exists.

Use in quality control charts

The materials can be used for quality control charts. Different CRM-units will give the same result as inhomogeneity was included in the uncertainties of the certified values.

10 Acknowledgments

The authors would like to acknowledge the support received from Jean Charoud-Got and John Seghers (IRMM) related to the processing of this CRM and from Maria Contreras Lopez (IRMM) concerning the set-up of the required isochronous studies.

Furthermore, the authors would like to thank Amalia Munoz-Pineiro, Evanthia Monogioudi, Robert Koeber, Andrea Held and Hendrik Emons (all IRMM) for reviewing of the certification report, Rainer Peters (ALV-Laser Vertriebsgesellschaft m-b.H., Langen, DE), Daniel Werner (Sympatec GmbH, Clausthal-Zellerfeld, DE) and Michael Kaszuba (Malvern Instruments Ltd., Malvern, UK) for their advice regarding DLS evaluation algorithms, as well as the experts of the Certification Advisory Panel "Physicochemical-physical properties", Mark Gee (NPL, Teddington, UK), Jan Mast (CODA-CERVA, Brussels, BE) and Ludwig Niewöhner (Bundeskriminalamt, Wiesbaden, DE) for their constructive comments.

11 References

1 ISO Guide 34, General requirements for the competence of reference materials producers, International Organization for Standardization, Geneva, Switzerland, 2009

2 ISO Guide 35, Reference materials – General and statistical principles for certification, International Organization for Standardization, Geneva, Switzerland, 2006

3 ISO/IEC 17025:2005, General requirements for the competence of testing and calibration laboratories, International Organization for Standardization, Geneva, Switzerland, 2005

4 ISO/IEC Guide 98-3, Guide to the Expression of Uncertainty in Measurement, (GUM 1995), International Organization for Standardization, Geneva, Switzerland, 2008

5 ISO/TS 27687, Nanotechnologies – Terminology and definitions for nano-objects – Nanoparticles, nanofibres and nanoplates, International Organization for Standardization, Geneva, Switzerland, 2008

6 Commission Recommendation of 18 October 2011 on the definition of nanomaterial, 2011/696/EU, 2011

7 M.N. Pons, H. Vivier, K. Belaroui, B. Bernard-Michel, F. Cordier, D. Oulhana, J.A. Dodds, Particle morphology: from visualisation to measurement, Powder Technol. 103 (1999) 44-57

8 G. Binnig, C.F. Quate, Ch. Gerber, Atomic force microscope, Phys. Rev. Lett. 56 (1986) 930-933

9 ISO 13318-1, Determination of particle size distribution by centrifugal liquid sedimentation methods – Part 1: General principles and guidelines, International Organization for Standardization, Geneva, Switzerland, 2001

10 ISO 13318-2, Determination of particle size distribution by centrifugal liquid sedimentation methods – Part 2: Photocentrifuge method, International Organization for Standardization, Geneva, Switzerland, 2007

11 ISO 13318-3, Determination of particle size distribution by centrifugal liquid sedimentation methods – Part 3: Centrifugal X-ray method, International Organization for Standardization, Geneva, Switzerland, 2004

12 T. Detloff, T. Sobisch, D. Lerche, Particle size distribution by space or time dependent extinction profiles obtained by analytical centrifugation, Part. Part. Syst. Charact. 23 (2006) 184-187

13 H. Cölfen, W. Wohlleben, Analytical ultracentrifugation of latexes, In: L.M. Gugliotta, J.R. Vega (eds), Measurement of particle size distribution of latexes, Research Signpost, Kerala, India, 2010, pp 183-222

14 B.J. Berne, R. Pecora, Dynamic light scattering with applications to chemistry, biology, and physics, Dover Publications Inc., New York, USA, 2000

15 D.E. Koppel, Analysis of macromolecular polydispersity in intensity correlation spectroscopy: the method of cumulants, J. Chem. Phys. 57 (1972) 4814-4820

16 ISO 13321, Particle size analysis – Photon correlation spectroscopy, International Organization for Standardization, Geneva, Switzerland, 2001

17 ISO 22412, Particle size analysis – Dynamic light scattering (DLS), International Organization of Standardization, Geneva, Switzerland, 2008

18 S.W. Provencher, CONTIN: a general purpose constrained regularization program for inverting noisy linear algebraic and integral equations, Comput. Phys. Commun. 27 (1982) 229-242

19 S.W. Provencher, A constrained regularization method for inverting data represented by linear algebraic or integral equations, Comput. Phys. Commun. 27 (1982) 213-227

20 L. Lawson, R. Hanson, Solving least squares problems, Prentice-Hall Inc., Englewood Cliffs, New Jersey, USA, 1974

21 S. Twomey, Introduction to the mathematics of inversion of remote sensing and indirect measurements, Dover Publications Inc. New York, USA, 2002

22 ISO 13322-1, Particle size analysis – Image analysis methods – Part 1: Static image analysis methods, International Organization for Standardization, Geneva, Switzerland, 2004

23 P.-J. De Temmerman, E. Van Doren, E. Verleysen, Y. Van der Stede, M.A.D. Francisco, J. Mast, Quantitative characterization of agglomerates and aggregates of pyrogenic and precipitated amorphous silica nanomaterials by transmission electron microscopy, J. Nanobiotech. 10 (2012) 24, 11p

24 P.-J. De Temmerman, J. Lammertyn, B. De Ketelaere, V. Kestens, G. Roebben, E. Verleysen, J. Mast, Measurement uncertainties of size, shape, and surface measurements using transmission electron microscopy of near-monodisperse, near-spherical nanoparticles, J. Nanopart. Res. 16 (2014) 2177, 20p

25 S.B. Rice, C. Chan, S.C. Brown, P. Eschbach, L. Han, D.S. Ensor, Stefaniak, A.B., J. Bonevich, A.E. Vladár, A.R.H. Walker, J. Zheng, C. Starnes, A, Stromberg, J. Ye, E.A. Grulke, Particle size distributions by transmission electron microscopy: an interlaboratory comparison case study, Metrologia 50 (2013) 663-678

26 O. Glatter, O. Kratky, Small angle X-ray scattering, Academic Press, London, UK, 1982

27 A. Guinier, G. Fournet, Small angle scattering from X-rays, Wiley, New York, USA, 1955

28 O. Glatter, A new method for the evaluation of small-angle scattering data, J. Appl. Crystallogr. 10 (1977) 415-421

29 T.P.J. Linsinger, J. Pauwels, A.M.H. van der Veen, H. Schimmel, A. Lamberty, Homogeneity and stability of reference materials, Accred. Qual. Assur. 6 (2001) 20-25

30 A. Lamberty, H. Schimmel, J. Pauwels, The study of the stability of reference materials by isochronous measurements, Fres. J. Anal. Chem. 360 (1998) 359-361

31 A. Braun, K. Franks, V. Kestens, G. Roebben, A. Lamberty, T. Linsinger, Certification of equivalent spherical diameters of silica nanoparticles in water – Certified reference material ERM-FD100, EUR Report 24620 – European Union, Luxembourg - 2011 – ISBN 978-92-79-18676-9

32 K. Franks, A. Braun, V. Kestens, G. Roebben, A. Lamberty, T. Linsinger, Certification of the equivalent spherical diameters of silica nanoparticles in aqueous solution – Certified reference material ERM-FD304, EUR Report 25018 – European Union, Luxembourg - 2012 – ISBN 978-92-79-21866-8

33 T.P.J. Linsinger, J. Pauwels, A. Lamberty, H. Schimmel, A.M.H. van der Veen, L. Siekmann, Estimating the Uncertainty of Stability for Matrix CRMs, Fres. J. Anal. Chem. 370 (2001) 183-188

34 H. Woehlecke, T. Detloff, K. Franks, V. Kestens, G. Roebben, D. Lerche, In-situ determination of the effective particle density of suspended colloidal silica particles by

means of analytical centrifugation, International Congress on Particle Technology (PARTEC), Nuremberg, Germany, 23-25 April 2013

35 ISO 9276-1, Representation of results of particle size analysis – part 1: Graphical representation, International Organization for Standardization, Geneva, Switzerland, 1998

36 ISO/FDIS 9276-2, Representation of results of particle size analysis – part 2: Calculation of average particle sizes/diameters and moments from particle size distributions, International Organization for Standardization, Geneva, Switzerland, 2014

37 T.P.J. Linsinger, ERM Application Note 1: Comparison of a measurement result with the certified value, www.erm-crm.org (last accessed on 28 January 2014)

38 P. Hole, K. Sillence, C. Hannell, C.M. Maguire, M. Roesslein, G. Suarez, S. Capracotta, Z. Magdolenova, L. Horev-Azaria, A. Dybowska, L. Cooke, A. Haase, S. Contal, S. Manø, A. Vennemann, J.-J. Sauvain, K.C. Staunton, S. Anguissola, A. Luch, M. Dusinska, R. Korenstein, A.C. Gutleb, M. Wiemann, A. Prina-Mello, M. Riediker, P. Wick, Interlaboratory comparison of size measurements on nanoparticles using nanoparticle tracking analysis (NTA), J. Nanopart. Res. 15 (2013) 2101

39 CIPM, Report of the 96th meeting (2007) – BIPM, Paris, FR

Annexes

Annex A: Results of the homogeneity measurements

The graph (Fig. A1) shows the ampoule averages of two replicates and their 95 % confidence intervals (error bars). These confidence intervals are based on the expanded measurement uncertainties (k = 2) that purely reflect the repeatability of the DLS and line-start CLS (disc centrifuge) methods, as obtained during in-house method validation studies. Absolute values do not necessarily agree with the certified value due to the potential laboratory bias, which is irrelevant for the evaluation of homogeneity.

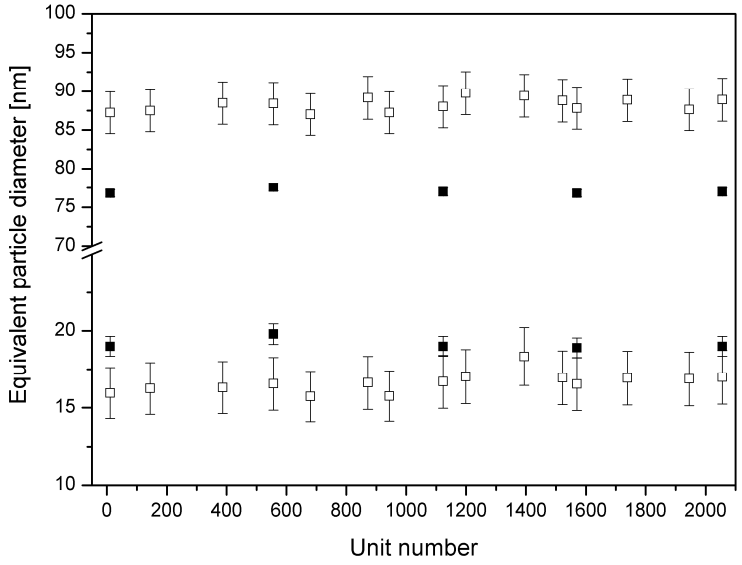

Fig. A1 Homogeneity data (average results of two replicates) of ERM-FD102; DLS NNLS light scattering intensity-weighted arithmetic mean particle diameter (open squares) and line-start CLS (disc centrifuge) light extinction intensity-weighted modal Stokes' particle diameter (solid squares); error bars correspond to the expanded measurement uncertainties (k = 2) for method repeatability, CLS measurement uncertainties for particle size results from size class B are only about 0.5 nm and error bars are therefore not visible in the graph.

Annex B: Results of the short-term stability measurements

Graphs depicted in Fig. B1 and Fig. B2 show the short-term stability data as obtained by DLS NNLS and line-start CLS (disc centrifuge) methods, respectively. Error bars are omitted in the graphs for reasons of clarity. The relative expanded uncertainties (k = 2) for single replicate DLS measurement results for size class A and size class B are 14.6 % and 4.4 %, respectively. The relative expanded uncertainties (k = 2) for single replicate CLS measurement results for size class A and size class B are 4.8 % and 0.8 %, respectively. These uncertainties purely reflect the repeatability of the DLS and line-start CLS (disc centrifuge) methods, as assessed during in-house method validation studies. Absolute values do not necessarily agree with the certified value due to the potential laboratory bias, which is irrelevant for the evaluation of stability.

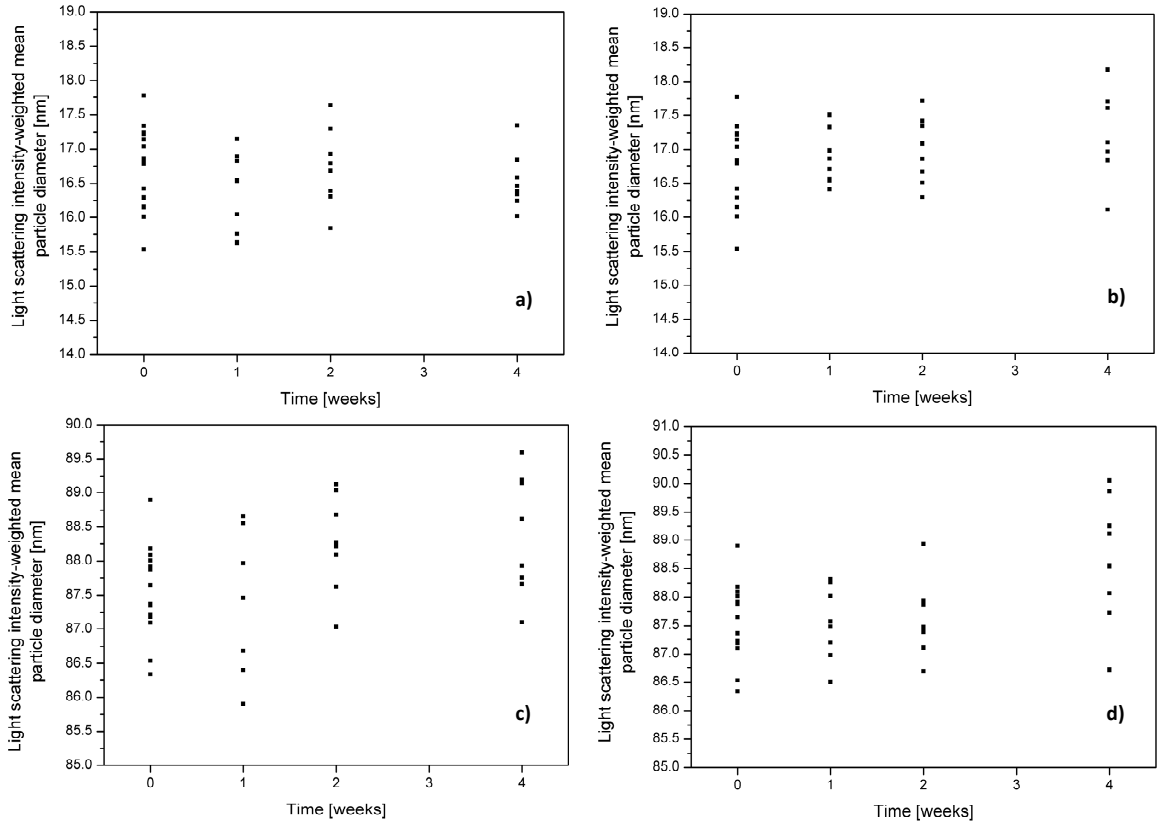

Fig. B1 Short-term stability data (results of individual replicates) of ERM-FD102; DLS NNLS light scattering intensity-weighted arithmetic mean particle diameter results of size class A and size class B, when stored for several weeks at 4 °C (a and c) and 60 °C (b and d), results at time point 0 weeks correspond to units that were stored at the reference temperature of 18 °C.

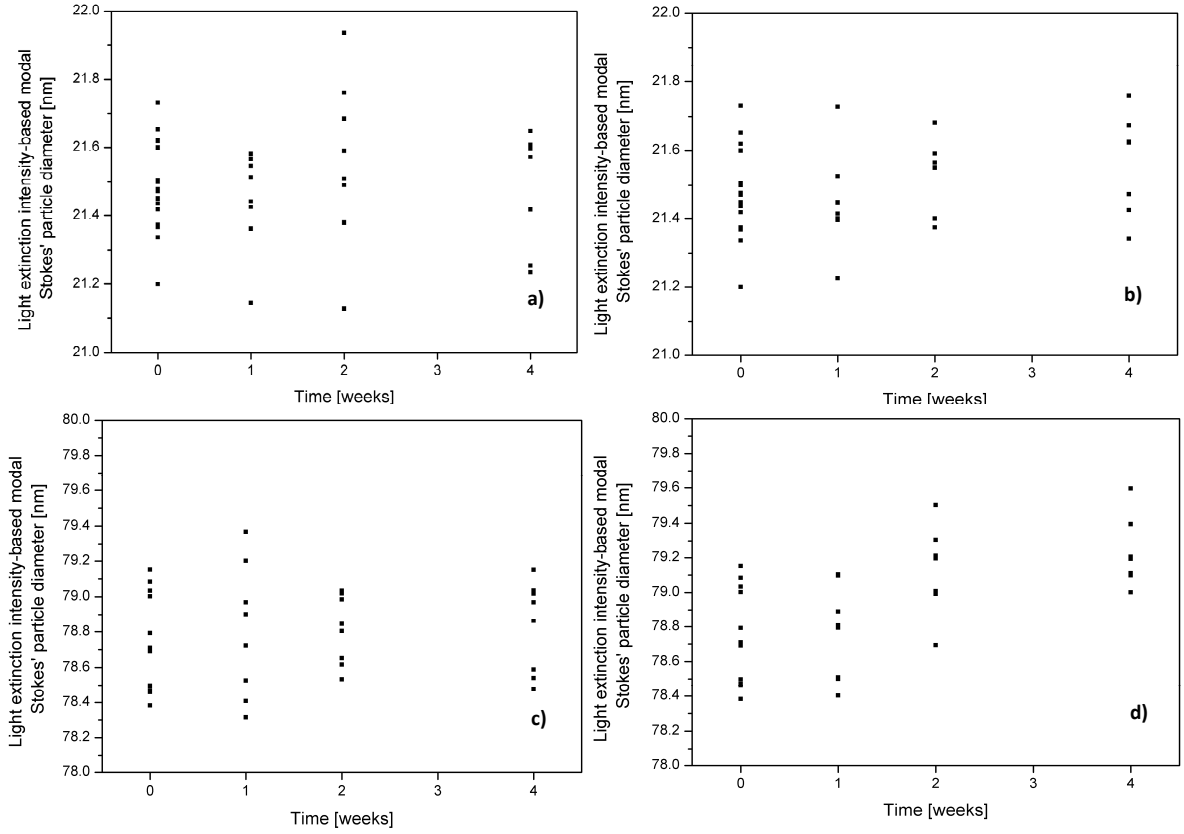

Fig. B2 Short-term stability data (results of individual replicates) of ERM-FD102; line-start CLS (disc centrifuge) light extinction intensity-weighted modal Stokes' particle diameter results of size class A and size class B, when stored for several weeks at 4 °C (a and c) and 60 °C (b and d), results at time point 0 weeks correspond to units that were stored at the reference temperature of 18 °C.

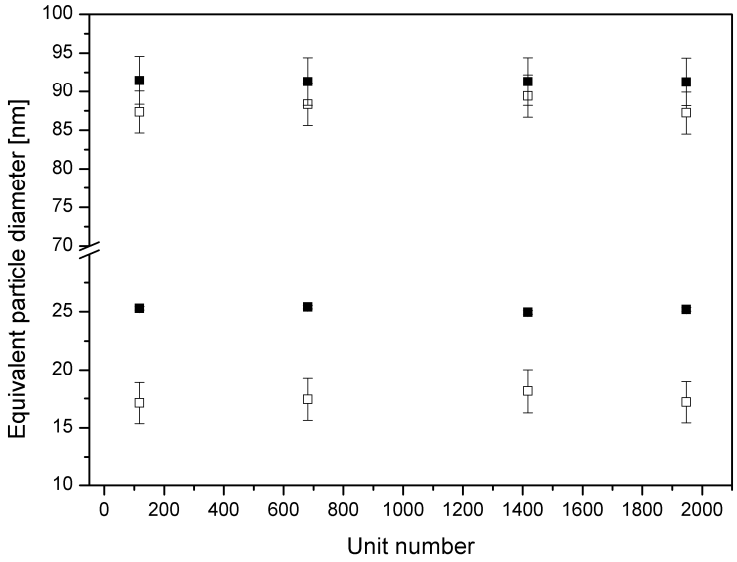

Fig. B3 Additional stability data (average of two replicates) of ERM-FD102 (size class A and size class B) when stored at 60 °C for three months; DLS NNLS scattered light intensity-weighted arithmetic mean particle diameter (open squares) and line-start CLS (disc centrifuge) light extinction intensity-weighted modal Stokes' particle diameter (solid squares); error bars correspond to the expanded measurement uncertainties (k = 2) for method repeatability, CLS measurement uncertainties for particle size results from size class B are only about 0.5 nm and error bars are therefore not visible in the graph.

Annex C: Results of the long-term stability measurements

Graphs depicted in Fig. C1 and Fig. C2 show the long-term stability data as obtained by DLS NNLS and line-start CLS (disc centrifuge) methods, respectively. Error bars are omitted in the graphs for reasons of clarity. The relative expanded uncertainties (k = 2) for single replicate DLS measurement results for size class A and size class B are 14.6 % and 4.4 %, respectively. The relative expanded uncertainties (k = 2) for single replicate CLS measurement results for size class A and size class B are 4.8 % and 0.8 %, respectively. These uncertainties purely reflect the repeatability of the DLS and line-start CLS (disc centrifuge) methods, as assessed during in-house method validation studies. Absolute values do not necessarily agree with the certified value due to the potential laboratory bias, which is irrelevant for the evaluation of stability.

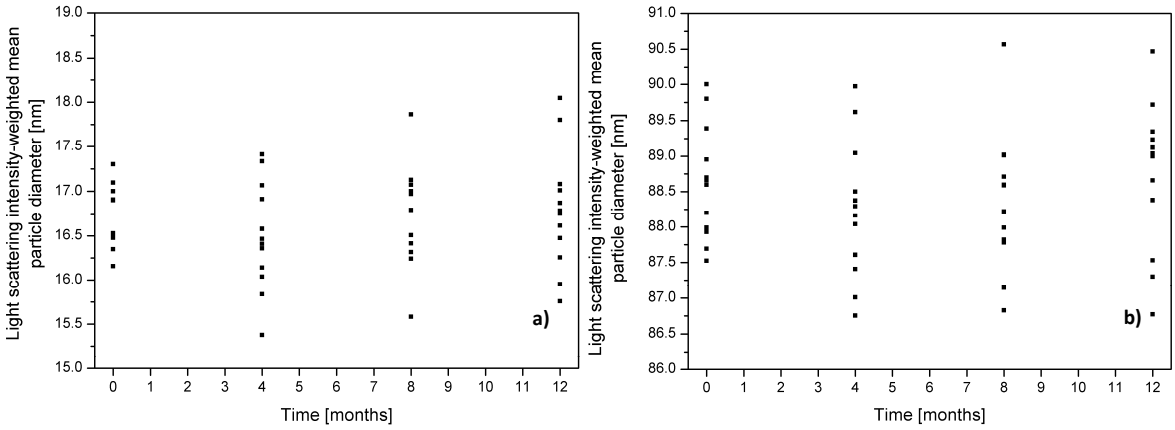

Fig. C1 Long-term stability data (results of individual replicates) of ERM-FD102; DLS NNLS scattered light intensity-weighted arithmetic mean particle diameter results of size class A (a) and size class B (b), when stored for several months at 18 °C, results at time point 0 months correspond to units that were stored at the reference temperature of 4 °C.

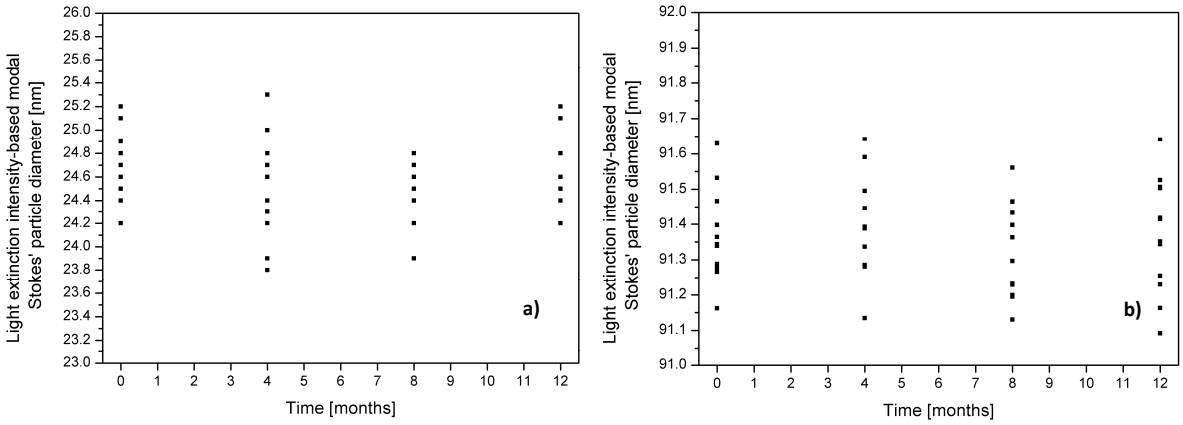

Fig. C2 Long-term stability data (results of individual replicates) of ERM-FD102; line-start CLS (disc centrifuge) light extinction intensity-weighted modal Stokes' particle diameter results of size class A (a) and size class B (b), when stored for several months at 18 °C, results at time point 0 months correspond to units that were stored at the reference temperature of 4 °C.

Annex D: Summary of methods used in the characterisation study

Table D.1 Atomic force microscopy: relevant instrumental and method details (as reported by the participants) for the measurements of ERM-FD102

Lab code	Instrument manufacturer Make Operation mode	Specimen preparation	AFM probe Type	Cantilever	Spring constant* [N/m]	Resonant frequency * [kHz]	Tip	Height response calibration Metrological traceability	Pixels	Image analysis software Image analysis strategy
L15	Asylum Research Inc. Cypher AFM system Closed loop / amplitude modulation (tapping)	100 µL taken from the as-received material and 20x diluted with ultrapure water 1 µL of diluted suspension brought onto a ~13 x 13 mm^2 piece of Si wafer (cleaned with isopropanol, blow-dried under a stream of argon), drying in air while the substrate was tilted at an angle of 45°	SSS-NCHR (Nanosensors)	Rectangular cantilever of 125 µm x 30 µm area, made of doped Si, with aluminium reflex coating on the detector side	42	280	Tip radius curvature smaller than 5 nm, half cone angle < 10° at 200 nm from the tip apex	Traceable blaze grating and 80 nm step height standard with relative uncertainty of 6 % (k = 2). The step height standard was calibrated using an interferometric microscope.	512 x 512	SPIP 6.0.13 Thresholds of 10 nm and 35 nm for particles of size class A and size class B, respectively. Particles touching the edge of the image and clusters of particles were manually omitted.
L25	Asylum Research Inc. MFP-3D-SA Closed loop / amplitude modulation (tapping)	20 µL taken from the as-received material and 100x and 1000x diluted with ultrapure water 50 µL of 0.1 % poly-L-lysine brought onto a freshly cleaved muscovite substrate (grade V-1) during 60 s. Poly-L-lysine rinsed off and blown dry with dry nitrogen. 50 µL of the diluted suspension brought onto the surface-modified mica substrate and incubated for 5 min. Suspension rinsed off and blown dry with dry nitrogen. Sample dried in oven at 60 C for 60 min.	Tap 150Al-G (Budget Sensors)	"Diving board" monolithic Si, reflective aluminium coating on back side	5	150	Monolithic Si with apex radius < 10 nm	PTB calibrated step height standards MicroMaschTGZ01C (nominal 20 nm ± 1.2 nm (k = 2)) and TGZ02C (nominal 100 nm ± 1.3 nm (k = 2)). Calibration measurements performed according to VDI/VDE 2656	2048 x 2048	SPIP 6.0.14 Image processing (plane correction), particle size analysis function using Watershed Packed Segments method to detect particles and identify particle height maxima

* Nominal values

Table D.2 Centrifugal liquid sedimentation: relevant instrumental and method details (as reported by the participants) for the measurements of ERM-FD102

Lab code	Instrument make	Type	Mode of operation	Rotational speed [rpm]	Type of optics	Laser wavelength [nm]	Density gradient		Sample volume [µL]	Calibrant		
							Type	Concentration interval [g/kg]		Type	Particle density [g/cm^3]	Assigned modal value [nm]
L1	Disc Centrifuge DC24000 (CPS Instruments Inc.)	Disc	Line-start	22000	Turbidity	405	Sucrose	80 to 240	300	PVC particles (CPS Instruments Inc.)	1.385	226
L3	Disc Centrifuge DC20000 (CPS Instruments Inc.)	Disc	Line-start	20000	Turbidity	405	Sucrose	20 to 80	300	PVC particles (CPS Instruments Inc)	1.385	223
L4	Disc Centrifuge DC20000 (CPS Instruments Inc.)	Disc	Line-start	20000	Turbidity	470	Sucrose	80 to 240	150	PVC particles (CPS Instruments Inc.)	1.385	377
L5	Optima XL-I (Beckman-Coulter)	Cuvette	Homogeneous	10000 20000 25000	Rayleigh interference	675	n.a.	n.a.	340	Counter balance cell	n.a.	n.a.
L7	Disc Centrifuge DC24000 (CPS Instruments Inc.)	Disc	Line-start	24000	Turbidity	470	Sucrose	80 to 240	500	Silica particles (Thermo Scientific)	1.83	490 ± 20
L10	Disc Centrifuge DC24000 (CPS Instruments Inc.)	Disc	Line-start	24000	Turbidity	470	Sucrose	80 to 1000	400	PVC particles (CPS Instruments Inc.)	1.385	377
L11	Optima XL-I (Beckman-Coulter)	Cuvette	Homogeneous	5000	Rayleigh interference	675	n.a.	n.a.	330	Counter balance cell	n.a.	n.a.
L14	Disc Centrifuge DC20000 (CPS Instruments Inc.)	Disc	Line-start	20000	Turbidity	405	Sucrose	80 to 240	1000	PVC particles (CPS Instruments Inc.)	1.385	377
L15	Disc Centrifuge DC20000 (CPS Instruments Inc.)	Disc	Line-start	20000	Turbidity	405	Sucrose	40 to 120	100	PVC particles (CPS Instruments Inc.)	1.385	223
L18	LUMiSizer 651 (LUM GmbH)	Cuvette	Homogeneous	4000	Turbidity	470	n.a.	n.a.	~ 1600	n.a.	n.a.	n.a.
L19	LUMiSizer 651 (LUM GmbH)	Cuvette	Homogeneous	4000	Turbidity	470	n.a.	n.a.	~ 1600	n.a.	n.a.	n.a.
L25	Disc Centrifuge DC24000 (CPS Instruments Inc.)	Disc	Line-start	24000	Turbidity	405	Sucrose	41 to 182	100	PVC particles (CPS Instruments Inc.)	1.385	263

n.a. = not applicable

Table D.3 Dynamic light scattering: relevant instrumental and method details (as reported by the participants) for the measurements of ERM-FD102

Lab code	Instrument type / make	Method	Laser			Detector		Sample cell			Data inversion algorithm	
			Source	Wave-length [nm]	Power [mW]	Type ‡	Angle [°]	Type	Cuvette dimension [mm]	Aliquot volume [mL]	Type	Regula-risation value
L2	Dawn Helios with WyattQELS	Correlation function analysis	GaAs linearly polarised	658	120	APD	90	Quartz glass microcuvette	10	0.15	Dynals	n.a.
L3	Malvern Zetasizer Nano ZS	Correlation function analysis	He-Ne	633	4	APD	173	Standard quartz glass cuvette	10	1	NNLS	0.01
L7	Coulter N4 PLUS Submicron Particle Sizer	Correlation function analysis	He-Ne	633	10	PMT	90	Standard polystyrene cuvette	10	4.7	SDP (CONTIN-based)	n.a.
L8	Malvern Zetasizer Nano ZS	Correlation function analysis	He-Ne	633	4	APD	173	Plastic disposable microcuvette	10	0.1	NNLS	0.001
L10	Malvern Zetasizer Nano ZS	Correlation function analysis	He-Ne	633	4	APD	173	Standard polystyrene cuvette	10	1	NNLS	0.001
L15	Malvern Zetasizer Nano ZS	Correlation function analysis	He-Ne	633	4	APD	173	UV transparent disposable cuvette	10	0.6	NNLS	0.01
L16	Sympatec NANOPHOX	3D-cross-correlation function analysis	He-Ne	633	10	PMT	90	Poly(methyl methacrylate) standard cuvette	10	0.3	NNLS	n.a.
L17a	Malvern Zetasizer Nano ZS	Correlation function analysis	He-Ne	633	4	APD	173	Standard quartz glass cuvette	10	1	NNLS	0.001
L17b	Malvern Zetasizer Nano ZS90	Correlation function analysis	He-Ne	633	4	APD	90	Standard quartz glass cuvette	10	1	NNLS	0.001
L20	Malvern Zetasizer Nano ZSP	Correlation function analysis	He-Ne	633	10	APD	173	Standard polystyrene cuvette	10	1	NNLS	0.001

L21a	Malvern HPPS	Correlation function analysis	He-Ne	633	3	APD	173	Polymethyl methacrylate standard cuvette	10	2	CONTIN-based	n.a.
L21b	Sympatec NANOPHOX	3D-cross-correlation function analysis	He-Ne	633	10	PMT	90	Poly(methyl methacrylate) standard cuvette	10	2	NNLS	n.a.
L22	Malvern Zetasizer Nano ZS	Correlation function analysis	He-Ne	633	4	APD	173	Standard polystyrene cuvette	10	1.2	NNLS	0.001
L23	Malvern Zetasizer Nano ZS	Correlation function analysis	He-Ne	633	4	APD	173	Standard polystyrene cuvette	10	3.5	NNLS	0.01
L24	Malvern Zetasizer Nano ZS	Correlation function analysis	He-Ne	633	4	APD	173	Poly(methyl methacrylate) standard cuvette	10	1.5	NNLS	0.001
L25	Malvern Zetasizer Nano ZS	Correlation function analysis	He-Ne	633	4	APD	173	Standard polystyrene cuvette	10	1	NNLS	0.001
L26	Coulter N4 PLUS Submicron Particle Sizer	Correlation function analysis	He-Ne	633	10	PMT	90	Poly(methyl methacrylate) standard cuvette	10	1.5	SDP (CONTIN-based)	n.a.
L28	Sympatec NANOPHOX	3D-cross-correlation function analysis	He-Ne	633	15	APD	90	Poly(methyl methacrylate) standard cuvette	10	2	NNLS	n.a.
L29	Horiba NanoPartica SZ-100Z	Correlation function analysis	Diode	532	10	PMT	90	UV transparent disposable microcuvette	5	0.05	Dynals	0.3
L30	Malvern Zetasizer Nano ZS	Correlation function analysis	He-Ne	633	4	APD	173	Standard quartz glass cuvette	10	3	NNLS	0.01

n.a. = not available or reported by participant

‡ APD, avalanche photodiode detector; PMT, photomultiplier tube

Table D.4 Electron microscopy: relevant instrumental and method details (as reported by the participants) for the measurements of ERM-FD102

Lab code	Instrument type Make Electron source	Acceleration voltage SEM working distance	Magnification calibration Metrological traceability	Specimen preparation	SEM electron detector type / TEM imaging mode	CCD camera type	Field of view [μm^2]	Image magnifi-cation [1000x]	Pixel size [nm]	Total number of particles counted	Image analysis software Image analysis strategy	Bin size [nm]
1a	TEM Philips Tecnai 10	80 kV	Pelco® optical diffraction cross-grating (No. 607) with 2160 lines/mm and 463 nm line spacing (Ted Pella, Inc.) Traceability statement not available	1000x diluted with ultrapure water 5 µL of diluted suspension brought onto Formvar® carbon-coated grid (Cu/Pd 300 mesh) and air dried in fume hood	n.a.	n.a.	A = 0.4 x 0.4 B = 3.2 x 2.4	A = 180 B = 26	A = 0.3 B = 2.4	n.a.	Tecnai User Interface Item solution Particles manually counted and measured	n.a.
1b	SEM JEOL JSM-7500F	3 kV 4 mm	Grid of 1000 mesh Traceability statement not available	100x diluted with ultrapure water (only for investigation of size class A) 20 µL of diluted suspension brought onto gold coated silicon chip and air dried in fume hood	n.a.	n.a.	A = 0.8 x 0.6 B = 4.0 x 6.0	A = 150 B = 30	A = 0.8 B = 3.9	n.a.	Analysis Station Particles manually counted and measured	n.a.
8	SEM FEI Helios Dual-Beam	5 kV 4 mm	NanoLattice™ standard with nominal 100 nm pitch (VLSI Standards, Inc.) Pitch size standard calibrated on metrological AFM, pitch value of	20 µL taken from the as-received material and 10x diluted with ultrapure water 50 µL of diluted suspension brought onto a single-crystal	Standard SE detector	n.a.	A = 0.4 x 0.4 B = 2.0 x2.0	A = 150 B = 30	A = 0.4 B = 1.9	A = 8947 B = 2019	ImageJ v1.47 Binarisation by baseline thresholding and automated particle size analysis and lognormal fit, particles touching each other or cut by image border were	A = < 0.1 B = < 0.1

			100.0 nm ± 1.5 nm (*k* = 2) traceable to SI Unit, metre	silicon chip that was pre-cleaned, etched and coated with poly-L-lysine							excluded	
9	TEM FEI Tecnai G2 Spirit LaB6	120 kV	Optical diffraction cross-grating (S106) with 2160 lines/mm and 463 nm line spacing (Agar Scientific) Traceability statement not available	500 µL taken from the as-received material and 500x diluted with ultrapure water Alcian blue pre-treated Pioloform® carbon-coated grid (Cu 400 mesh) placed on a drop (15 µL) of diluted suspension, 10 min incubation, washed and air dried	Bright-field with objective aperture of 150 µm	Eagle CCD Bottom-mount Pixels 4k x 4k	A = 2.4 x 2.4 B = 9.2 x 9.2	A = 18.5 B = 4.8	A = 0.6 B = 2.3	A = 64399 B = 2520	iTEM (Olympus Soft Imaging Solutions GmbH) and Sigmaplot® Manual grey-scale thresholding, 5x5 filter for reducing background noise (only for small particles) and automated particle size analysis, lognormal fit using Fityk software	A = < 0.1 B = 0.5
10	TEM Philips CM200 LaB6	80 kV	Optical diffraction cross-grating (No. 607) with 2160 lines/mm and 463 nm line spacing (Ted Pella, Inc.) Reference polystyrene particles with certified mean diameters of 112 nm (S130-1), 305 nm (S130-5) and 1036 nm (S130-7) (Plano GmbH) Traceability statement not available	2.5 µL of the as-received suspension brought onto a Carbon-coated grid (Cu 200 mesh) and vacuum dried	Bright-field with objective aperture of 20 µm	Olympus SIS Megaview II CCD Pixels 1k x 1k	A = 0.5 x 0.5 B = 2.1 x 2.1	A = 135 B = 34	A = 0.9 B = 3.8	A = 6503 B = 2034	iTEM (Olympus Soft Imaging Solutions GmbH) Manual optimisation of image brightness/contrast manual particle size analysis by approaching individual particles either by a 3-point circle (small) or a polygon (large)	A = 1 B = 4

11a	TEM Carl Zeiss Libra 120 LaB6	120 kV	Optical diffraction cross-grating (S106) with 2160 lines/mm and 463 nm line spacing) (Plano GmbH) Traceability statement not available	20 µL taken from the as-received material and 1000x and 400x diluted with ultrapure water for measuring the size of particles belonging to size class A and size class B, respectively 2 µL of the diluted suspension brought onto a carbon-coated grid (Cu 400 mesh) and air dried in a clean room	Bright-field with objective aperture of 30 µm	TRS slow scan CCD Pixels 2k x 2k	A = 0.7 x 0.7 B = 1.5 x 1.5	A = 40 B = 20	A = 0.3 B = 0.7	A = 6000 B = 1800	iTEM (Olympus Soft Imaging Solutions GmbH) Manual grey-scale thresholding, touching particles were manually excluded, particle sizes were automatically measured.	A = 0.1 B = 0.2
11b	SEM Carl Zeiss Neon-40-EsB FEG Schottky emitter ZrO/W	5 kV 5 mm	Critical dimension standard (IMS-HR 083641-01380) with certified pitch sizes (Plano GmbH) Certified pitch sizes traceable to SI Unit, metre	20 µL taken from the as-received material and 1000x and 400x diluted with ultrapure water for measuring the size of particles belonging to size class A and size class B, respectively 2 µL of the diluted suspension brought onto a carbon-coated grid (Cu 400 mesh) that was placed on a carbon pad and air dried in a clean room	In-lens SE, aperture of 30 µm	n.a.	A = 1.0 x 0.8 B = 1.0 x 0.8	A = 150 B = 100	A = 0.7 B = 1.1	A = 6000 B = 1800	iTEM and ImageJ Manual grey-scale thresholding, touching particles were manually excluded, particle sizes were automatically measured	A = 0.1 B = 0.2

16	SEM Carl Zeiss Ultra 55 Schottky (termal-assisted field emitter)	5 kV 4.5 mm	400 nm pitch spacing standard (Chinese Academy of Sciences) Pitch size standard SI traceably calibrated on metrological AFM	100 µL taken from the as-received material and 100x diluted with ultrapure water 20 µL of the diluted suspension brought onto a silicon chip	In-lens SE, aperture 30 µm	n.a.	A = 0.6 x 0.4 B = 3.8 x 2.8	A = 200 B = 30	A = 0.6 B = 3.7	A = 6187 B = 1976	SPIP Automated thresholding and particle size analysis	A = 1 B = 2
24	TEM LEO 912AB (nowadays Carl Zeiss) LaB6	120 kV	Mag*I*Cal single-crystal silicon reference standard (Technoorg-Linda Ltd.) Traceable to SI Unit, metre, through interplanar lattice spacing of a silicon crystal	100 µL taken from the as-received material and 20x diluted with ultrapure water 7 µL of the diluted suspension brought onto a Pioloform® carbon-coated grid (Cu 200 mesh)	Bright-field with objective aperture of 500 µm	Slow scan CCD Pixels 2k x 2k	A = 1.0 x 1.0 B = 2.0 x 2.0	A = 20 B = 10	A = 0.5 B = 0.9	A = 10336 B = 2676	iTEM version 5.2 (Olympus Soft Imaging Solutions GmbH) 5x5 filter, grey-scale thresholding, particles cut by the field of view were omitted, particles manually selected and analysed	A = 1.4 B = 1.6
25	TEM JEOL 2100 LaB6	100 kV	Colloidal silica certified reference material ERM-FD100 (IRMM) Certified value and uncertainty, 19.4 nm ± 1.3 nm (k = 2) traceable to SI Unit, metre	5 µL taken from the as-received material and 2000x diluted with 0.1 µm filtered ultrapure water (18.2 MΩ.cm) 200 µL of the diluted suspension nebulised onto a Lacey carbon coated grid (Cu 400 mesh), 10 min of initial drying in fume	Bright-field with objective aperture of 40 µm	Gatan Ultrascan 1000 CCD Pixels 2k x 2k	A = 0.7 x 0.7 B = 0.7 x 0.7	A = 30 B = 30	A = 0.7 B = 0.7	A = 14378 B = 1583	ImageJ version 1.45s Semi-automated particle detection, manual setting of contrast and brightness, 7x7 filter, particles touching or cut by field of view excluded from analysis	A = 1.0 B = 1.0

				hood followed by > 1 hr drying in cytotoxic cabinet								
27	TEM JEOL JEM-1011 W filament	80 kV	Catalase crystal diffraction standard with lattice spacing of 8.6 nm ± 0.2 nm Traceability statement not available	100 µL taken from the as-received material and 200x diluted with ultrapure water 10 µL of the diluted suspension brought onto a carbon coated grid (Cu 200 mesh), incubated for 1 min, excess liquid blotted, after drying 10 µL of uranyl acetate for negative colouring, 30 s of incubation and excess liquid removed with filter paper	Bright-field with objective aperture of 50 µm	Olympus SIS Keenview II CCD Pixels 1k x 1k	A = 1.0 x 1.3 B = 3.8 x 5.0	A = 20 B = 5	A = 1.0 B = 3.8	A = 7748 B = 744	Scandium SIS (Olympus Soft Imaging Solutions GmbH) Touching particles were automatically excluded from analysis based on aspect ratio and sphericity	A = 3.0 B = 5.0

A = size class A

B = size class B

Pioloform® = polyvinyl butyral

Formvar® = polyvinyl formal

Table D.5 Particle tracking analysis: relevant instrumental and method details (as reported by the participants) for the measurements of ERM-FD102

Lab code	Instrument type / make	Aliquot preparation	Laser			Camera Type	Aliquot volume [mL]	Measurement duration [s]	Camera shutter	Analysis software	Bin width [nm]
			Source	Wave-length [nm]	Power [mW]						
L6	NanoSight NS500	Aliquots were prepared in a class II cabinet. Test portions were taken from the ampoule with a clean pipette using a new tip for each aliquot. 10 µL of the as-received material was gravimetrically diluted 1000-5000 times with ultrapure water that was passed through a PVDF membrane syringe filter with nominal pore sizes of 0.1 µm.	Diode	405	< 60	EMCCD	0.25	60	636	NTA2.2	4
L12	NanoSight LM10HSB	10 µL test portions taken from the ampoules were 5000x diluted in pre-filtrated ultrapure water that was passed through a filter with nominal pore sizes of 0.1 µm.	Diode	405	< 40	sCMOS	0.5	90	n.a.	NTA2.3	n.a.
L16	NanoSight LM20	10 µL of the as-received material was diluted (1000x to 2000x) by ultrapure water. Sample preparation was done in a clean room (class 6).	Diode	638	40	CCD	0.25	60	n.a.	n.a.	n.a.

Table D.6 Small-angle X-ray scattering: relevant instrumental and method details (as reported by the participant) for the measurements of ERM-FD102

Lab code	Instrument type / make	Aliquot preparation	X-ray generator	X-ray source	Detector	Sample holder	Scattering angular range [°]	Aliquot volume [µL]
L13	SAXSess	Test samples were analysed as-received. Before loading of the capillary, each capillary was rinsed with tap water for 30 s then rinsed with *iso*-propanol and air-dried.	General Electric ID3003	Sealed tube, Cu-Kα λ = 0.1542 nm, 40 kV, 50 mA, line collimation	Mythen 1k, strip size 50 µm	Quartz capillary	0.03-2.84	25

Table D.7 Asymmetrical flow field-flow fractionation: relevant instrumental and method details (as reported by the participant) for the measurements of ERM-FD102

Lab code	Instrument type / make	Aliquot preparation	Measurement parameters	Calibration	Signal evaluation
L11	- Agilent Infinity 1260 isochratic pump - Wyatt DUALTEC separation system - Wyatt Dawn 8^+ multi-angle laser light detector - Agilent Infinity 1260 refractive index detector	Test samples were diluted to 1 mg/mL using ultrapure water	Channel length: 17.3 cm Elution flow: 1.0 mL/min Cross flow: 0.5 mL/min Focus position: 12.4 % Solvent viscosity: 1.157 mPa s Elution flow: 1.0 mL/min	Polystyrene standard 40 nm ± 1 nm	FFF theory

Table D.8 Zeta potential, pH and electrolytic conductivity: relevant instrumental and method details (as reported by the participant) for the measurements of ERM-FD102

Lab code	Physical property	Instrument type / make / specifications	Aliquot preparation	Instrument calibration	Sample holder	Aliquot volume [mL]
L3	Zeta potential	Malvern Zetasizer Nano ZS Light source: He-Ne Power 4 mW Wavelength 633 nm Detector: APD 13° angle Model: Smoluchowski	Test samples were analysed as-received. Before loading of the sample, the measurement cell was pre-rinsed with ethanol of analytical grade and abundantly rinsed with ultrapure water.	n.a.	Polycarbonate folded capillary cell with gold-plated beryllium/copper electrodes	0.85
L3	pH	744 pH Meter (Metrohm AG) Solitrode electrode with Pt1000 temperature sensor (Metrohm AG)	Test samples were analysed as-received.	2-point calibration using buffer solutions (Metrohm AG) with nominal pH values of 9.00 ± 0.02 (art. no. 6.2305.030) and 4.00 ± 0.02 (art. no. 6.2305.010)	Glass beaker	3
L3	Electrolytic conductivity	InoLab Cond730 (WTW Wissenschaftlich-Technische Werkstätten)	Test samples were analysed as-received	The cell constant was determined using a 0.01 mol/L KCl solution (Certipur®, Merck KGaA) with assigned electrolytic conductivity of 1.41 mS/cm.	Glass beaker	6

Annex E1: Results of the characterisation measurements – AFM

Table E1-1 Modal maximum particle height results associated to size class A of the number-based PSD, obtained by AFM

Lab-code	Replicate results [nm]						Mean [nm]	*s* [1] [nm]	*U* [2] [nm]
	1	2	3	4	5	6			
L15	16	18	18	18	14	17	17	2	4
L25	18	17	16	16	16	18	17	1	1

[1] Standard deviation of the individual replicate results

[2] Expanded (k = 2) uncertainty as reported by the participant

Table E1-2 Modal maximum particle height results associated to size class B of the number-based PSD, obtained by AFM

Lab-code	Replicate results [nm]						Mean [nm]	*s* [1] [nm]	*U* [2] [nm]
	1	2	3	4	5	6			
L15	79	79	76	81	78	79	79	2	19
L25	82	84	80	79	81	82	81	2	3

[1] Standard deviation of the individual replicate results

[2] Expanded (k = 2) uncertainty as reported by the participant

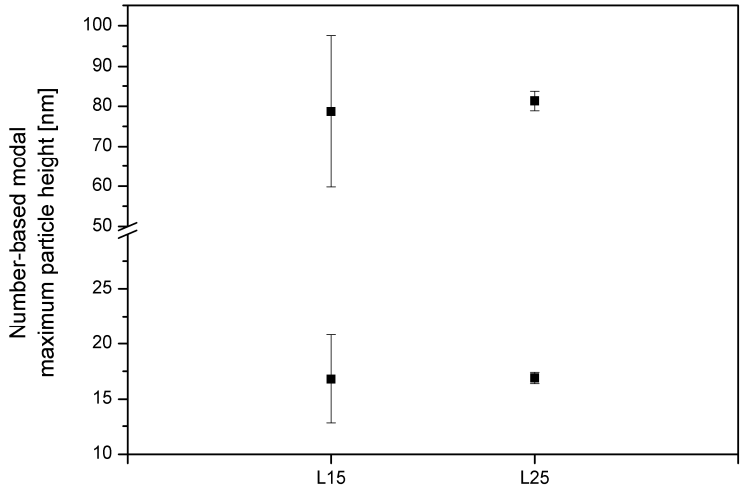

Fig. E1 Laboratory mean values of the number-weighted modal maximum particle heights as obtained by two laboratories by AFM; the error bars indicate the expanded (k = 2) measurement uncertainties as reported by the participants

Laboratory 15 performed all requested measurements according to the provided measurement scheme and successfully analysed the QC sample. The obtained QC result (mean of two replicate results) of 78.5 nm ± 18.8 nm (k = 2) agreed with the assigned value (81.0 nm ± 3.0 nm) of the polystyrene latex QC sample (3080A). All results were reported with a relative standard measurement uncertainty of 12 %. The laboratory estimated this measurement uncertainty by combining uncertainty contributions from method repeatability (2 %), intermediate precision (2 %), calibration (6 %) and deformation bias (10 %). The latter uncertainty component covers the elastic deformation that occurs during tip-sample contact. The precision of the method was assessed by repeatedly imaging and measuring 20 nm gold nanoparticles during different days.

Laboratory 25 performed all requested measurements according to the provided measurement scheme and successfully analysed the QC sample. The obtained QC result (mean of two replicate results) of 79.8 nm ± 2.4 nm (k = 2) agreed with the assigned value (81.0 nm ± 3.0 nm) of the polystyrene latex QC sample (3080A). The results for size class A and size class B were reported with relative standard measurement uncertainties of 1.6 % and 1.5 %, respectively. These uncertainties were estimated by the laboratory by combining uncertainty contributions from repeatability (0.7 % for size class A and 0.4 % for size class B), intermediate precision (1.4 % for size class A and size class B) and trueness (< 0.1 % for size class A and size class B). The uncertainty due to repeatability was estimated by dividing the standard deviation of a set of mean particle heights determined from a series of images of the same sample area by the average of those mean particle heights. The uncertainty due to day-to-day variation or intermediate precision was estimated by dividing the standard deviation of a set of step heights determined from measurements of the same step height artefact (20.0 nm ± 0.9 nm) taken on different days by the average of the set of measured step heights. The uncertainty associated to the method trueness was estimated from the two step-height gratings that were used to calibrate the height response of the AFM instrument.

Annex E2: Results of the characterisation measurements – CLS

Table E2-1 Light extinction intensity-weighted modal Stokes' particle diameter results associated to size class A of the PSD, obtained by CLS with turbidimetric detection

Lab-code	Replicate results [nm]						Mean [nm]	s [1] [nm]	U [2] [nm]
	1	2	3	4	5	6			
L1	25.1	25.2	25.5	25.0	25.0	25.0	25.2	0.2	7.3
L3*	23.6	24.3	24.0	23.8	23.7	23.9	23.9	0.3	3.8
L7	23.6	23.9	26.4	26.2	24.6	24.7	24.9	1.2	2.8
L10	23.9	23.7	22.2	25.5	23.4	24.8	23.9	1.1	2.9
L14	27.0	26.1	24.8	26.1	27.2	25.4	26.1	0.9	4.4
L15	22.9	23.1	22.8	23.1	22.6	22.8	22.9	0.2	2.8
L19	20.2	20.0	19.5	20.0	19.5	19.9	19.9	0.3	0.4
L25	24.2	24.1	23.7	24.5	24.4	24.3	24.2	0.3	1.9
Results not used for certification									
L18	19.5	20.0	18.6	19.5	19.7	19.4	19.5	0.5	0.4

[1] Standard deviation of the individual replicate results

[2] Expanded (k = 2) uncertainty as reported by the participant

[*] L3 provided nine replicate results, additionally including 24.4 nm, 23.8 nm, 23.7 nm

Table E2-2 Light extinction intensity-weighted modal Stokes' particle diameter results associated to size class B of the PSD, obtained by CLS with turbidimetric detection

Lab-code	Replicate results [nm]						Mean [nm]	s [1] [nm]	U [2] [nm]
	1	2	3	4	5	6			
L1	90.7	90.5	91.2	91.2	90.4	90.6	90.8	0.4	7.1
L3*	87.9	88.6	88.0	88.2	88.2	88.5	88.3	0.2	14.1
L7	80.0	80.5	79.2	81.8	82.5	82.5	81.1	1.4	8.9
L10	99.0	96.1	92.0	93.9	92.0	96.6	94.9	2.8	13.7
L14	88.1	88.4	86.8	88.9	88.2	88.3	88.1	0.7	13.4
L15	86.4	86.0	86.2	86.0	86.2	86.2	86.2	0.2	10.4
L19	88.2	86.0	83.8	85.8	83.8	87.9	85.9	1.9	1.7
L25	88.8	88.6	88.3	88.8	88.8	88.5	88.6	0.2	6.4
Results not used for certification									
L18	83.6	85.3	83.9	84.4	81.5	83.7	83.7	1.3	1.7

[1] Standard deviation of the individual replicate results

[2] Expanded (k = 2) uncertainty as reported by the participant

[*] L3 provided nine replicate results, additionally including 88.1 nm, 88.4 nm, 88.5 nm

Table E2-3 Light extinction intensity-weighted modal Stokes' particle diameter results associated to size class A of the PSD, obtained by CLS with Rayleigh interference optics

Lab-code	Replicate results [nm]						Mean [nm]	*s* [1)] [nm]	*U* [2)] [nm]
	1	2	3	4	5	6			
L5	17.7	17.7	17.7	17.4	17.4	17.5	17.6	0.2	0.2
L11	18.4	18.4	18.7	18.1	18.9	18.4	18.5	0.3	0.7

[1)] Standard deviation of the individual replicate results

[2)] Expanded (k = 2) uncertainty as reported by the participant

Table E2-4 Light extinction intensity-weighted modal Stokes' particle diameter results associated to size class B of the PSD, obtained by CLS with Rayleigh interference optics

Lab-code	Replicate results [nm]						Mean [nm]	*s* [1)] [nm]	*U* [2)] [nm]
	1	2	3	4	5	6			
L5	91.5	89.9	91.3	89.6	89.9	87.0	89.9	1.6	3.3
L11	86.0	88.3	89.6	87.0	86.4	85.1	87.1	1.6	3.2

[1)] Standard deviation of the individual replicate results

[2)] Expanded (k = 2) uncertainty as reported by the participant

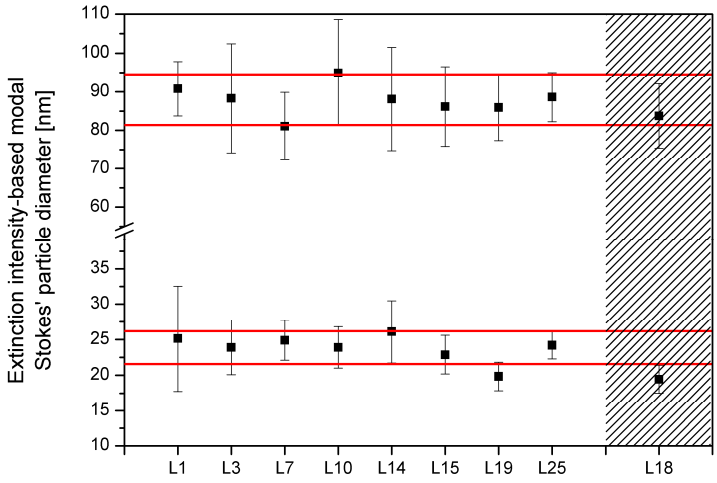

Fig. E2-1 Laboratory mean values of the light extinction intensity-weighted modal particle diameters as obtained by nine laboratories by CLS with turbidimetric detection; the error bars indicate the expanded (k = 2) measurement uncertainties as reported by the participants; the two sets of horizontal lines reflect the certified ranges; technically invalid results are indicated in the hatched region

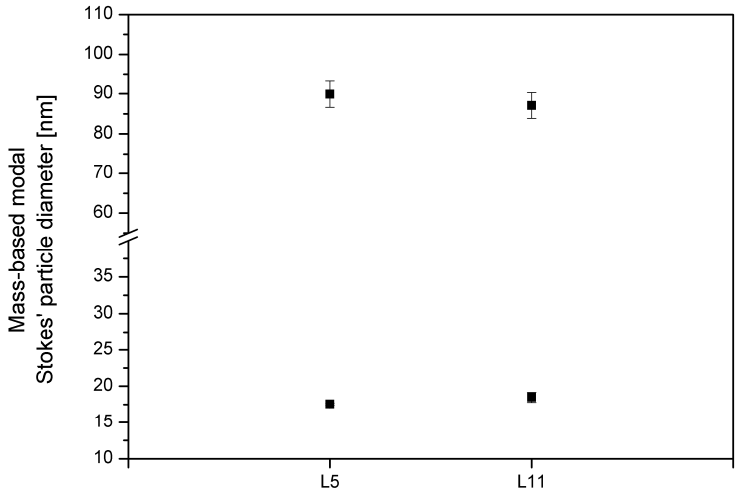

Fig. E2-2 Laboratory mean values of the mass-weighted modal particle diameters as obtained by two laboratories by CLS with Rayleigh interference optics; the error bars indicate the expanded (k = 2) measurement uncertainties as reported by the participants

Laboratory 1 performed all measurements according to the provided measurement protocol and successfully analysed the monomodal colloidal silica QC sample (ERM-FD304). The obtained QC result (mean of six replicate results) of 34.7 nm ± 8.2 nm (k = 2) agreed with the certified value (33.0 nm ± 3.0 nm) of the QC sample. For ERM-FD102, the modal results of size class A and size class B of the PSD were reported with relative standard measurement uncertainties of 14.4 % and 3.9 %, respectively. These combined uncertainties were estimated from method precision and trueness studies.

Laboratory 3 performed all measurements according to the provided measurement protocol and successfully analysed the monomodal colloidal silica QC sample (ERM-FD304). The obtained QC result (mean of two replicate results) of 32.4 nm ± 4.7 nm (k = 2) agreed with the certified value (33.0 nm ± 3.0 nm) of the QC sample. For ERM-FD102, the modal results of size class A and size class B were reported with a relative standard measurement uncertainty of 8.0 %. These uncertainties were estimated following a top-down approach whereby the standard uncertainties from method trueness, precision, calibration and effective particle density were combined.

Laboratory 4 performed all measurements according to the provided measurement protocol, but reported results only on a volume-basis. In addition, the monomodal colloidal silica QC sample (ERM-FD304) could not be successfully analysed. The obtained QC result (mean of two replicate results) of 63 nm significantly differed from the certified value (33.0 nm ± 3.0 nm) of the QC sample. As a result, the submitted dataset for ERM-FD102 was considered to be technically invalid and was therefore not included in the value assignment procedure.

Laboratory 5 performed all measurements according to the provided measurement protocol and successfully analysed the monomodal polystyrene latex QC sample (3080A). The obtained QC result (mean of two replicate results) of 80.0 nm ± < 0.1 nm (two times standard deviation) agreed with the assigned value (81.0 nm ± 3.0 nm) of the QC sample. The reported relative standard measurement uncertainties for the mode of size class A and size class B of the PSD of ERM-FD102 were 0.4 % and 1.8 %, respectively. These uncertainties are based on the combined contributions from intermediate precision and trueness. The

results from a previous ILC study, during which a homogeneous and stable monomodal colloidal silica test material was analysed, were used to estimate the uncertainty for intermediate precision. The uncertainty for method trueness was calculated from limited measurements performed on a polystyrene latex size standard (102 nm ± 3.0 nm).

Laboratory 7 performed all measurements according to the provided measurement protocol and successfully analysed the monomodal colloidal silica QC sample (ERM-FD304). The obtained QC result (mean of two replicate results) of 30.3 nm ± 3.3 nm (k = 2) agreed with the certified value (33.0 nm ± 3.0 nm) of the QC sample. For ERM-FD102, the modal results of size class A and size class B were reported with a relative standard measurement uncertainty of 5.5 %. These uncertainties were estimated following a bottom-up approach whereby the standard uncertainties from calibration, instrument operation and handling were combined.

Laboratory 10 performed all measurements according to the provided measurement protocol and successfully analysed the monomodal colloidal silica QC sample (ERM-FD304). The obtained QC result (mean of two replicate results) of 35.3 nm ± 2.0 nm (k = 2) agreed with the certified value (33.0 nm ± 3.0 nm) of the QC sample. For ERM-FD102, the modal results of size class A and size class B of the intensity-based PSD were reported with a relative standard measurement uncertainty of 6.1 % and 7.2 %, respectively. These uncertainties were estimated following a top-down approach whereby the standard relative uncertainties from intermediate precision (2.9 %) and trueness (5.4 %) were combined.

Laboratory 11 performed all measurements according to the provided measurement protocol and successfully analysed the monomodal polystyrene latex QC sample (3080A). The obtained QC result (mean of two replicate results) of 80.2 nm ± 3.0 nm (k = 2) agreed with the assigned value (81.0 nm ± 3.0 nm) of the QC sample. The reported relative standard measurement uncertainty (1.8 %) was based mainly on the method's trueness which was evaluated from measurement results obtained on a polystyrene latex standard with assigned particle size value of 199 nm.

Laboratory 14 performed all measurements according to the provided measurement protocol and successfully analysed the monomodal colloidal silica QC sample (ERM-FD304). The obtained QC result (mean of two replicate results) of 34.6 nm ± 0.6 nm (two times standard deviation) agreed with the certified value (33.0 nm ± 3.0 nm) of the QC sample. For ERM-FD102, the modal results of size class A and size class B of the intensity-based PSD were reported with a relative standard measurement uncertainty of 8.5 % and 7.6 %, respectively. These uncertainties include a contribution from method trueness (7.5 %).

Laboratory 15 performed all measurements according to the provided measurement protocol and successfully analysed the monomodal colloidal silica QC sample (ERM-FD304). The obtained QC result (mean of two replicate results) of 32.4 nm ± 3.9 nm (k = 2) agreed with the certified value (33.0 nm ± 3.0 nm) of the QC sample. For ERM-FD102, the modal results of size class A and size class B of the intensity-based PSD were reported with a relative standard measurement uncertainty of 6.0 %. These uncertainties were estimated following a top-down approach whereby the standard relative uncertainties from repeatability (1.5 %), intermediate precision (0.5 %) and trueness (6.0 %) were combined. In the evaluation of the trueness uncertainty, the laboratory assumed that the values provided by the ILC measurement protocol for the effective particle density of both the QC and ERM-FD102 samples were correct within 2 % and 2.5 %, respectively. An additional potential source of uncertainty is the lack of accurate knowledge of the shape of the particles. For the given study, the shape of the particles is assumed to be spherical, whereas this might not be the case. However, the uncertainty associated with non-sphericity should be less than 5 % in diameter for rigid particles of uniform density. Another source of uncertainty may come from the fact that the nanoparticles of the QC and ERM-FD102 samples are different in size and density compared to the PVC calibrant and therefore experience a subtly different

sedimentation regime within the CLS instrument. Detailed analysis indicates that this effect contributes for less than 1 % uncertainty.

Laboratory 18 performed all measurements according to the provided measurement protocol, however, the monomodal polystyrene latex QC sample (3080A) could not be successfully analysed. The obtained QC result (mean of two replicate results) of 68.5 nm ± 1.4 nm (k = 2) significantly differed from the assigned value (81.0 nm ± 3.0 nm) of the QC sample. As a result, the credibility of the submitted dataset could not be guaranteed and was hence excluded from the study.

Laboratory 19 performed all measurements according to the provided measurement protocol and successfully analysed the monomodal polystyrene latex QC sample (3080A). The obtained QC result (mean of two replicate results) of 79.8 nm ± 1.6 nm (k = 2) agreed with the assigned value (81.0 nm ± 3.0 nm) of the QC sample. The low relative expanded measurement uncertainty is due to the fact that the instrument (cuvette type) does not require calibration with a particle size standard. For ERM-FD102, the modal results of size class A and size class B of the intensity-based PSD were reported with a relative standard measurement uncertainty of 5 %. The estimation of the measurement uncertainty has been done on the basis of participation to an ILC of a previous certification study (ERM-FD100) and an in-house study where a control material (colloidal silica with nominal particle size of 0.5 μm) was measured with six similar CLS instruments. The instruments varied from each other with respect to their optical system (wavelength of the laser light, optical path length).

Laboratory 25 performed all measurements according to the provided measurement protocol and successfully analysed the monomodal colloidal silica QC sample (ERM-FD304). The obtained QC result (mean of two replicate results) of 33.0 nm ± 2.5 nm (k = 2) agreed with the certified value (33.0 nm ± 3.0 nm) of the QC sample. For ERM-FD102, the modal results of size class A and size class B of the intensity-based PSD were reported with a relative standard measurement uncertainty of 3.9 %. These uncertainties include contributions from method repeatability, intermediate precision and trueness. Whereas the relative standard uncertainties for repeatability and intermediate precision are about 1 %, it was found that the major source of uncertainty (about 3 %) stemmed from the CRM that was used for trueness assessment. In addition to the two modes of size class A and size class B, the laboratory reported the presence of third small mode with modal value of 47.6 nm ± 3.5 nm (k = 2) which could be clearly distinguished from the other modes. Compared to the relative contributions (in terms of extinction intensity) from the two other particle populations, the third mode is rather negligible.

Annex E3: Results of the characterisation measurements – DLS

Table E3-1 Light scattering intensity-weighted arithmetic mean particle diameter results associated to size class A of the PSD, obtained by DLS

Lab-code	Aliquot mean results [nm]									Mean [nm]	s [1] [nm]	U [2] [nm]
	1	2	3	4	5	6	7	8	9			
L3	16.5	16.4	17.0	16.8	16.6	17.3	16.7	16.7	16.8	16.8	0.3	1.6
L7	18.8	20.3	*	18.8	20.3	19.3	21.4	19.6	26.0	20.6	2.4	1.9
L8	17.2	16.4	16.7	16.8	16.4	17.3	17.0	17.2	17.1	16.9	0.4	2.2
L10	17.3	17.8	17.7	17.7	17.4	17.4	17.2	17.6	17.4	17.5	0.2	0.3
L15	17.2	17.4	16.8	17.2	17.4	17.1	17.1	18.0	16.8	17.2	0.4	5.6
L17a	18.1	17.3	18.4	17.4	17.5	17.3	17.7	17.3	17.8	17.7	0.4	4.2
L17b	17.4	17.0	17.6	16.5	17.1	15.4	16.7	17.8	16.6	16.9	0.7	4.2
L20	18.8	17.4	17.8	18.1	17.4	17.1	18.4	17.9	17.2	17.8	0.6	4.2
L21a	18.3	17.9	18.1	18.0	17.8	17.9	16.5	18.5	17.1	17.8	0.6	2.2
L22	17.5	17.8	17.8	17.8	17.6	17.6	17.8	17.6	17.7	17.7	0.1	0.4
L23	18.7	18.3	17.6	17.9	18.1	18.5	18.4	18.3	18.7	18.3	0.4	1.2
L24	17.4	18.2	18.4	17.4	17.3	18.0	17.4	17.1	17.7	17.7	0.5	1.4
L25	17.9	17.6	17.6	17.4	18.1	18.0	17.4	18.0	17.8	17.8	0.3	2.9
L26	17.3	18.5	17.7	17.7	17.5	17.7	19.3	18.7	18.7	18.1	0.7	1.5
L28	18.5	17.8	17.2	17.0	16.6	16.6	17.2	16.4	16.9	17.1	0.7	0.9
L29	18.8	18.6	18.7	18.3	18.5	18.2	18.3	18.6	18.7	18.5	0.2	1.0
L30	17.6	18.8	17.5	18.2	17.8	18.4	17.4	18.9	17.8	18.0	0.6	0.8
Results not used for certification												
L2	n.d.	n.d.	n.d.	n.d.	n.d.	n.d.	n.d.	n.d.	n.d.	n.a.	n.a.	n.a.

[1] Standard deviation of the mean aliquot results

[2] Expanded (k = 2) uncertainty as reported by the participant

n.d. = not detectable, amount of light scattering below method's limit of detection

* technically invalid result

Table E3-2 Light scattering intensity-weighted arithmetic mean particle diameter results associated to size class B of the PSD, obtained by DLS

Lab-code	Aliquot mean results [nm]									Mean [nm]	s [1] [nm]	U [2] [nm]
	1	2	3	4	5	6	7	8	9			
L3	87.7	87.7	88.7	88	87.8	88.9	88.3	88	88.7	88.2	0.5	3.7
L7	87.3	89.5	*	89.4	89.4	88.7	90.7	89.7	94.0	89.8	1.9	8.4
L8	82.8	82.1	82.0	82.7	81.6	83.5	82.8	82.9	83.2	82.6	0.6	4.5
L10	88.6	89.2	89.3	89.8	88.3	88.8	88.4	89.1	88.7	88.9	0.5	1.6
L15	88.8	89.5	89.7	89.2	90.2	89.2	89.5	90.5	89.3	89.5	0.5	18.0
L17a	89.6	88.4	90.1	88.6	89.0	88.4	89.5	88.4	88.8	89.0	0.6	6.8
L17b	90.4	91.0	91.7	89.6	89.7	83.6	90.1	90.7	90.4	89.7	2.4	6.8
L20	89.8	88.4	88.9	89.8	88.5	87.4	89.2	88.3	87.8	88.7	0.8	6.8
L21a	88.3	89.7	89.5	89.7	88.5	88.9	86.5	89.4	87.4	88.6	1.1	5.0
L22	88.2	88.2	88.0	88.9	89.1	89.0	88.4	88.1	88.6	88.5	0.4	7.1
L23	90.5	90.2	88.8	89.1	89.4	90.4	90.0	89.9	91.0	89.9	0.7	2.0
L24	88.5	89.5	90.9	89.8	88.3	90.1	88.4	87.2	88.7	89.0	1.1	6.8
L25	89.9	89.0	88.5	88.4	89.5	88.8	90.4	89.5	89.1	89.2	0.7	7.6
L26	85.1	87.5	84.0	84.5	84.3	83.1	88.1	86.0	86.3	85.4	1.7	6.9
L28	88.1	85.6	84.2	86.3	83.9	83.5	85.9	85.0	85.6	85.3	1.4	2.9
L29	94.6	92.9	92.5	90.4	92.2	89.8	91.9	91.8	91.4	92.0	1.4	3.8
L30	89.1	90.0	87.9	89.9	89.2	90.7	87.9	89.9	89.5	89.3	0.9	3.6
Results not used for certification												
L2	83.2	84.6	83.5	83.3	83.3	79.7	77.8	79.8	83.6	82.1	2.4	13.2

[1] Standard deviation of the mean aliquot results

[2] Expanded (k = 2) uncertainty as reported by the participant

* technically invalid result

Table E3-3 Light scattering intensity-weighted harmonic mean particle diameter results associated to size class A of the PSD, obtained by DLS

Lab-code	Aliquot mean results [nm]									Mean [nm]	s [1] [nm]	U [2] [nm]
	1	2	3	4	5	6	7	8	9			
L28	17.4	16.8	16.2	16.5	15.8	16.0	16.4	16.0	16.5	16.4	0.5	2.7
L29	18.5	18.2	18.3	18.0	18.2	17.9	17.9	18.3	18.4	18.2	0.2	1.0

[1] Standard deviation of the mean aliquot results

[2] Expanded (k = 2) uncertainty as reported by the participant

Table E3-4 Light scattering intensity-weighted harmonic mean particle diameter results associated to size class B of the PSD, obtained by DLS

Lab-code	Aliquot mean results [nm]									Mean [nm]	s [1] [nm]	U [2] [nm]
	1	2	3	4	5	6	7	8	9			
L28	87.6	85.0	83.7	86.1	83.6	83.1	85.6	84.8	85.4	85.0	1.4	6.0
L29	86.6	85.3	84.4	83.7	85.0	83.1	84.1	85.1	84.0	84.6	1.0	2.9

[1] Standard deviation of the mean aliquot results

[2] Expanded (k = 2) uncertainty as reported by the participant

Table E3-5 Light scattering intensity-weighted geometric mean particle diameter results associated to size class A of the PSD, obtained by DLS

Lab-code	Aliquot mean results									Mean	s [1]	U [2]
	1	2	3	4	5	6	7	8	9			
L28	18.0	17.3	16.7	16.8	16.2	16.3	16.8	16.2	16.7	16.8	0.6	2.7

[1] Standard deviation of the mean aliquot results

[2] Expanded (k = 2) uncertainty as reported by the participant

Table E3-6 Light scattering intensity-weighted geometric mean particle diameter results associated to size class B of the PSD, obtained by DLS

Lab-code	Aliquot mean results [nm]									Mean [nm]	s [1] [nm]	U [2] [nm]
	1	2	3	4	5	6	7	8	9			
L28	87.9	85.3	84.0	86.2	83.8	83.3	85.8	84.9	85.5	85.2	1.4	6.0

[1] Standard deviation of the mean aliquot results

[2] Expanded (k = 2) uncertainty as reported by the participant

Table E3-7 Light scattering intensity-weighted modal particle diameter results associated to size class A of the PSD, obtained by DLS

Lab-code	Aliquot mean results [nm]									Mean [nm]	s [1] [nm]	U [2] [nm]
	1	2	3	4	5	6	7	8	9			
L16	18.4	17.8	18.8	17.8	19.0	17.7	17.9	18.8	18.3	18.3	0.5	1.6
L21a	17.6	17.2	17.5	17.5	16.9	17.4	15.9	18.1	16.5	17.2	0.7	2.3
L21b	14.7	16.7	16.0	18.7	17.5	18.4	16.5	16.9	18.0	17.0	1.3	1.4

[1] Standard deviation of the mean aliquot results

[2] Expanded (k = 2) uncertainty as reported by the participant

Table E3-8 Light scattering intensity-weighted modal particle diameter results associated to size class B of the PSD, obtained by DLS

Lab-code	Aliquot mean results [nm]									Mean [nm]	s [1] [nm]	U [2] [nm]
	1	2	3	4	5	6	7	8	9			
L16	88.7	88.5	89.2	86.6	89.1	87.3	86.9	89.1	86.0	87.9	1.2	5.1
L21a	79.5	79.9	79.5	82.2	78.0	80.4	75.6	81.5	75.4	79.1	2.4	8.5
L21b	81.1	77.6	81.5	88.6	81.0	81.4	81.3	84.0	87.8	82.7	3.5	25.8

[1] Standard deviation of the mean aliquot results

[2] Expanded (k = 2) uncertainty as reported by the participant

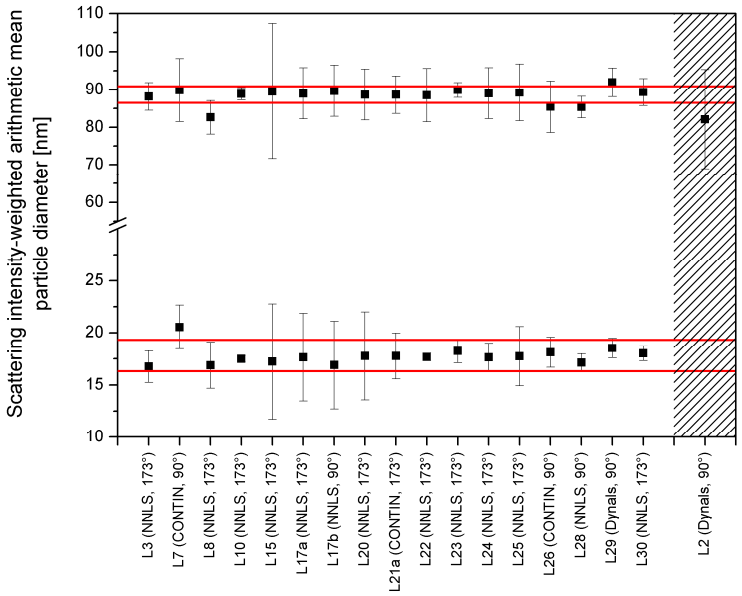

Fig. E3-1 Laboratory mean values of the light scattering intensity-weighted arithmetic mean particle diameters as obtained by 17 laboratories by DLS, the error bars indicate the expanded (k = 2) measurement uncertainties as reported by the participants, the two sets of horizontal lines reflect the certified ranges, technically invalid results are indicated in the hatched region

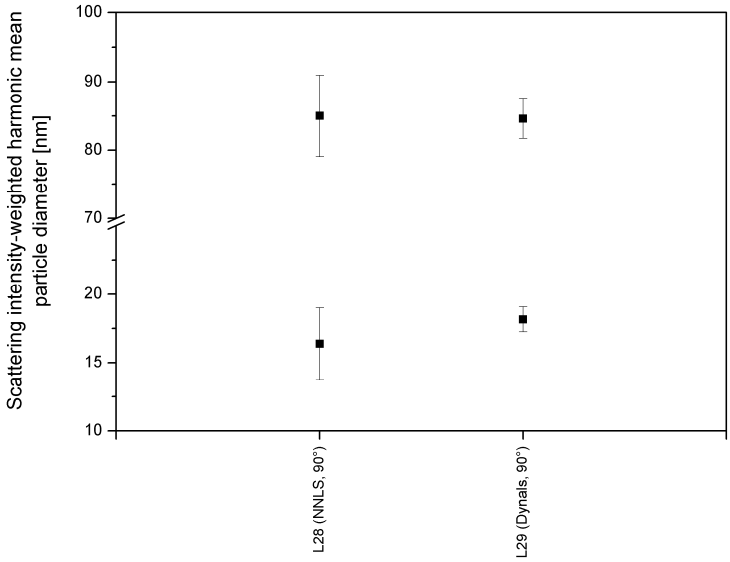

Fig. E3-2 Laboratory mean values of the light scattering intensity-weighted harmonic mean particle diameters as obtained by two laboratories by DLS, the error bars indicate the expanded (k = 2) measurement uncertainties as reported by the participants

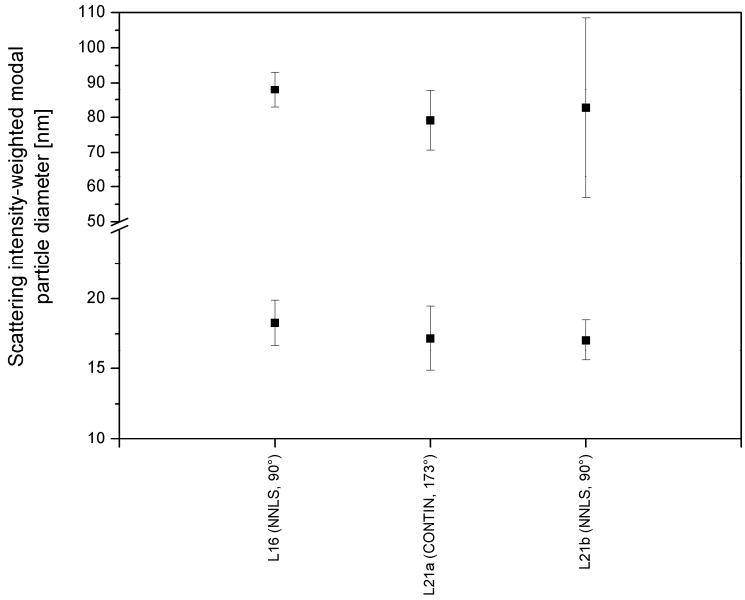

Fig. E3-3 Laboratory mean values of the light scattering intensity-weighted modal particle diameters as obtained by two laboratories by DLS, the error bars indicate the expanded (k = 2) measurement uncertainties as reported by the participants

Laboratory 2 performed all measurements according to the provided measurement protocol. Measurements were conducted at 29 °C, the obtained results were corrected for a temperature of 25 °C. The monomodal colloidal silica QC sample (ERM-FD304) could not be successfully analysed. The obtained QC result (mean of three replicate results) of 33.7 nm ± 5.4 nm (k = 2) significantly differed from the assigned value (42.1 nm ± 0.3 nm) of the QC sample. As a result, the credibility of the submitted dataset could not be guaranteed and was therefore excluded from the value assignment procedure.

Laboratory 3 performed all measurements according to the provided measurement protocol and successfully analysed the monomodal colloidal silica QC sample (ERM-FD304). The obtained QC result (mean of two aliquot means; three consecutive measurements per aliquot) of 42.2 nm ± 0.8 nm (k = 2) agreed with the certified value (42.1 nm ± 0.3 nm) of the QC sample. For ERM-FD102, the mean results of size class A and size class B of the intensity-based PSD were reported with a relative standard measurement uncertainty of 4.5 % and 2.1 %, respectively. These uncertainties were estimated following a top-down approach whereby the standard relative uncertainties from repeatability, intermediate precision and trueness were combined.

Laboratory 7 performed all measurements according to the provided measurement protocol and successfully analysed the monomodal colloidal silica QC sample (ERM-FD304). The obtained QC result (mean of two aliquot means; three consecutive measurements per aliquot) of 40.8 nm ± 3.7 nm (k = 2) agreed with the certified value (42.1 nm ± 0.3 nm) of the QC sample. For ERM-FD102, the mean results of size class A and size class B of the intensity-based PSD were reported with a relative standard measurement uncertainty of 4.5 %. This uncertainty reflects the full uncertainty budget including all individual steps (bottom-up). According to the supplier of the DLS equipment, the merely device-related uncertainty is 3 %. Given an additional 0.4 % temperature uncertainty plus sample- as well as handling-related contributions, an overall relative standard uncertainty of about 4.5 % is considered to be realistic. Seven out of the 24 PSDs showed to be trimodal instead of being bimodal. This additional third mode, which is much smaller than the modal value of size class A, repeatedly appears in the particle diameter range of 11 nm to 15 nm and surprisingly shifts the means of size class A and size class B to about 40 nm and 105 nm, respectively. Based on prior knowledge on the two raw materials that were used for developing ERM-FD102 and on results from other complementary techniques (e.g., electron microscopy), the third mode can be regarded as a false positive peak. The appearance of false positive peaks in DLS PSDs is a well-known phenomenon that is typically triggered by the ill-posed algorithms as response on detected baseline noise. Data from these trimodal PSDs were excluded from the evaluation.

Laboratory 8 performed all measurements according to the provided measurement protocol and successfully analysed the monomodal colloidal silica QC sample (ERM-FD304). The obtained QC result (mean of two aliquot means; five consecutive measurements per aliquot) of 42.0 nm ± 0.2 nm (k = 2) agreed with the certified value (42.1 nm ± 0.3 nm) of the QC sample. For ERM-FD102, the mean results of size class A and size class B of the intensity-based PSD were reported with a relative standard measurement uncertainty of 6.5 % and 2.7 %, respectively. These uncertainties were based on significant contributions from repeatability, reproducibility and method trueness. The repeatability of DLS measurements was determined by calculating the standard deviation of five replicate measurements. The reproducibility was determined for each ampoule by calculating the standard deviation of the aliquot means. Estimation of uncertainty contribution from trueness was based on comparison of intensity-weighted mean values of 100-nm gold particles measured in the presence and absence of a second mode.

Laboratory 10 performed all measurements according to the provided measurement protocol and successfully analysed the monomodal colloidal silica QC sample (ERM-FD304). The obtained QC result (mean of two aliquot means; five consecutive measurements per aliquot) of 42.6 nm ± 0.8 nm (k = 2) agreed with the certified value (42.1 nm ± 0.3 nm) of the QC

sample. For ERM-FD102, the mean results of size class A and size class B of the intensity-based PSDs were reported with a relative standard measurement uncertainty of 0.9 %. This uncertainty stems from measurements performed on a NIST nanosphere standard of nominal 50 nm. The relative standard deviation calculated across the different replicate results was in the same order of magnitude.

Laboratory 15 performed all measurements according to the provided measurement protocol and successfully analysed the monomodal colloidal silica QC sample (ERM-FD304). The obtained QC result (mean of two aliquot means; three consecutive measurements per aliquot) of 42.2 nm ± 4.2 nm (k = 2) agreed with the certified value (42.1 nm ± 0.3 nm) of the QC sample. For ERM-FD102, the mean results of size class A and size class B of the intensity-based PSD were reported with a relative standard measurement uncertainty of 16.0 % and 10.0 %, respectively. The laboratory estimated the overall measurement uncertainties following a top-down approach whereby individual relative standard uncertainties for method repeatability, intermediate precision and trueness were combined. Both uncertainties for repeatability and intermediate precision were estimated from the measurements performed on different days on the materials provided in this study. The uncertainty for trueness was evaluated from a combination of experimental data and expert judgement.

Laboratory 16 performed all measurements according to the provided measurement protocol and successfully analysed the monomodal colloidal silica QC sample (ERM-FD304). The obtained QC result (mean of two aliquot means; three consecutive measurements per aliquot) of 42.9 nm ± 0.8 nm (k = 2) agreed with the certified value (42.1 nm ± 0.3 nm) of the QC sample. For ERM-FD102, the modal results of size class A and size class B of the intensity-based PSD were reported with a relative standard measurement uncertainty of 4.4 % and 2.9 %, respectively. The laboratory evaluated the measurement uncertainties by combining Type B standard uncertainties associated to the Boltzmann constant, temperature, refractive index of the solvent, scattering angle, decay rate and solvent viscosity with Type A standard uncertainties from repeatability and intermediate precision. The Type A relative standard uncertainties, which are less than 1.2 %, are based on periodic instrument verification measurements performed on monomodal polystyrene latex size standards.

Laboratory 17 performed all measurements according to the provided measurement protocol and successfully analysed the monomodal colloidal silica QC sample (ERM-FD304). The laboratory submitted two datasets (further referred to as L17a and L17b); each dataset was obtained by a different DLS instrument. The obtained QC results (mean of two aliquot means; three consecutive measurements per aliquot) of 42.5 nm ± 0.8 nm (k = 2) for L17a and 42.0 nm ± 0.8 nm (k = 2) for L17b agreed with the certified value (42.1 nm ± 0.3 nm) of the QC sample. For ERM-FD102, the mean results of size class A and size class B of the intensity-based PSD were reported with a relative standard measurement uncertainty of 11.9 % and 3.8 % for L17a and 12.4 % and 3.8 % for L17b. These uncertainties were estimated from an in-house prepared mixture of two monomodal polystyrene latex size standards with nominal particle diameters of 20 nm and 80 nm.

Laboratory 20 performed all measurements according to the provided measurement protocol and successfully analysed the monomodal colloidal silica QC sample (ERM-FD304). The obtained QC result (mean of two aliquot means; three consecutive measurements per aliquot) of 42.2 nm ± 0.8 nm (k = 2) agreed with the certified value (42.1 nm ± 0.3 nm) of the QC sample. For ERM-FD102, the mean results of size class A and size class B of the intensity-based PSD were reported with a relative standard measurement uncertainty of 11.8 % and 3.8 %, respectively. These uncertainties were estimated from an in-house prepared mixture of two monomodal polystyrene latex size standards with nominal particle diameters of 20 nm and 80 nm.

Laboratory 21 performed all measurements according to the provided measurement protocol and successfully analysed the monomodal colloidal silica QC sample (ERM-FD304). The laboratory submitted two datasets (further referred to as L21a and L21b); each dataset was obtained by a different DLS instrument and data evaluation software. The obtained QC results (mean of two aliquot means; three consecutive measurements per aliquot) of 42.5 nm ± 1.9 nm (k = 2) for L21a and 41.6 nm ± 1.9 nm (k = 2) for L21b agreed with the certified value (42.1 nm ± 0.3 nm) of the QC sample. For ERM-FD102, the mean results (L21a) of size class A and size class B of the intensity-based PSD were reported with a relative standard measurement uncertainty of 6.2 % and 2.8 %. These uncertainties reflect the methods' repeatability and intermediate precision performance as they were calculated from the three tested aliquots and their corresponding consecutive measurements. Dataset L21b was excluded from the study because the laboratory reported modal values from transformed density functions. The instrument software did not allow computing of the arithmetic mean values of the different peaks.

Laboratory 22 performed all measurements according to the provided measurement protocol and successfully analysed the monomodal colloidal silica QC sample (ERM-FD304). The obtained QC result (mean of two aliquot means; three consecutive measurements per aliquot) of 42.0 nm ± 0.1 nm (two times standard deviation) agreed with the certified value (42.1 nm ± 0.3 nm) of the QC sample. For ERM-FD102, the mean results of size class A and size class B of the intensity-based PSD were reported with a relative standard measurement uncertainty of 1.0 % and 4.0 %, respectively. The laboratory evaluated these measurement uncertainties by combining (bottom-up) Type B standard uncertainties associated to the Boltzmann constant, temperature, refractive index of the solvent, scattering angle, decay rate and solvent viscosity.

Laboratory 23 performed all measurements according to the provided measurement protocol and successfully analysed the monomodal colloidal silica QC sample (ERM-FD304). The obtained QC result (mean of two aliquot means; three consecutive measurements per aliquot) of 42.8 nm ± 0.5 nm (two times standard deviation) agreed with the certified value (42.1 nm ± 0.3 nm) of the QC sample. For ERM-FD102, the mean results of size class A and size class B of the intensity-based PSD were reported with a relative standard measurement uncertainty of 3.1 % and 1.1 %, respectively. These uncertainties are equivalent to the standard deviations that were calculated across the results obtained on the different ampoules and aliquots.

Laboratory 24 performed all measurements according to the provided measurement protocol and successfully analysed the monomodal colloidal silica QC sample (ERM-FD304). The obtained QC result (mean of two aliquot means; three consecutive measurements per aliquot) of 42.1 nm ± 3.2 nm (k = 2) agreed with the certified value (42.1 nm ± 0.3 nm) of the QC sample. For ERM-FD102, the mean results of size class A and size class B of the intensity-based PSD were reported with a relative standard measurement uncertainty of 3.8 %. These uncertainties, which were calculated according to the guidelines provided by the ILC coordinator, include contributions from method repeatability (0.5 %), intermediate precision (1.1 %) and trueness (3.6 %). The aforementioned method performance parameters were quantitatively assessed from method validation data and established control charts.

Laboratory 25 performed all measurements according to the provided measurement protocol and successfully analysed the monomodal colloidal silica QC sample (ERM-FD304). The obtained QC result (mean of two aliquot means; six consecutive measurements per aliquot) of 42.0 nm ± 4.1 nm (k = 2) agreed with the certified value (42.1 nm ± 0.3 nm) of the QC sample. For ERM-FD102, the mean results of size class A and size class B of the intensity-based PSD were reported with a relative standard measurement uncertainty of 8.0 % and 4.2 %, respectively. These uncertainties, which were calculated according to the guidelines provided by the ILC measurement protocol, include contributions from method repeatability, intermediate precision and trueness. The relative standard uncertainty for repeatability

(4.4 % for size class A and 1.8 % for size class B) was estimated from the standard deviation of the six repeated measurements of the QC sample and ERM-FD102 samples. The relative standard uncertainty for intermediate precision (6.2 % for size class A and 3.2 % for size class B) was calculated by monitoring a given sample of ERM-FD102 over six days and comparing the obtained standard deviations. The relative standard uncertainty for trueness (2.3 % for size class A and 1.9 % size class B) was estimated from an in-house prepared bimodal mixture of nominally 20 nm and 100 nm gold nanoparticles. This material was one of the test samples measured in a recent ILC study, and the values were compared to the consensus values arising from that ILC study.

Laboratory 26 performed all measurements according to the provided measurement protocol and successfully analysed the monomodal colloidal silica QC sample (ERM-FD304). The obtained QC result (mean of two aliquot means; six consecutive measurements per aliquot) of 39.5 nm ± 3.2 nm (k = 2) agreed with the certified value (42.1 nm ± 0.3 nm) of the QC sample. For ERM-FD102, the mean results of size class A and size class B of the intensity-based PSD were reported with a relative standard measurement uncertainty of 4.0 %. This uncertainty was estimated from measurement results that were obtained on four samples of the Coulter N4 Series Reference Standards (batch no. 0008). The four samples were all measured on seven different days.

Laboratory 28 performed all measurements according to the provided measurement protocol and successfully analysed the monomodal colloidal silica QC sample (ERM-FD304). The obtained QC result (mean of two aliquot means; three consecutive measurements per aliquot) of 41.2 nm ± 3.3 nm (k = 2) agreed with the certified value (42.1 nm ± 0.3 nm) of the QC sample. For ERM-FD102, the laboratory reported arithmetic, harmonic and geometric mean values as well as the modal and median values of individual peaks associated to size class A and size class B. The results for size class A and size class B were accompanied with relative standard measurement uncertainties of 8.0 % and 3.5 %, respectively. The relative standard uncertainties were equivalent to the obtained standard deviations.

Laboratory 29 performed all measurements according to the provided measurement protocol and successfully analysed the monomodal colloidal silica QC sample (ERM-FD304). The obtained QC result (mean of two aliquot means; three consecutive measurements per aliquot) of 42.0 nm ± 1.2 nm (k = 2) agreed with the certified value (42.1 nm ± 0.3 nm) of the QC sample. For ERM-FD102, the harmonic and arithmetic mean results of size class A and size class B of the intensity-based PSD were reported with a relative standard measurement uncertainty of 2.5 % and 1.7 %, respectively. The relative standard measurement uncertainties were equivalent to the obtained standard deviations.

Laboratory 30 performed all measurements according to the provided measurement protocol and successfully analysed the monomodal colloidal silica QC sample (ERM-FD304). The obtained QC result (mean of two aliquot means; three consecutive measurements per aliquot) of 41.2 nm ± 1.6 nm (k = 2) agreed with the certified value (42.1 nm ± 0.3 nm) of the QC sample. For ERM-FD102, the mean results of size class A and size class B of the intensity-based PSD were reported with a relative standard measurement uncertainty of 2.0 %. The reported uncertainty was based on expert judgement.

Annex E4: Results of the characterisation measurements – EM

Table E4-1 Number-weighted modal area-equivalent particle diameter results associated to size class A of the PSD, obtained by EM

Lab-code	Method	Replicate results [nm]						Mean [nm]	s [1] [nm]	U [2] [nm]
		1	2	3	4	5	6			
L8	SEM	18.2	17.8	17.7	18.2	17.3	17.5	17.8	0.4	3.0
L9	TEM	18.3	18.4	18.7	18.6	18.3	19.2	18.6	0.3	1.0
L10	TEM	20.5	18.5	17.5	17.1	20.5	17.5	18.6	1.5	1.2
L11a	TEM	16.7	16.6	16.8	17.5	17.6	17.5	17.1	0.5	1.1
L11b	SEM	19.1	18.9	18.0	18.5	18.9	19.0	18.7	0.4	1.2
L16	SEM	18.1	19.0	17.3	17.3	20.0	20.3	18.7	1.3	3.6
L24	TEM	18.2	16.8	16.8	16.8	16.8	16.8	17.1	0.6	1.4
L25	TEM	19.0	18.0	19.0	19.0	18.0	17.0	18.3	0.8	3.0
L27	TEM	19.8	20.4	17.6	19.5	19.8	19.2	19.4	1.0	1.4
Results not used for certification										
L1a	TEM	18.2	17.1	19.4	17.1	16.1	18.4	17.7	1.2	1.8
L1b	SEM	18.3	16.4	16.8	19.2	22.8	19.2	18.8	2.3	1.9

[1] Standard deviation of the individual replicate results
[2] Expanded (k = 2) uncertainty as reported by the participant

Table E4-2 Number-weighted modal area-equivalent particle diameter results associated to size class B of the PSD, obtained by EM

Lab-code	Method	Replicate results [nm]						Mean [nm]	s [1] [nm]	U [2] [nm]
		1	2	3	4	5	6			
L8	SEM	82.1	81.6	83.0	83.2	82.5	82.1	82.4	0.6	3.2
L9	TEM	83.0	84.0	82.9	83.8	83.5	83.6	83.5	0.4	4.0
L10	TEM	83.7	83.7	83.7	84.2	80.7	80.1	82.7	1.8	5.0
L11a	TEM	83.9	82.8	84.9	85.0	84.9	84.9	84.4	0.9	5.1
L11b	SEM	85.2	85.4	85.0	85.3	85.8	85.8	85.4	0.3	5.2
L16	SEM	82.2	80.7	82.6	85.0	84.0	84.4	83.2	1.6	4.0
L24	TEM	83.4	86.6	80.2	85.0	83.4	80.2	83.1	2.6	6.7
L25	TEM	90.0	87.0	85.0	87.0	85.0	88.0	87.0	1.9	14.0
Results not used for certification										
L1a	TEM	84.0	78.0	73.0	74.0	71.0	74.0	75.7	4.7	9.4
L1b	SEM	96.0	95.0	87.0	86.0	91.0	91.0	91.0	4.0	9.1
L27	TEM	94.0	n.a.	98.7	n.a.	90.4	n.a.	94.4	4.2	6.6

[1] Standard deviation of the individual replicate results
[2] Expanded (k = 2) uncertainty as reported by the participant

Table E4-3 Number-weighted median area-equivalent particle diameter results associated to size class A of the PSD, obtained by EM

Lab-code	Method	Replicate results [nm]						Mean [nm]	s [1] [nm]	U [2] [nm]
		1	2	3	4	5	6			
L8	SEM	18.7	18.4	18.3	18.9	18.0	18.2	18.4	0.3	3.1
L9	TEM	18.5	18.6	18.9	18.7	18.5	19.5	18.8	0.4	1.2
L10	TEM	19.9	18.4	17.7	18.1	19.8	18.0	18.7	1.0	1.1
L11a	TEM	16.7	16.8	16.9	17.1	16.8	17.1	16.9	0.2	1.0
L11b	SEM	19.1	19.1	18.2	18.5	19.4	19.1	18.9	0.5	1.1
L16	SEM	18.1	18.9	17.5	17.3	19.9	20.3	18.7	1.2	3.5
L24	TEM	17.5	16.7	16.9	16.1	16.8	17.3	16.9	0.5	1.4
L25	TEM	18.3	17.4	17.8	19.2	17.3	17.6	17.9	0.7	2.2
L27	TEM	18.8	18.6	19.5	19.2	19.7	19.3	19.2	0.4	1.3
Results not used for certification										
L1a	TEM	17.8	17.2	17.6	17.0	16.6	16.1	17.1	0.6	1.7
L1b	SEM	18.3	19.5	16.9	19.1	22.9	19.6	19.4	2.0	1.9

[1] Standard deviation of the individual replicate results

[2] Expanded (k = 2) uncertainty as reported by the participant

Table E4-4 Number-weighted median area-equivalent particle diameter results associated to size class B of the PSD, obtained by EM

Lab #	Method	Replicate results [nm]						Mean [nm]	s [1] [nm]	U [2] [nm]
		1	2	3	4	5	6			
L8	SEM	82.3	81.7	83.1	83.3	82.6	82.2	82.5	0.6	3.1
L9	TEM	82.2	82.2	82.1	81.6	82.3	82.6	82.2	0.3	3.9
L10	TEM	79.4	79.9	80.6	81.3	79.0	77.8	79.7	1.2	4.8
L11a	TEM	83.1	83.0	84.8	84.3	85.2	85.3	84.3	1.0	5.1
L11b	SEM	85.2	85.4	85.1	85.6	85.8	86.0	85.5	0.3	5.1
L16	SEM	81.7	80.9	82.6	84.7	84.4	83.8	83.0	1.5	4.0
L24	TEM	83.5	83.4	81.5	84.4	82.7	79.8	82.6	1.7	6.6
L25	TEM	88.7	85.9	84.8	88.3	84.9	86.5	86.5	1.7	10.4
Results not used for certification										
L1a	TEM	84.0	78.0	73.0	74.0	71.0	74.0	75.7	4.7	9.4
L1b	SEM	98.0	99.0	91.0	88.0	91.0	91.0	93.0	4.4	9.3
L27	TEM	94.0	n.a.	94.6	n.a.	94.0	n.a.	94.2	0.3	6.6

[1] Standard deviation of the individual replicate results

[2] Expanded (k = 2) uncertainty as reported by the participant

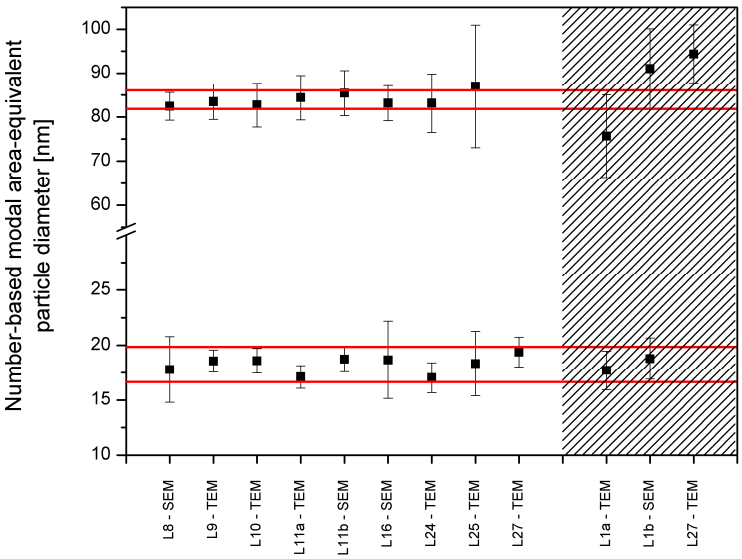

Fig. E4-1 Laboratory mean values of the number-weighted modal area-equivalent particle diameters as obtained by nine laboratories by EM; the error bars indicate the expanded (k = 2) measurement uncertainties as reported by the participants; the two sets of horizontal lines reflect the certified ranges; technically invalid results are indicated in the hatched region

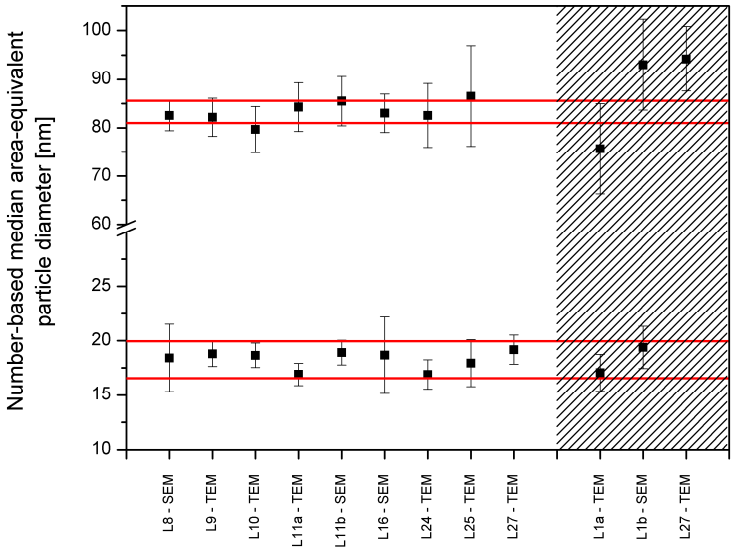

Fig. E4-2 Laboratory mean values of the number-weighted median area-equivalent diameters as obtained by nine laboratories by EM; the error bars indicate the expanded (k = 2) measurement uncertainties as reported by the participants; the two sets of horizontal lines reflect the certified ranges; technically invalid results are indicated in the hatched region

Laboratory 1 participated in the ILC study with both TEM and SEM methods. The datasets of the TEM and SEM methods are further referred to as L1a and L1b, respectively. The laboratory performed all measurements according to the provided measurement scheme. However, particle size measurements were performed by drawing a line through the centre of the particle and measuring the length of the line, rather than measuring the requested area-equivalent circular diameter. For dataset L1a, the mean of the two replicate modal results, obtained for the monomodal polystyrene latex QC sample (3100A), was 102.5 nm ± 10.3 nm (k = 2). This result agreed with the assigned value (102.0 nm ± 3.0 nm). However, the mean of the two replicate modal results, obtained for the monomodal colloidal silica QC sample (ERM-FD100), was 16.5 nm ± 1.6 nm (k = 2). This result was about 20 % below the corresponding certified modal value and uncertainty (19.4 nm ± 1.3 nm). For dataset L1b, the mean of the two replicate modal results, obtained for the monomodal polystyrene latex QC sample (3100A), was 93.8 nm ± 9.4 nm (k = 2), and agreed with the assigned value (102.0 nm ± 3.0 nm). For the monomodal colloidal silica QC sample (ERM-FD100), the mean of the two replicate modal results was 23.0 nm ± 2.3 nm (k = 2). This result only overlaps with the certified value and uncertainty by less than 0.1 nm and the experimental bias was found to be significant following the guidelines described in ERM Application Note 1 [**Error! Bookmark not defined.**].For ERM-FD102, the mean results of the modal and median particle diameters associated to size class A and size class B of the number-based PSDs were reported with a relative standard measurement uncertainty of 5.0 %. This uncertainty was estimated from the results obtained during a previous ILC study and from expert judgement. Because the results (L1a and L1b) for ERM-FD100 did not agree with the certified value, and because results originate from a different measurand, both ERM-FD102 datasets were excluded from the value assignment procedure.

Laboratory 8 participated in the ILC study with SEM and performed all measurements according to the provided measurement protocol. For the monomodal polystyrene latex QC sample (3100A), the mean of the two replicate modal results was 100.6 nm ± 3.0 nm (k = 2). This result agreed with the assigned value (102.0 nm ± 3.0 nm). The mean of the two replicate modal results, obtained for the monomodal colloidal silica QC sample (ERM-FD100), was 19.5 nm ± 2.9 nm (k = 2). This agreed with the certified modal value and uncertainty (19.4 nm ± 1.3 nm). For ERM-FD102, the mean results of the modal and median particle diameters associated to size class A and size class B of the number-based PSDs were reported with a relative standard measurement uncertainty of 8.4 % and 1.9 %, respectively. These measurement uncertainties are based on the assessment of significant contributions from repeatability, reproducibility, the threshold correction and background uncertainty, determination of the particle boundary, and the X, Y calibration and image drift. The repeatability of SEM measurements was determined for each size by grouping the data into subsets, calculating the arithmetic mean for each subset separately, and then computing the standard deviation of the means from the overall mean value. To assure statistically meaningful estimation of repeatability for the large particles, sizes < 60 nm were excluded from the calculation. The reproducibility of SEM measurements is determined for each ampoule by calculating the standard deviation of the two EM test sample modal diameters obtained from distribution fitting with a lognormal function.

Laboratory 9 participated in the ILC study with TEM and performed all measurements according to the provided measurement protocol. For the monomodal polystyrene latex QC sample (3100A), the mean of the two replicate modal results was 101.4 nm ± 4.1 nm (k = 2). This result agreed with the assigned value (102.0 nm ± 3.0 nm). The mean of the two replicate modal results, obtained for the monomodal colloidal silica QC sample (ERM-FD100), was 20.1 nm ± 0.8 nm (k = 2) and agreed with the certified modal value and uncertainty (19.4 nm ± 1.3 nm). For ERM-FD102, the mean results of the modal particle diameters associated to size class A and size class B of the number-based PSDs were reported with a relative standard measurement uncertainty of 2.7 % and 2.4 %, respectively. The mean results of the median particle diameters associated to size class A and size class B of the number-based PSDs were reported with a relative standard measurement

uncertainty of 3.1 % and 2.4 %, respectively. All measurement uncertainties originate from a validation study during which the method repeatability, reproducibility and trueness was investigated. The calculated Type A uncertainties were complemented with a Type B uncertainty for TEM calibration. In addition to size class A and size class B, the laboratory also indicated the presence of a third minor population between 40 nm and 50 nm.

Laboratory 10 participated in the ILC study with TEM and performed all measurements according to the provided measurement protocol. For the monomodal polystyrene latex QC sample (3100A), the mean of the two replicate modal results was 98.3 nm ± 5.9 nm (k = 2). This result agreed with the assigned value (102.0 nm ± 3.0 nm). The mean of the two replicate modal results, obtained for the monomodal colloidal silica QC sample (ERM-FD100), was 20.0 nm ± 1.2 nm (k = 2) and agreed with the certified modal value and uncertainty (19.4 nm ± 1.3 nm). For ERM-FD102, the mean results of the modal and median particle diameters associated to size class A and size class B of the number-based PSDs were reported with a relative standard measurement uncertainty of 3.0 %. This uncertainty was estimated based on the relative uncertainty for a single measurement and on the relative standard error for the arithmetic mean of the distribution. Relative standard errors for the arithmetic mean were found to be always between 0.4 % and 0.6 %. The relative uncertainty for a single measurement was estimated at 3.0 %. This includes the combined effect of the method trueness (2.0 %) and the repeatability and intermediate precision (combined effect also 2.0 %). The effect of the latter will be negligible on the final result for mode and median since they cancel out due to their random nature, especially since the number of particles counted was quite large. The effect of the method trueness, however, remains important as it is a systematic uncertainty. Combining therefore the value for method trueness (2.0 %) and the relative standard error (at most 0.6 %), it can be stated that the cumulative measurement uncertainty on the number-weighted modal and median particle diameter values is approximately 3.0 %.

Laboratory 11 participated in the ILC study with both TEM and SEM methods. The datasets of the TEM and SEM methods are further referred to as L11a and L11b, respectively. The laboratory performed all measurements according to the provided measurement protocol. For dataset L11a, the mean of the two replicate modal results, obtained for the monomodal polystyrene latex QC sample (3100A), was 96.0 nm ± 5.8 nm (k = 2). For dataset L11b, the result was 99.0 nm ± 5.9 nm (k = 2). Both results agreed with the assigned value (102.0 nm ± 3.0 nm). For the monomodal colloidal silica QC sample (ERM-FD100), the means of the two replicate modal results for datasets L11a and L11b were 17.6 nm ± 1.1 nm (k = 2) and 18.9 nm ± 1.1 nm (k = 2). Both results agreed with the certified modal value and uncertainty (19.4 nm ± 1.3 nm). For ERM-FD102, the mean results of the modal and median particle diameters associated to size class A and size class B of the number-based PSDs were reported with a relative standard measurement uncertainty of 3.0 %. This uncertainty is mainly based on the trueness of the TEM and SEM methods.

Laboratory 16 participated in the ILC study with SEM and performed all measurements according to the provided measurement protocol. For the monomodal polystyrene latex QC sample (3100A), the mean of the two replicate modal results was 100.9 nm ± 4.8 nm (k = 2). This result agreed with the assigned value (102.0 nm ± 3.0 nm). The mean of the two replicate modal results, obtained for the monomodal colloidal silica QC sample (ERM-FD100), was 22.1 nm ± 4.1 nm (k = 2) and agreed with the certified modal value and uncertainty (19.4 nm ± 1.3 nm). For ERM-FD102, the mean results of the modal and median particle diameters associated to size class A and size class B of the number-based PSDs were reported with a relative standard measurement uncertainty of 9.4 % and 2.4 %, respectively. These measurement uncertainties were estimated from the method repeatability for multiple measurements, magnification calibration, stage drift, threshold selection for particle separation and stigmatism of the beam spot. The modal diameters were estimated by fitting the histogram with normal distribution.

Laboratory 24 participated in the ILC study with TEM and performed all measurements according to the provided measurement protocol. For the monomodal polystyrene latex QC sample (3100A), the mean of the two replicate modal results was 98.6 nm ± 7.9 nm (k = 2). This result agreed with the assigned value (102.0 nm ± 3.0 nm). The mean of the two replicate modal results, obtained for the monomodal colloidal silica QC sample (ERM-FD100), was 18.2 nm ± 1.5 nm (k = 2) and agreed with the certified modal value and uncertainty (19.4 nm ± 1.3 nm). For ERM-FD102, the mean results of the modal and median particle diameters associated to size class A and size class B of the number-based PSDs were reported with a relative standard measurement uncertainty of 4.0 %. This measurement uncertainty was estimated from the method repeatability (1.5 %), intermediate precision (2.8 %) and trueness (2.5 %), as recommended by the ILC measurement protocol.

Laboratory 25 participated in the ILC study with TEM and performed all measurements according to the provided measurement protocol. For the monomodal polystyrene latex QC sample (3100A), the mean of the two replicate modal results was 100.5 nm ± 14.1 nm (k = 2). This result agreed with the assigned value (102.0 nm ± 3.0 nm). The mean of the two replicate modal results, obtained for the monomodal colloidal silica QC sample (ERM-FD100), was 19.0 nm ± 2.7 nm (k = 2) and agreed with the certified modal value and uncertainty (19.4 nm ± 1.3 nm). For ERM-FD102, the mean results of the modal particle diameters associated to size class A and size class B of the number-based PSDs were reported with a relative standard measurement uncertainty of 8.0 %. The mean results of the median particle diameters associated to size class A and size class B of the number-based PSDs were reported with a relative standard measurement uncertainty of 6.0 %. The uncertainty for repeatability was calculated by dividing the standard deviation of particle measurements from multiple individual images from three different TEM grids, prepared from the same reference material aliquot (ERM-FD100), and measured on the same day, by the average measured value. The relative uncertainty due to day-to-day variation or intermediate precision was calculated by dividing the standard deviation of measurement results of the average equivalent circular particle diameter of the calibration material (ERM-FD100) from images generated on different days, by the average measured value (in pixel). The uncertainty due to method trueness takes into account uncertainty contributions from the TEM scaling calibration, the diameter measurements and the binning procedure.

Laboratory 27 participated in the ILC study with TEM. The laboratory deviated from the provided measurement protocol regarding the analysis of size class B. Measurements for size class A were performed according to the protocol. For the monomodal polystyrene latex QC sample (3100A), the mean of the two replicate modal results was 98.8 nm ± 13.8 nm (k = 2). This result agreed with the assigned value (102.0 nm ± 3.0 nm). The mean of the two replicate modal results, obtained for the monomodal colloidal silica QC sample (ERM-FD100), was 18.8 nm ± 1.3 nm (k = 2) and agreed with the certified modal value and uncertainty (19.4 nm ± 1.3 nm). For ERM-FD102, the mean results of the modal and median particle diameters associated to size class A and size class B of the number-based PSDs were reported with a relative standard measurement uncertainty of 3.5 %. This combined uncertainty includes the contribution of both Type A (repeatability, sample variability and number of particles) and Type B (size calibration and magnification) standard uncertainties. The uncertainty for repeatability was estimated by performing three repeated measurements on each of three different samples. The repeatability is expected to be within 2 % of the average of the peak diameter. For a reference material, it is assumed that sample-to-sample variability is not a problem. The third Type A uncertainty depends on the number of particles that are measured and the use of Poisson statistics to convert this to an uncertainty. For a total number of 1000 small and 300 large particles, the contribution to the total uncertainty is estimated to be less than 1 %. The uncertainty (about 0.5 %) due to the size calibration was estimated for nominally 100 nm particles. The uncertainty of the magnification was about 1 %. The as-received material was 200 times diluted. At this dilution, images contained only few particles of size class B compared to the number particles of size class A. As a result, many images had to be analysed to identify and measure the required number of 300 large

particles. Analysing of a less diluted sample resulted in the nominally 20 nm particles (size class A) sticking to the larger particles (size class B). As a result, reliable measurements of the large particles became uncertain. From a practical viewpoint, the laboratory measured at least 200 particles. Since the measurement protocol prescribed at least 300 of the nominally 80 nm particles to be analysed, the dataset (size class B) was excluded from the value assignment procedure.

Annex E5: Results of the characterisation measurements – PTA

Table E5-1 Number-weighted modal hydrodynamic particle diameter results associated to size class B of the PSD, obtained by PTA

Lab-code	Aliquot mean results [nm]									Mean [nm]	*s* [1] [nm]	*U* [2] [nm]
	1	2	3	4	5	6	7	8	9			
L6	77.6	81.0	80.4	79.6	77.6	78.2	81.2	79.6	78.8	79.3	1.4	2.6
L12	78.0	78.3	78.6	77.5	78.3	78.9	77.6	77.1	78.3	78.1	0.6	5.5
L16	77.0	78.0	75.0	75.7	76.0	75.3	75.3	76.3	74.3	75.9	1.1	4.1

[1] Standard deviation of the mean aliquot results

[2] Expanded (k = 2) uncertainty as reported by the participant

Table E5-2 Number-weighted mean hydrodynamic particle diameter results associated to size class B of the PSD, obtained by PTA

Lab-code	Aliquot mean results [nm]									Mean [nm]	*s* [1] [nm]	*U* [2] [nm]
	1	2	3	4	5	6	7	8	9			
L6	85.0	81.4	78.2	79.2	81.6	80.0	82.0	80.0	81.2	81.0	2.0	4.0
L12	81.4	82.8	84.1	82.3	80.8	81.7	83.0	79.7	82.7	82.1	1.3	9.4
L16	84.8	83.7	85.2	82.5	83.5	85.2	84.7	83.7	84.3	84.2	0.9	4.5

[1] Standard deviation of the mean aliquot results

[2] Expanded (k = 2) uncertainty as reported by the participant

Table E5-3 Number-weighted median hydrodynamic particle diameter results associated to size class B of the PSD, obtained by PTA

Lab-code	Aliquot mean results [nm]									Mean [nm]	*s* [1] [nm]	*U* [2] [nm]
	1	2	3	4	5	6	7	8	9			
L6	82.0	79.6	78.6	79.4	79.0	79.6	80.6	79.4	n.a.	79.8	1.1	2.2
L12	78.6	79.1	80.1	78.6	77.6	78.0	78.8	77.1	79.2	78.6	0.9	4.6
L16	79.8	78.7	81.0	79.0	77.7	78.0	80.0	80.0	79.2	79.3	1.1	4.3

[1] Standard deviation of the mean aliquot results

[2] Expanded (k = 2) uncertainty as reported by the participant

Table F5-4 Particle concentration [10^8 particles/mL] associated to size class B of the PSD, obtained by PTA

Lab-code	Aliquot mean results									Mean	s [1)]	U [2)]
	1	2	3	4	5	6	7	8	9			
L6	5.4	6.8	7.6	6.8	6.4	6.5	6.4	7.2	6.6	6.6	0.6	2.2
L12	6.0	6.1	5.1	5.9	6.1	5.9	5.8	6.0	6.4	5.9	0.4	2.3
L16	2.0	1.7	2.3	1.2	4.9	0.9	1.0	0.9	1.0	1.8	1.3	n.a.

[1)] Standard deviation of the mean aliquot results

[2)] Expanded (k = 2) uncertainty as reported by the participant

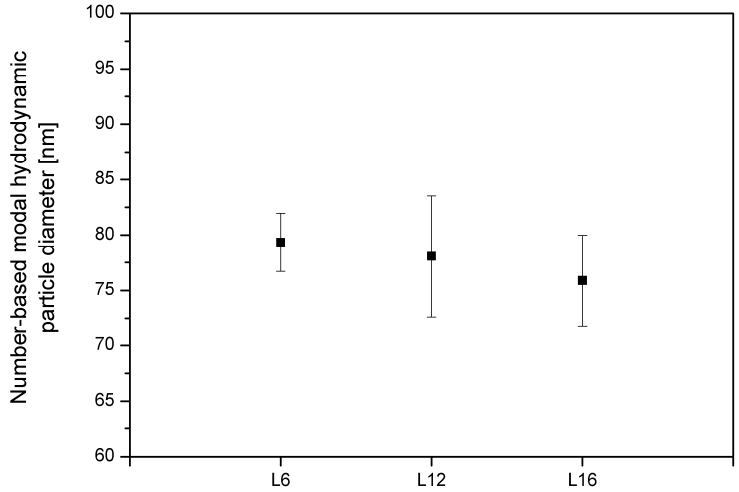

Fig. E5-1 Laboratory mean values of the number-weighted modal hydrodynamic particle diameters as obtained by three laboratories by PTA; the error bars indicate the expanded (k = 2) measurement uncertainties as reported by the participants

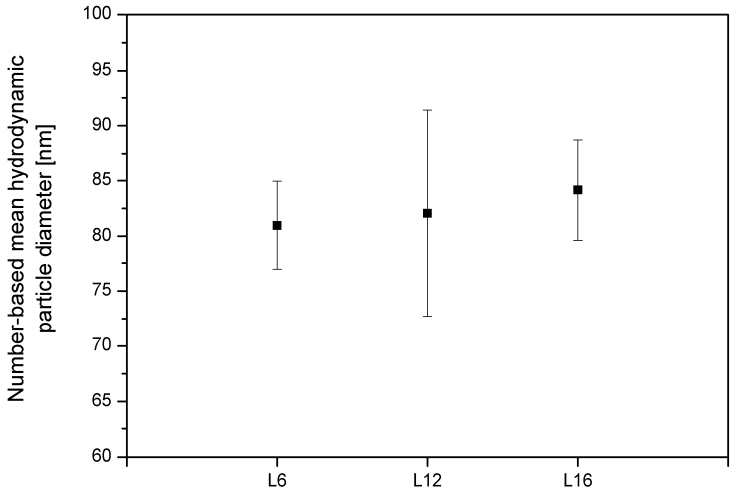

Fig. E5-2 Laboratory mean values of the number-weighted mean hydrodynamic particle diameters as obtained by three laboratories by PTA; the error bars indicate the expanded (k = 2) measurement uncertainties as reported by the participants

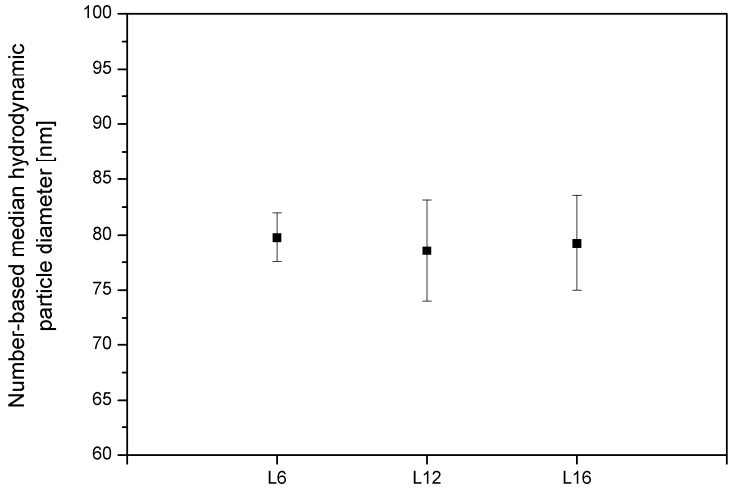

Fig. E5-3 Laboratory mean values of the number-weighted median hydrodynamic particle diameters as obtained by three laboratories by PTA; the error bars indicate the expanded (k = 2) measurement uncertainties as reported by the participants

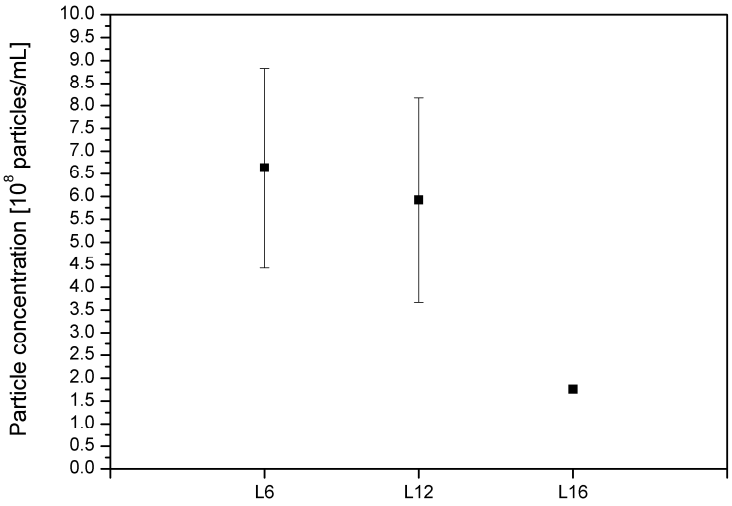

Fig. E5-4 Laboratory mean values of the particle concentration results as obtained by three laboratories by PTA; the error bar indicate the expanded (k = 2) measurement uncertainty as reported by the participant; L16 did not provide a measurement uncertainty

Laboratory 6 performed all measurements according to the provided measurement scheme and protocol, and successfully analysed the monomodal colloidal polystyrene latex QC sample (3080A). The obtained QC result (mean of two aliquot results; six consecutive measurements per aliquot) of 78.6 nm ± 6.0 nm (k = 2) agreed with the assigned value (81.0 nm ± 3.0 nm) of the QC sample. For ERM-FD102, the modal, mean and median values determined for the number-based PSDs were associated with relative standard measurement uncertainties of 1.7 %, 2.5 % and 1.4 %, respectively. To estimate these measurement uncertainties, the laboratory calculated first the averages of the replicate results (of the modal particle diameters) obtained on each aliquot, thereby arriving at nine independent size values. Then, using ANOVA, the day-to-day variation and repeatability uncertainty components were calculated. Because a suitable CRM does not exist, the laboratory could not estimate the uncertainty due to method trueness. The effect of the measurement temperature was experimentally investigated at 22 °C, 25 °C and 28 °C. Due to the non-significance of the obtained results, an additional uncertainty component for temperature was not considered in the precision uncertainty budget.

Laboratory 12 performed all measurements according to the provided measurement scheme and protocol, and successfully analysed the monomodal colloidal polystyrene latex QC sample (3080A). The obtained QC result (mean of two aliquot results; 10 consecutive measurements per aliquot) of 82.3 nm ± 2.6 nm (two times standard deviation) agreed with the assigned value (81.0 nm ± 3.0 nm) of the QC sample. For ERM-FD102, the mode, mean and median values determined for the number-based PSDs were associated with a relative standard measurement uncertainty of 3.5 %, 5.7 % and 2.9 %, respectively. These uncertainties, which are related to single PTA measurements, were estimated by series of repeated measurements of polystyrene latex and silica nanoparticles. Method trueness, which was estimated from measurements of 46 nm and 102 nm polystyrene latex beads according to the method described in ERM Application Note 1 [31], was found to be 2.0 %. The uncertainty associated with repeatability and intermediate precision was estimated from measurements on the bimodal colloidal silica CRM that were performed under repeatability and intermediate precision conditions. The uncertainty due to repeatability was calculated as 2.8 %, and although the uncertainty associated to intermediate precision could not be determined ($MS_{between} < MS_{within}$), the maximum variation that could be hidden by method

repeatability was estimated to be 0.7 %. Combination of these three uncertainty components by taking the root of the sum of squares indicates an estimated combined relative standard measurement of 3.5 %. The laboratory reported that with a shorter recording time (30 s) a second particle population was visible as shoulder to the main PSD.

Laboratory 16 performed all measurements according to the provided measurement scheme and protocol, and successfully analysed the monomodal colloidal polystyrene latex QC sample (3080A). The obtained QC result (mean of two aliquot results; 5 consecutive measurements per aliquot) of 83.1 nm ± 4.5 nm (k = 2) agreed with the assigned value (81.0 nm ± 3.0 nm) of the QC sample. For ERM-FD102, the modal, mean and median values determined for the number-based PSDs were associated with a relative standard measurement uncertainty of 2.7 %. This uncertainty includes contributions from method trueness and repeatability. The former was investigated and quantified by performing five repeated measurements on a polystyrene latex particle size standard (100 nm ± 3 nm) and combining the calculated standard error and standard uncertainty from the particle size standard. The obtained uncertainty for trueness (1.8 %) was then combined with a standard uncertainty estimated for method repeatability (2.0 %).

European Commission

EUR 26656 EN – Joint Research Centre – Institute for Reference Materials and Measurements
Title: **The certification of equivalent diameters of a mixture of silica nanoparticles in aqueous solution: ERM®- FD102**
Author(s): V. Kestens and G. Roebben
Luxembourg: Publications Office of the European Union
2014 – 106 pp. – 21.0 x 29.7 cm
EUR – Scientific and Technical Research series – ISSN 1831-9424
ISBN 978-92-79-38396-0
doi:10.2787/95996

Abstract
This report describes the production of ERM®-FD102, silica nanoparticles in an aqueous solution certified for different equivalent diameters. The material was produced following ISO Guide 34:2009.
The certified reference material (CRM), which has been produced by the Institute for Reference Materials and Measurements (IRMM) of the European Commission's Joint Research Centre (JRC), is a mixture of two monomodal populations of silica nanoparticles with distinct nominal particle sizes of 20 nm and 80 nm. These nominally 20 nm and 80 nm particle populations are further referred to as size class A and size class B, respectively. The CRM was prepared from two commercially available silica sols, moderately diluted in an aqueous solution and bottled in 10 mL pre-scored amber glass ampoules.
Between unit-homogeneity was quantified and stability during dispatch and storage were assessed in accordance with ISO Guide 35:2006. The minimum sample intake for the different methods was determined from the results and information provided by the laboratories that participated in the interlaboratory comparison (ILC) exercises of the characterisation study.
The material was characterised, for size classes A and B, by an intercomparison amongst laboratories of demonstrated competence and adhering to ISO/IEC 17025. Technically invalid results were removed but no outlier was eliminated on statistical grounds only.
Uncertainties of the certified values were calculated in accordance with the Guide to the Expression of Uncertainty in Measurement (GUM) and include uncertainty contributions related to possible inhomogeneity and instability and to characterisation.
The material is intended for quality control and assessment of method performance. As any reference material, it can also be used for control charts or validation studies. In addition, ERM-FD102 can be used for calibration of electron microscopy methods. The CRM is available in amber glass ampoules containing about 9 mL of suspension.
The CRM was accepted as European Reference Material (ERM®) after peer evaluation by the partners of the European Reference Materials consortium.

As the Commission's in-house science service, the Joint Research Centre's mission is to provide EU policies with independent, evidence-based scientific and technical support throughout the whole policy cycle.

Working in close cooperation with policy Directorates-General, the JRC addresses key societal challenges while stimulating innovation through developing new methods, tools and standards, and sharing its know-how with the Member States, the scientific community and international partners.

Key policy areas include: environment and climate change; energy and transport; agriculture and food security; health and consumer protection; information society and digital agenda; safety and security, including nuclear; all supported through a cross-cutting and multi-disciplinary approach.

LA-NA-26656-EN-N

Publications Office

ISBN: 978-92-79-38396-0